Spring 1-1-2015

Don't Soil Your Chances with Solar Energy: Experiments of Natural Dust Accumulation on Solar Modules and the Effect on Light Transmission

Liza Boyle
University of Colorado Boulder, liza.boyle@colorado.edu

DON'T SOIL YOUR CHANCES WITH SOLAR ENERGY: EXPERIMENTS OF NATURAL DUST ACCUMULATION ON SOLAR MODULES AND THE EFFECT ON LIGHT TRANSMISSION

by

Liza Boyle

B.S., University of the Pacific, 2009

M.S., University of Colorado Boulder, 2012

A thesis submitted to the

Faculty of the Graduate School of the

University of Colorado in partial fulfillment

of the requirements for the degree of

Doctor of Philosophy

Department of Mechanical Engineering

2015

This thesis entitled:
DON'T SOIL YOUR CHANCES WITH SOLAR ENERGY: EXPERIMENTS OF NATURAL DUST ACCUMULATION ON SOLAR MODULES AND THE EFFECT ON LIGHT TRANSMISSION
written by Liza Boyle
has been approved for the Department of Mechanical Engineering

_____
Prof. Michael P. Hannigan

_____
Prof. Jana B. Milford

Date _____

The final copy of this thesis has been examined by the signatories, and we find that both the content and the form meet acceptable presentation standards of scholarly work in the above mentioned discipline.

Boyle, Liza (Ph.D., Mechanical Engineering)

DON'T SOIL YOUR CHANCES WITH SOLAR ENERGY: EXPERIMENTS OF NATURAL DUST ACCUMULATION ON SOLAR MODULES AND THE EFFECT ON LIGHT TRANSMISSION

Thesis directed by Prof. Michael P. Hannigan

Dust accumulation, or soiling, on solar energy harvesting systems can cause significant losses that reduce the power output of the system, increase pay-back time of the system, and reduce confidence in solar energy overall. Developing a method of estimating soiling losses could greatly improve estimates of solar energy system outputs, greatly improve operation and maintenance of solar systems, and improve siting of solar energy systems. This dissertation aims to develop a soiling model by collecting ambient soiling data as well as other environmental data and fitting a model to these data.

In general a process-level approach is taken to estimating soiling. First a comparison is made between mass of deposited particulates and transmission loss. Transmission loss is the reduction in light that a solar system would see due to soiling, and mass accumulation represents the level of soiling in the system. This experiment is first conducted at two sites in the Front Range of Colorado and then expanded to three additional sites. Second mass accumulation is examined as a function of airborne particulate matter (PM) concentrations, airborne size distributions, and meteorological data. In depth analysis of this process step is done at the first two sites in Colorado, and a more general analysis is done at the three additional sites. This step is identified as less understood step, but with results still allowing for a general soiling model to be developed. Third these two process steps are combined, and spatial variability of these steps are examined. The three additional sites (an additional site in the Front Range of Colorado, a site in Albuquerque New Mexico, and a site in Cocoa Florida) represent a much more spatially and climactically diverse set of locations than the original two sites and provide a much broader sample space in which to develop the combined soiling model. Finally a few additional parameters, precipitation, micro-meteorology, and some sampling artifacts, are cursorily examined. This is to provide a broader context for these results and to help future researchers in understanding the strengths and weaknesses of this dissertation and the results presented within.

Acknowledgements

This work would not be possible without the continuous support of my wonderful advisor Prof. Mike Hannigan. My deepest appreciation to him for the guidance (and frustration) that he has provided me. I would also like to thank Prof. Jana Milford for her insight in both research and teaching that have lead me examine my work and continually improve. A huge thanks to my other committee members, Dr. Bruce King, Prof. Peter Hamlington, and Dr. Michael Brandemuehl, your thoughts and advice has been very helpful in the conducting of this research.

There are many people who have helped make research and field work go much smoother than I could have ever hoped for. The students and researchers at CU especially Holly Flinchpaugh, but also Tori Danner, Tiffany Duhl, John Ortega, Alex Murray, Alison Moore, Kyle Gustafson, and all the graduate students who have shared time with me in the Hannigan lab. And the many helpful folks at all the locations I have had field sites especially Daniel Wolfe and Bruce Bartram of NOAA, Bradley Rink of CDPHE, Bruce King, Patrick Burton, and Charles Robinson of SNL, Ken Blackwell of FSEC, and Bill Sekulic, Mathew Dabney, and Chris Deline of NREL. Thank you all!

Finally, I would like to thank all of my friends and family who have tolerated me these last several years. Your constant support, encouragement, and understanding has made my graduate studies not only bearable but generally very enjoyable. This is all possible because of you.

This material is based upon work supported by the National Science Foundation Graduate Research Fellowship Program under Grant No. DGE 1144083. This work was supported by the U.S. Department of Energy SunShot Initiative.

Contents

Chapter

Tables

Table

Figures

Figure

Chapter 1

INTRODUCTION

1.1 Motivation for Research

Many factors have lead to a growing interest in renewable energy. Climate change, caused in large part by burning fossil fuels for electricity and transportation, is causing immense damage around the world with more powerful storms, more severe drought, and melting glaciers and ice caps. Concerns about how much longer fossil fuels will last, as reserves dwindle and extraction costs subsequently increase. Air quality and human health issued caused by the released of pollutants in the burning of fossil fuels. And finally the need for energy systems in remote and harsh environments where stable grid systems are nonexistent, resupplying fuel sources is not feasible, or the environment is not suitable for relying on combustion (the space station for example). These and many other concerns have lead to the growing increase in installed renewable energy systems.

While renewable energy systems used to be almost exclusively small scale systems (providing energy to power a single home, or small system), now large utility-scale systems are being deployed. These large systems often require investor financing, and utility support for implementation which requires a strong understanding of how these systems will perform over time and the payback time of the system. Currently there are several models that estimate power output over time and payback period of the system. For photovoltaic (PV) systems these models estimating power output from individual panels, string losses, losses from maximum power point tracking, and inverter losses, as well as financial information like electricity rate, cost of system and installation. These models have proved valuable in assessing system feasibility both

residentially and commercially.

While these models are generally quite accurate, there are some areas where large errors are introduced. For solar energy modeling one the largest of these is in soiling losses. Soiling is the natural accumulation of dust and particulates on the surface of the solar panel which reduces light transmission (or reflection). Current models require users to estimate the soiling losses in their system. Often a default value of between 1-10% is used, and rarely are these loss estimates based on any real information about where the system is located, or how the system is installed.

In addition to adding uncertainty to system output, soiling can significantly reduce the output from a solar energy system. Previous research has found a wide range of losses from soiling, averaging from one or two percent [32], to more than 80% [25] [30]. A comprehensive review of losses caused by soiling can be found elsewhere [57] [60]. These losses can increase the payback time of the system, reduce confidence in solar energy, and waste valuable energy, but are completely reversible with simple cleaning techniques. Because this a completely reversible loss, understanding of soiling has the added benefit of increasing knowledge of when to clean systems (at what point is it worth the cost).

1.2 Overview of Research Methods

Soiling is a multi-step process. In order for particulates to scatter or absorb the incoming solar radiation, they must be deposited on the surface. To be deposited on the surface they must have become airborne, and to be come airborne they must have come from some original source. In this way we can thinking of soiling as a three step process. First particulates end up in the air. This can come from resuspension - wind blowing dust up into the air, emission - power plants, factories, or other sources releasing particles into the atmosphere, or reaction, condensation, or coagulation- gaseous airborne particles react or condense to form particles, or coagulate to form larger particles from very small ones. Once particles are airborne they must be deposited onto the surface of the solar panel. This happens either by dry or wet deposition. Dry deposition can happen by gravitational settling for large particle or by Brownian diffusion for smaller particles, or impaction for all particles. Wet deposition happens when precipitation scavenges

particles from the atmosphere and deposits them with the precipitation. Once particles have deposited they are able to interfere with incoming solar radiation to reduce the transmitted radiation primarily by absorbing, reflecting, or scattering the light. All of these steps are represented pictorially in Figure 1.1. Throughout all of these steps the chemistry of the particulates can have an effect. For example: darker particles will absorb more light, denser particles will deposit more easily, and hydrophilic particles will be more easily deposited by wet-deposition.

Because airborne ambient particulates cause negative health and environmental effects they are regulated and monitored by the US Environmental Protection Act under the Clean Air Act. There has been extensive previous research into the sources of airborne particulate matter (PM), and the concentrations of these particulates is monitored at thousands of locations across the US. Therefore this step of the soiling process is not examined in this work, and instead PM data is assumed to be a readily available data stream in predicting soiling losses.

This research differs from previous work, and advances soiling knowledge in several different ways. First a novel approach to collecting soiling data is developed and appropriate analysis tools are developed. Second, long time series of data were collected (more than a year at most sites), which is different than the one week to several month studies that are typical in soiling research. Third we examine PM. This has not been done in soiling research and represents perhaps the best metric we have for predicting soiling losses in diverse locations. Finally we collect a spatially diverse data set. This has been done in some previous studies [11] [44], but it is uncommon. Previous work that has looked at spatial variability of soiling has not examined any methods for generalizing results such as monitoring mass of deposited particulates, or ambient PM concentrations, both of which are done in this work.

1.3 Thesis Organization

This reminder of this dissertation is organized into a method development chapter, Chapter 2, followed by four research chapters. The first three research chapters represent independent articles that have or will be published independently, and the final research chapter is some additional work that I have done

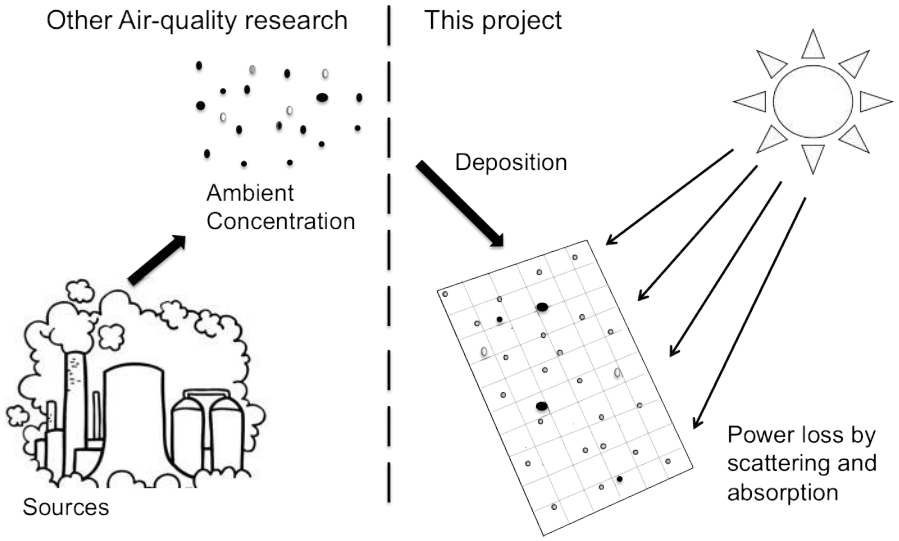

Figure 1.1: An overview of the processes required for soiling of solar energy systems. This work examines how ambient PM concentrations effect deposition, and how deposited particulates effect light transmission.

on the topic but that does not easily fit into the three previous chapters. Chapters 3 and 4 examine the steps in the soiling process. Specifically Chapter 3 examines how deposited particulates effect light transmission including the effect of angle of incidence. This chapter is also the most detailed in error analysis and the errors that are associated with the data collected in this dissertation. Chapter 4 examines how ambient particulates are related to mass accumulation. This chapter examines several methods of estimating mass accumulation, specifically dry deposition, from a simple linear model to a much more complex and established deposition model. Chapter 5 combines these and focuses on examining spatial variability of soiling for wide implementation of these and previous results. Finally Chapter 6 examines precipitation both as a cleaning and a contamination method, micrometeorology, and some effects of my sampling strategy, focusing on how all of these things relate to the larger picture of this research and broadly implementing this soiling model.

Chapter 2

IDENTIFYING IMPORTANT PARAMETERS AND DEVELOPING A METHOD FOR AMBIENT SAMPLING

2.1 State of the Literature

Previous studies of soiling generally fall into one, or more, of three main categories. The first are studies that examine the extent of the problem, or how much energy is lost because of soiling. These are typically field studies done at one location, sometimes more, and the main soiling results are just the percentage losses seen at that location at that time. These studies provide an understanding of the soiling losses that will be seen in that and similar locations, and help motivate further research in soiling. The second type of studies are laboratory studies that typically address basic parameters related to soiling and the effect of those parameters. These studies use very controlled environments, and simplified methods to understand what factors most effect soiling while keeping other factors constant. These studies are great for understanding the most important factors and processes in soiling, but lack the certainty that they apply to actual soiling situations. The final category of previous research are studies that attempt in some way to generalize their results. These studies are similar to the first category of studies but do some additional analysis or research and add additional information to make their research relevant to soiling happening in any location. The remainder of this section examines a subset of the literature in these three categories and what is currently known about soiling. Several more comprehensive reviews of soiling literature have been put together. For a more detailed examination of the literature readers are referred to an article by Mani and Pillai [42], an article by Sarver and collaborators [57], and an article by Sayyah and collaborators [59]. The

following is an overview of the literature presented to help frame the work that is done in this dissertation in the context of other work that has been done in the field, motivate the work that is done here, and provide a foundation for the methods used in this work. Specifically studies that represent significant improvements in understanding of soiling are presented, as well as studies that are most applicable to the ambient studies that are conducted in this dissertation.

2.1.1 Category One: How Bad Is It?

The first study of soiling was done by Hottel and Woertz in Cambridge Massachusetts in 1942, and found that soiling accounted for at most a 4.2% reduction in energy loss for a solar hot water system, and on average around 1% loss [32]. These results were found by comparing actual and theoretical output of solar hot water system mounted on the roof of a test building. This study was by far the first and seems to have set the stage for the thought, initially, that soiling was not a significant factor in solar energy harvesting. More recent studies, have seen much higher losses due to soiling. A study published in 1974 by Garg found transmission losses of up to 20% after 30 days for a horizontally deployed glass plate in Roorkee India, an average soiling rate (or increase of losses caused by soiling) of 0.67%/day [25]. Another study, published in 1978 by Sayigh, found 27% losses after two months for an uncleaned flat plate solar hot water heater compared to an identical cleaned collector when both were deployed horizontally in Riyadh Saudi Arabia [58]. These, and other similar studies, have shown that large losses from soiling are possible. Since then results have been published for many locations and results have covered a wide range of losses. A study by Nahar and Gupta in the Thar desert in India found transmission losses averaging as high as 7.12%, for horizontally deployed PVC samples, and as low as 1.36%, for vertically deployed glass, when a variety of tilt angles and materials were investigated [46]. Losses of 14% have been seen in Bangkok Thailand [43], and over 25% in Minia Egypt [30], both after just 30 days. Other studies conducted in less dusty locations have seen lower losses caused by soiling. A study by Kimber and collaborators found average losses between 1 and 6% for real systems when compared with theoretical outputs at a variety of locations across California [37]. A study by Appels and collaborators in Belgium found transmission losses of less than 6% for horizontally deployed glass plates, and even lower losses for tilted samples after two months

[3].

These studies, and many others, demonstrate both the severity of the problem, but also the variability. Location is clearly a factor, but beyond that the only factors that are explored are surface characteristics (plastic compared with glass), and angle of deployment. While these factors seem capable of explaining differences caused by these factors they are not widely generalizable to other locations, and do not explain the processes responsible for these differences. Category one primarily set the stage for later studies in the other two categories of research in soiling. They provide justification for continued research into soiling by demonstrating its large effect and variability, but are not able to provide details on why or how soiling varies in any generalized terms.

2.1.2 Category Two: What Factors Are Important? - Laboratory Studies

Many laboratory studies have been conducted to examine individual factors, or groups of factors, that may affect soiling. One such factor is ambient particle concentration. Not surprisingly a study conducted by Goosens and Kerschaever found that increasing particle concentrations that a PV module was exposed to in a wind tunnel decreased the power output from that module [28]. However this study doesn't provide any quantification of the relationship between particle concentration and losses. Overall this research indicates that increasing particle concentrations increases soiling losses and provides evidence that this factor should be examined in future soiling studies.

Another factor that has been examined in laboratory studies is wind speed. Wind speed does not have as large an effect on soiling losses as does particle concentration however, the study by Goosens and Kerschever, cited above, did find that increasing the wind speed in the wind tunnel experiment, for the same particle concentrations deposited on the solar panel, decreased the losses [28]. They hypothesize that this is due to ripples and patterning forming at higher wind speeds that allowed particles to pile on top of each other more than at lower wind speeds, but again quantification of the results is not done.

Deposited particle size and chemistry can be hard to differentiate as different particle chemistries typically have different sizes. Many studies have looked at the chemistry of deposited particles by either depositing a single type of particle, or a mixture of particles on glass or PV panels and measuring the

transmission or the power output. A study by Kaldellis and Kapsali looked at the effect of red soil, limestone, and fly ash, and found marked differences between the three with fly ash having the greatest impact on performance (per mass deposited), and red soil having the least [34]. Another study by Burton and King examined differing ratios of Arizona road dust and soot, and found that the higher the concentration of soot the greater the impact on transmission (per mass deposited) [8]. For these studies, size is not examined, and it is unknown how much of the difference is due to varying sizes, and how much is due to varying optical properties of the particles. While chemistry and size seem to be important factors how this relates to the ambient environment is not know.

Size, independently, has been shown to be a significant factor in soiling losses per mass deposited. A study by El-Shobokshy and Hussein found that Limestone particles of 80 µm, 60 µm, and 50 µm in mean particle diameter created very different power outputs for the same mass deposited on a PV panel [20]. This study also examined 10 µm diameter cement particles, and 5 µm carbon particles and found the same trend [20], but the lack of numerical relationship development makes applying these results broadly difficult.

2.1.3 Category Three: How Do We Generalize? - Field and Modeling Studies

Field based studies that go beyond reporting the amount of soiling observed fall into the third category of current soiling studies. This is the broadest group, and includes studies that examine a broad range of factors. One of the most influential factors that has been examined is mass accumulation. A relationship between mass of accumulated particulates, and the loss of transmission for samples deployed in the ambient environment was first shown by Hegazy in 2001 for samples collected in Minia Egypt. This paper fit an error function equation to the relationship:

$$\Delta\tau = 34.37erf(0.17\omega^{0.8473}) \tag{2.1}$$

where $\Delta\tau$ is the transmission loss in percent and ω is the mass of deposited particulates in g/m^2. This equation is shown to be valid between 0 and 10 g/m^2 [30]. A study in 2006 by Elminir found a similar relationship for samples collected in Cairo Egypt:

$$\Delta\tau = 0.0381\omega^4 - 0.8626\omega^3 + 6.4143\omega^2 - 15.051\omega + 16.769 \tag{2.2}$$

for dust accumulation between 1.5 and 9 g/m^2 [21]. These studies are some of the most useful field studies that have generalized their results, because they show clear and similar trends and have developed quantitative relationships. This strong correlation between mass accumulation and transmission loss makes the use of a simple equation an easy way to generalize soiling loss results. However predicting mass accumulation is not done, and this step may be difficult. Additionally the applicability of these results beyond where they were developed is not known, and how they may change with changing sources of particulates or ambient environments has not been explored.

Meteorological parameters have been shown to affect soiling losses in the ambient environment. A study in 2003 found that wind speed and direction, relative to the direction that glass windows were facing, was important in light attenuation [64]. A study in 2014 by Ghazi and Ip found that humidity was a contributing factor to soiling losses, with increasing humidity increasing soiling [26]. While these studies are not as significant or broadly useful as other category three studies, they have attempted to find variables that predict soiling losses, and have shown some success which is why they are placed in this category. However all of these studies have failed to quantitatively generalize their results.

Finally, two studies are included in this category for presenting frameworks for soiling models. The first model, presented by Kimber and collaborators, proposes a soiling model that allows for precipitation above a threshold to completely clean panels, and a pre-determined soiling rate to be constantly applied after a cleaning. In the implementation of the model they allowed for a grace period, of a pre-determined number of days, where negligible soiling occurs after rain. When these elements are combined a saw-tooth type soiling loss estimation plot over time is developed which can be combined with other solar energy harvesting models to understand soiling losses [37]. For locations in California this model has been shown to give good results [11]. This framework is useful for thinking about soiling but requires many parameters that are not known including soiling rate, grace period, and the amount of precipitation necessary for cleaning.

The second study that provides a model for soiling was presented by Qasem and collaborators. This model uses meteorological, PV system, and air quality inputs to estimate soiling over time. This model allows for variable soiling rates, and predicts total PV system output, as opposed to just soiling loss [50]. However the details of the model are unclear, and validation has only been done in one very dusty location,

Kuwait.

From the previous research many things about soiling are understood and many contributing factors have been identified. The model proposed by Kimber and collaborators provides a framework for a soiling model but requires knowing the grace period, precipitation effects, and most importantly the soiling rate. The model developed by Qasem and collaborators attempts to fill this gap by providing understanding of soiling rates, but lacks the details and validation to be used widely. There is still a need to be able to predict soiling rates at any location, using routinely collected data.

The remainder of this chapter will cover the development of methods used in this dissertation. Several experiments are presented to provide justification of the methods selected, more details on these experiments can be found in Chapter 6. The discussion here is aimed at providing a background and framework for understanding results that come later and the strengths and limitations of the methods used throughout the dissertation.

2.2 Method Development

As seen above there are many factors that can drive soiling. These factors include, the amount and type of particulates in the atmosphere, or even more generally the type and quantity of sources of particulates, meteorological conditions including wind, humidity, and precipitation, and panel orientation and surface characteristics. In conducting soiling research it is important to understand the factors that can affect soiling, and control for, or identify, those factors. The overarching goal of the experiments discussed in this dissertation are to generate results that are applicable to actual solar energy systems, and generalize beyond a single location. The focus of this research is to develop a method to predict soiling rates (or the loss caused by soiling per some unit in time). The following discussion of method development highlights some key experimental design parameters and the reason for their selection.

2.2.1 Samples

Previous studies have followed one of two routes for collecting samples. They either use actual PV or solar hot water panels, or they use surrogate surfaces, glass or plastic pieces that are similar to those used as the cover plates for PV or solar hot water application. The advantages of using actual panels is that they more accurately represent the system - panels get hot during the day, may have interesting edge effects or respond to uneven soiling in certain ways - and using panels accounts for these factors. However PV panels can degrade over time which makes collecting accurate loss measurements difficult, additionally different types of panels have different responses to varying light spectrum, soiling non-uniformity, and temperature which may make results not widely generalizable across technologies, and collecting and measuring the deposited dust is much more challenging. Using surrogate surfaces has the advantage of allowing for easy collection and storage of surfaces and easy measurements that can be generalized (e.g. transmission measurements can be taken using a spectroradiometer which allows for measuring transmission across a broad spectrum which can allow for application to any technology). Surrogate surfaces do not necessarily allow for understanding panel geometry or heat effects, or permanent degradation of panels that may occur due to soiling. Because of the overarching goal of this research to generalize soiling, surrogate surfaces were used instead of panels. In addition to this method being more generalizable, it plays to the strengths and tools that exist in the air-quality lab where this research was conducted.

PV panels are typically covered with a tempered glass surface, and for this reason the original samples used in this study were 10 cm by 10cm by 0.48 cm tempered glass plates that were made in the glass shop at the University of Colorado Boulder. When additional samples were needed 10 cm by 10 cm by 0.32 cm transparent conductive oxide glass, available from Pilkington (NSG TEC^{TM}), was used. This is glass that is actually used in many thin film PV applications. When smaller samples were needed 5 cm by 6 cm by 0.32 cm low iron glass was purchased from Swift Glass (Elmira Heights, New York). While these are different types of glass, they were all seen to have similar deposition and soiling results. Previous studies have shown that flat surfaces tend to accumulate very similar amounts of particulates [27], providing additional evidence that these samples should yield similar soiling results, and also providing evidence that the

results presented in this dissertation should be broadly applicable to varying solar energy systems so long as they use a flat surface.

2.2.2 Wet and Dry Deposition

Particles can deposit on the surface of a solar panel in one of two ways. The first is by dry deposition, or the accumulation of particles without precipitation. This is particles either 'falling' out of the air by gravitational settling, or arriving at the surface by diffusion or impaction. The second is by wet deposition, when rain or other precipitation collects particles from the atmosphere and brings them to the surface where they are deposited. In soiling, precipitation can also have a cleaning effect by washing away deposited particles. Previous studies have found cleaning of PV systems with precipitation, but the actual amount of precipitation necessary varys widely. A study by Kimber and collaborators in 2006 found that 0.4 inches of rain was necessary, but suggested that precipitation rate be examined [37]. Caron and Littmann found 0.04 inches of rain to be effective [11] and Garcia collaborators found 0.16-0.2 inches of rain was necessary [24]. Meji and Kleissl actually found an increase in soiling with less than 0.1 inches of rain [44]. It is unknown why such varying results are found.

To examine the effects of precipitation, identical samples were exposed side-by-side at a site in Commerce City, Colorado. One set of samples was covered with a roof to prevent wet deposition or cleaning by precipitation, and the other was uncovered to allow for cleaning and wet deposition. A comparison between the mass accumulation on the two samples is shown in Figure 2.1. These samples span more than a year, beginning in March of 2013 and running through September of 2014. This figure shows that the covered set-up regularly accumulates more mass than the uncovered set-up. This indicates that at this location, rain is cleaning the set-ups and that wet deposition is not a significant contributor to mass accumulation, and is important for removing particles (or cleaning). Rain data was obtained from Denver International Airport weather station (KDEN) maintained by the National Oceanic and Atmospheric Administration (NOAA), and Figure 2.1 is also color coded for the time since the last 'significant' rain, where significant is taken as more than 0.05 inches of precipitation in one hour. The samples with the greatest difference between the covered and uncovered samples correspond with the most recent significant rain (and cleaning), while the remaining

samples were generally clustered just below the 1:1 line. More details on this experiment can be found in Chapter 6.

These results comparing precipitation affected and unaffected samples indicate that dry deposition is the primary source of particle deposition and that for predicting a soiling rate (or loss over time) dry deposition should be the primary consideration. Therefore the majority of the remaining experiments in this dissertation examine dry deposition, and do not account for precipitation effects.

To prevent cleaning or deposition by precipitation a roof was placed over all of the samples while they were deployed. The roof may decrease the accumulation of particulates on the surface by preventing them from reaching the surface. To reduce this effect the deposition of a particle with a 100 μm aerodynamic diameter depositing by gravitation settling was considered. The terminal velocity of this particle in the atmosphere is approximately 30 cm/sec. In Denver an analysis of micro variations in wind speed during calm or low wind speeds found a reasonable lowest wind speed of approximately 50 cm/sec. If we use a roof that is 122 cm by 122 cm (half of a full sheet of plywood) so that the farthest a sample can be from a side is 61 cm, then the roof needs to be approximately 37 cm above the sample to allow for large particles (up to 100 μm in aerodynamic diameter) to settle onto the samples in low wind conditions. The actual roofs were designed to be 67 cm above the samples, but with a slight tilt to allow water to run off for long term life of the sampling structure.

Figure 2.1 shows that the covered samples rarely accumulate more mass than the uncovered samples. In addition to this being caused by precipitation, this is an indication that the roof is not significantly affecting the mass of particles accumulating. This is difficult to prove because during no deployment time was there no rain, however the clustering below the 1:1 line indicates that the roof is not affecting deposition.

2.2.3 Ambient Particle Concentrations

Particles have to be suspended into the air in some manner in order to be deposited, and it therefore makes sense that the concentration of deposited particles will be related to the concentration of ambient particles in the atmosphere. Previous research has found this to be true [61], with actual dry deposition being also dependent on particle parameters (such as size, and density), ambient meteorological conditions

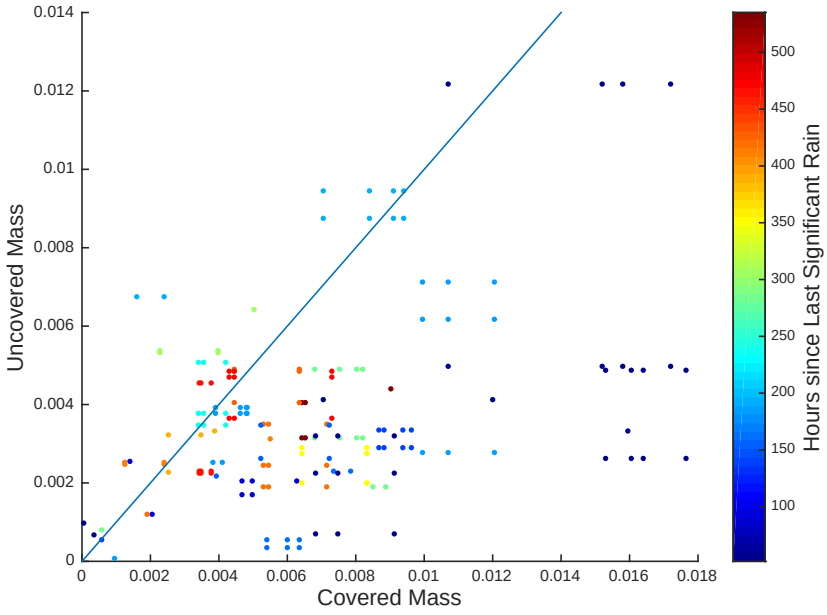

Figure 2.1: Comparison of mass accumulation on the samples with and without a roof.

(such as wind speed and temperature), and location and surface parameters (such as surface roughness). In a very basic form this is represented as:

$$m_{accumulated} = v_d * PM \tag{2.3}$$

where $m_{accumulated}$ is the mass of particles accumulated, v_d is the deposition velocity (where all the dependence on particles, surfaces, surrounding environment and meteorology happens), and PM is mass of ambient airborne particulates. In order to generalize the soiling results found, it makes sense that ambient particulates and meteorology should be measured.

There are many options available for measuring ambient particles, and the most important decision is which sizes of particles should be sampled. Deposition velocity is very size dependent, and ideal sampling would allow for collection of the ambient particle size distribution, however this can be quiet costly. Two different approaches to sampling particles are taken in these experiments. The first is to use a dichotomous filter sampler, that has previously been developed and validated [12] . This sampler simultaneously samples both $PM_{2.5}$, or particles with aerodynamic diameter smaller than 2.5 µm, and $PM_{10\text{-}2.5}$, or particles with aerodynamic diameters between 10 µm and 2.5 µm. These can be combined to obtain a PM_{10} measurement as well. The advantages to using this system are that it gives some information about the size distribution by collecting two sizes of particles, $PM_{2.5}$ and PM_{10}, which are widely collected in the United States due to their regulation under the Clean Air Act, and that they have a reliable and known size cut. The second samplers that are used in this study are Hi-Volume Total Suspended Particulate (TSP) samplers. These samplers collect roughly PM_{100} with variation happening with wind and pressure changes. The advantage to using these samplers is that they collect many more of the ambient particulates, which much more closely correspond to what is depositing, and the majority of the particles that contribute to mass accumulation. Additionally these samplers are much cheaper both to purchase and to maintain.

Collecting meteorological data was not done explicitly in this work, and instead sites were chosen where active meteorological samplers were already in place. This was a key factor in choosing site locations.

2.2.4 Sample Arrangement

Solar energy systems are installed at varying angles based on latitude, environment, and ease of installation. Previous soiling studies have seen that angle plays a significant role in soiling [46] [30] [21] [29] [3]. This topic has been widely covered in previous research and this experiment deployed samples at several angles only for cursory understanding of angle of deployment. In these experiments samples were deployed horizontally to examine maximum soiling, and establish a baseline soiling, 40° to examine the situation for panels tilted at an ideal angle in central Colorado and to provide one angle of comparison for tilted panels, and also at 180° to examine the effect that deposition by diffusion has in comparison to deposition by gravitational settling. In theory, particles that would deposit by gravitational settling would deposit on the horizontal and 40° samples, but not on the 180° samples whereas particles that deposit by diffusion would deposit equally on all three samples. This sample methodology allows for the examination of different dry deposition methods, and comparison with systems titled at latitude in the local area Colorado Front Range area. Finally two samples were deployed horizontally to allow for duplicate samples to be collected. This can be very valuable in examining uncertainty, and experimental error.

Another important factor in deploying sampling equipment, is how far away things can be. In these experiments the sampling equipment was placed between 2 and 10 meters apart. This should reduce sampling equipment having a direct impact on each other, which could be the case if they were placed immediately adjacent, but allows them to not be exposed to different conditions. The exact spacing needed can be hard to validate thoroughly, but we can examine the scales on which soiling varies significantly. To do this we can compare the mass accumulation on samples that are co-deployed similar to those when examining wet precipitation, but where both are covered with a roof. This is shown as the blue dots in Figure 2.2. The 1:1 is also plotted to show that there is no significant (p=0.2) or systematic difference between the two measurements. The red dots in this figure represent a changing of the configuration of sampling to attempt to affect small scale meteorology, but again the difference was not significant (p=0.2) and systematic differences were not seen between the samples. The red data have lower mass accumulation that the majority of the blue data because these samples used the smaller 5 cm by 6 cm samples instead of the

larger 10 cm by 10 cm samples. More details about this experiment can be found in Chapter 6.

Beyond this experiment the results shown in Figure 2.2 indicate that soiling has negligible variability on the meter scale. This provides evidence that we can use a single soiling value for an entire solar energy system, and that small local changes to environment are likely to have a negligible effect on soiling (this would include things like inverters, additional strings of panels, or chimneys (unless they are emitting particles). Additionally this justifies having samplers within several meters of each other due to the lack of small scale variations in soiling.

2.3 Conclusion

The method development presented here provides the framework for sampling that is used in subsequent chapters. There are many factors that affect soiling, but the methodology used in this study is designed to examine many of the most important ones. Validation experiments indicate that dry deposition is the dominant factor for particle accumulation and soiling in the Front Range of Colorado, and the method developed and used in this dissertation is designed to examine dry deposition.

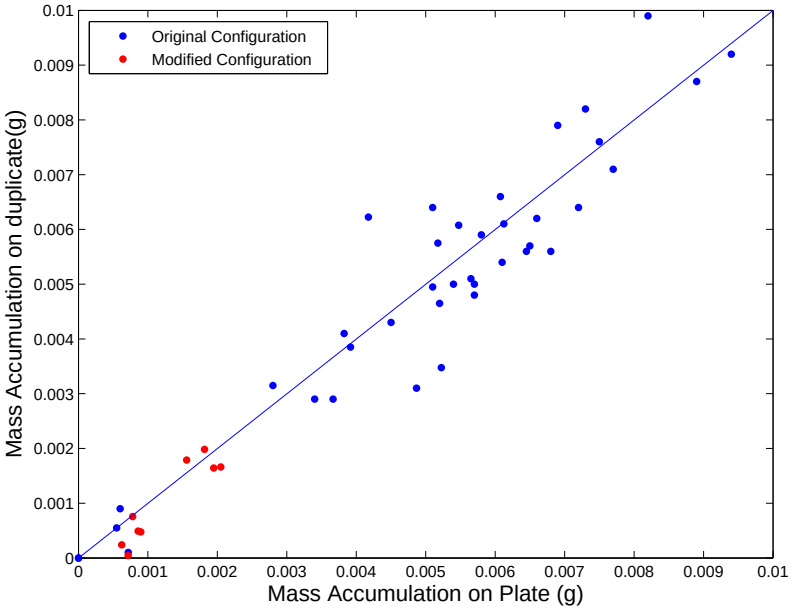

Figure 2.2: Comparison of mass accumulation of co-located samples. The blue data are from identically deployed samples, and the red data are from one set-up being slightly modified in an attempt to more significantly change the micrometeorology seen by the two set-ups.

Chapter 3

NATURAL SOILING OF PHOTOVOLTAIC COVER PLATES AND THE IMPACT ON TRANSMISSION

Liza Boyle, Holly Flinchpaugh, Michael P. Hannigan

Department of Mechanical Engineering

University of Colorado, Boulder, Colorado, USA

3.1 Abstract

Photovoltaic (PV) and other solar energy systems are known to lose efficiency as a result of the accumulation of dust on the surface of the panels. These losses have been difficult to predict and vary widely across geographical regions. In this work dust is allowed to naturally accumulate on PV cover plates at two sites in the Front Range of Colorado. Mass accumulation rates are measured, as well as light transmission reduction. Mass accumulation rates between 1 and 50 mg/m^2/day were observed and varied with time of year, location, and angle of deployment. Total mass accumulations up to 2 g/m^2 were observed after 1-5 week deployments. Transmission reductions up to 11% were found. Transmission varied linearly with the mass of dust accumulated and it was not affected by the angle of incidence of incoming irradiance, angle of deployment of the panel, or location of deployment. Light transmission was found to be reduced by 4.1% for every g/m^2 of dust accumulated on the PV cover plate; this relationship was derived from a linear regression of the data. A linear fit to the data is shown to be sufficient, and the uncertainties of the measurements and calculations are found.

3.2 Introduction and Background

Renewable energy sources are gaining prominence around the globe as energy demand increases, costs of fossil and other non-renewable fuels increase, and issues including climate change and the health effects of poor air quality influence energy production decisions. Renewable energy sources are estimated to have accounted for 16.7% of all energy consumption in 2010 [53]. Solar energy, in particular, is growing at an extraordinary rate with an increase of 75% in the installed photovoltaic (PV) capacity in 2010 (from 40 GW to 70 GW) [53]. The installation of PV is often hindered by economic concerns that are being constantly addressed by increasing panel efficiency and reducing panel cost. However, little research has been done to examine the performance of panels once they have been deployed.

Dust accumulation on the surface of PV and solar heat collector panels as well as Concentrating Solar Power (CSP) mirrors has been reported to create losses of between < 1 [32] and 88 [25] percent under ambient conditions. This wide range has been attributed to tilt angle [46] [54], location [11], and cleaning factors [54] [24]. The first published study of natural dust accumulation on panels found losses of up to 4.2%, but averages of less than 1% for solar heat collectors in Cambridge, Massachusetts [32]. Similar results were found by Nahar and Gupta [46] in India with transmission losses of 1-6% per month for glass samples when tilted from 0° to 90°. However, more recent studies in dustier locations in Egypt found transmission losses up to 25% [30] after one month and 28% [21] after seven months. In Saudi Arabia, Said found a 7% and an 11% loss per month over varying length of tests [55], indicating a significantly larger loss. These studies, while useful in developing an understanding of the problem caused by particle deposition do not help to explain what might happen in locations besides where they were conducted, or present ideas for mitigation strategies; research on the processes involved is needed to take that step.

Those critical processes are (1) airborne particle deposition onto the glazing, and (2) light transmission through deposited particles. Some studies have investigated one or both of these processes in more controlled environments. Using a wind tunnel Goossens and Kerschaever found that increasing the airborne concentration of particulates decreased the power output of a PV cell, and decreasing the wind speed decreased the power output of a PV cell [28]. El-Shobokshy and collaborators deposited varying

amounts of sized limestone, cement, and carbon and showed that for the same amount of deposited mass smaller particles decrease the power output from a PV panel more than larger particles [20]. These studies provide useful information about the relationships between airborne particles, environmental parameters, deposited particles, and power loss but real world studies are needed to improve their utility.

A handful of studies have focused on the process of light transmission through deposited particles, with the focus on developing a relationship between deposited mass and light transmission or power loss. Al-Hasan created a theoretical relationship between the mass of particles deposited on the surface and the amount of light transmitted [2], however this relationship requires information on the number and size of particles deposited on the surface, which is rarely known. Mastekvayeva used a curve fit to experimental data to determine the relationship between dust deposition and light transmission, however this was only valid in the heavily deposited range of 5 g/m^2 to 15 g/m^2 [43] which is observed only in the dustiest locations. Elminir and co-workers as well as Hegazy both conducted experiments in Egypt to quantify loss as a function of the amount of dust deposited. Elminir and co-workers developed the relationship:

$$\Delta\tau = 0.0381\omega^4 - 0.8626\omega^3 + 6.4143\omega^2 - 15.051\omega + 16.769 \tag{3.1}$$

where $\Delta\tau$ is the transmission loss in percent and ω is the dust deposition in g/m^2, by curve fitting data [21]. This relationship was valid between 1.5< ω < 9 g/m^2 which is useful for large deposition values, however deposition values less than 1.5 g/m^2 are common in the Colorado area, and likely many other parts of the world. Hegazy used a similar method to develop a more general equation:

$$\Delta\tau = 34.37erf(0.17\omega^{0.8473}) \tag{3.2}$$

(2) which is valid over 0 < ω < 10 g/m^2 [30]. While these studies were similar in the location and amount of material that was deposited, they resulted in different relationships, and it is unknown how these equations relate to other locations.

Other parameters in addition to the amount of dust deposited may affect light transmission. The angle of incidence of incoming light could affect the amount of light transmitted through the accumulated dust [2]. The wind speed at which dust deposits effects how much light is transmitted likely caused by ripples being formed when dust deposits at higher wind speeds [28]. The surface or glazing on which

the dust accumulates may affect both how the dust accumulates, and light transmission [45]. It has been theorized that the airborne particulate chemistry is important, however has not been demonstrated in the real world [34].

This paper will take a broader process-level approach to the problem of dust accumulation and its resulting impact on light transmission. First, mass accumulation of particles will be examined. Then, the mass accumulation effect on light transmission will be explored so that the deposition values can be related to solar energy loss. Additionally, uncertainty in all measurements and calculations are analyzed to validate and provide context for the results.

3.3 Methods

3.3.1 General Approach

Glass plates, similar to those used as cover plates for solar energy technologies were exposed to the ambient atmosphere in two locations in the Front Range of Colorado. At each location the plates were deployed at angles of 0°, 40°, and 180° from the horizontal. The plates were covered with a roof that minimized precipitation impacts but still allowed ambient particle deposition. The plates were weighed before and after being deployed to find the mass deposited on the plates, and the transmission of all plates was taken using an ASD Inc. Field Spec Pro 2 spectroradiometer.

3.3.2 Measurements and Locations

Two sites in the Colorado Front Range were used for this study. The first was on the roof of a one-story elementary school in Commerce City, Colorado, approximately 10 km northeast of downtown Denver. This site was located in a mixed industrial and residential area with many sources nearby including one major freeway passing 0.6 km to the northwest, and a second major freeway just over 1.5 km to the south-west. Additionally there was a 611 MW coal fired power plant which was being partially decommissioned for conversion to natural gas over the time span of these measurements, and a 98,000 barrel per day oil refinery 3 km to the southwest, as well as an open pit gravel mine less than 0.7 km to the west. The second

site is located at the base of the Boulder Atmospheric Observatory tower in Erie, Colorado. This site is located in a rural area 30 km north of downtown Denver and is surrounded by open fields and farmland. The only other major source is a freeway 2 km to the east. Land use around both sites is shown in Table 3.1. Fractional land use by class was determined using the 2001 National Land Cover Dataset (NLCD; `http://www.mrlc.gov/nlcd2001`).

Table 3.1: Land use around the sites from the 2001 National Land Cover Dataset

Site	100m radius from site	1000m radius from site
Commerce City	Low Intensity Developed - 41% Developed, Open Space - 38% Medium Intensity Developed - 21%	Low Intensity Developed - 37% Medium Intensity Developed - 34% High Intensity Developed- 11% Open Water - 9% Developed, Open Space - 5% Woody Wetlands - 3% Deciduous Forest <1% Evergreen Forest <1% Emergent Herbaceous Wetland <1%
Erie	Herbaceous - 100%	Cultivated Crops - 79% Herbaceous - 14% Developed, Open Space - 5% Woody Wetlands - 1% Developed, Low Intensity <1% Barren Land <1% Deciduous Forest <1%

A meteorological monitoring site located between the two sampling locations, which has been in operation for more than 30 years, provided typical meteorological data for the region. The site was 16.8 km south of the Erie site and 10.5 km northwest of the Commerce City site. Average meteorological data for three decades from 1981 to 2010 are given in Table 3.2 [1]. The monthly average temperatures range from around freezing in winter to 23° C in the summer. Average total precipitation is 36.4 cm per year, and comes primarily in the spring and summer.

Table 3.2: 30 year averaged meteorological data for the Colorado Front Range from a site between the two field sites used in this study.

	Average Precipitation (cm)	Average Daily Minimum Temp (° C)	Average Daily Temp (° C)	Average Daily Maximum Temp (° C)
Jan	0.94	-7.4	0.9	9.2
Feb	0.94	-6.4	1.9	10.4
Mar	3.05	-2.2	6.0	14.2
Apr	4.67	1.4	9.7	17.9
May	5.61	6.8	15.1	23.3
Jun	4.24	11.6	20.5	29.4
Jul	4.75	14.5	23.8	33.2
Aug	3.89	13.9	22.9	31.8
Sep	2.57	8.9	18.1	27.2
Oct	2.46	2.8	11.4	20.1
Nov	1.88	-3.1	5.1	13.2
Dec	1.42	-7.7	0.3	8.3

3.4 Description of Measurements

3.4.1 Measurement Locations

In Commerce City two deposition set-ups were deployed, and in Erie one deposition set-up was deployed. For each of these set-ups, four identical plates were deployed. Over the course of the measurements described here two types of plates were used. The first were 10 cm x 10 cm x 0.48 cm tempered glass plates with a mean square surface roughness of 1.06 nm and 2.18 nm for the two sides found using atomic force microscopy (AFM). The second were 10 cm x 10 cm x 0.32 cm transparent conductive oxide glass available from Pilkington (NSG TEC^{TM}) with a mean square surface roughness of 2.7 nm and 15.2 nm for the two sides, obtained using AFM. In general the less rough side was exposed to the environment for soiling, however this was not always controlled for and no significant difference in results was found depending on which side of the plate was exposed. For a subset of weeks, the two plate types were both deployed to investigate if the material properties differentially impacted particle deposition. The two types of plates were found to not vary statistically in mass accumulation (N=18, p=0.6229). In each set-up two plates were deployed horizontally, labeled as East and West to distinguish the two plates, one plate was deployed with an angle of 40° from the horizontal and pointed in a southward direction, and a fourth plate

was deployed upside down (180° from the horizontal). The 40° inclination was chosen because it is the ideal tilt at the sites, which are at a 40° latitude. Half way through the sampling campaign 180° plates stopped being collected because they were not accumulating any significant mass. All of the plates were deployed 55 centimeters above the ground in acrylic and wood frames as seen in Figure 3.1. The plates were covered with a roof to prevent precipitation from reaching the plates. This prevented natural cleaning from precipitation, and allowed only the consideration of dry deposition. Soiling is a complex process, and the roof covering reduces the number of variables affecting soiling. This allows for the examination of only deposition and resuspension processes without precipitation effects. The plates were deployed for 1 to 5 weeks, with the typical deployment spanning 2 weeks. Plates are placed in deposition set-ups and removed by hand. Nitrile gloves were worn at all times when handling plates. Additionally the acrylic parts of the set-up that the plates contacted were cleaned with a mixture of ultra-pure water and isopropanol between each plate changing and small circles of pre-cleaned aluminum foil approximately 45 mm in diameter were used to separate the glass plates from the acrylic. Field blanks were used throughout all analysis. Field blanks were washed, weighed, and carried to the field in the same manner as all the samples. Additionally the field blanks were placed in the deposition set-ups and removed during deployment of plates. Field blanks were used separately for each site and were taken each time a new set of plates was deployed. Field blanks are used to correct for any contamination that may occur on the samples because of transport or storage, and incidental contamination from the deposition set-ups.

Before being deployed the plates were thoroughly cleaned. This was done by first soaking the plates in a solution of tap water and Alconox detergent for at least 24 hours and then rinsing the plates with ultrapure water, isopropyl alcohol and hexanes before baking the plates at 500° C for at least 12 hours. This reduces quantities of organics, and other contaminants from the plates. Additionally optical cleanliness is checked visually before each plate is used. The plates were transported in cleaned glass petri dishes covered with aluminum foil. The petri dishes were cleaned in the same manner as the plates. After being deployed the plates were stored in the same petri dishes in which they were transported and kept in a freezer at -20 $\pm$ 5° C to ensure that none of the deposited material volatilized during long-term storage.

Figure 3.1: Set-up used for the deployment of PV cover plates in this study. This is at the Erie site, the Commerce City site used two nearly identical set-ups placed side by side.

3.4.2 Mass Accumulation Measurements

The mass of the plates was measured before and after being deployed. Measurements were taken using a LabServe model BP210D microbalance with an accuracy of 0.1 mg. The microbalance is in an environmentally controlled chamber that allows the temperature and relative humidity to be controlled. The details of the chamber were described by Dutton and collaborators [19]. The plates were conditioned in this chamber for at least 24 hours to ensure that the plates were equilibrated to the chamber's temperature and relative humidity. Each plate was weighed at least twice. If the two mass measurements differed by more than 0.1 mg a third mass was taken. The average of the masses was used, and in the case of a third mass measurement, the two closest mass measurements were averaged to obtain the mass of the plate. Plates were weighed in batches of five or smaller and for each batch two control plates were weighed in the same manner. The control plates remained in the environmentally controlled chamber during the duration of the experiment and were used only in understanding variations in the scale. To account for any spurious noise in the scale, differences in the control plates were subtracted from the differences in the plate masses when calculating the mass accumulation on the plates. This was determined to be the correct approach when examining the variation in masses of the control plates as discussed in Section 3.5.3. Mass accumulation was calculated by:

$$m_{accumulated} = [m_{post} - m_{pre}]_{plate} - [m_{post} - m_{pre}]_{control} \tag{3.3}$$

and the mass accumulation rate on the plates is calculated by:

$$\dot{m}_{accumulated} = \frac{m_{accumulated}}{A_{plate}\Delta t} \tag{3.4}$$

where $\dot{m}_{accumulated}$ is the rate of mass accumulated on the plate, A_{plate} is the area of the plate, and Δt is the length of time the plates were deployed.

3.4.3 Transmission Measurements

Transmission tests were conducted on clear sky days (no cloud cover) at the Solar Radiation Research Laboratory at the National Renewable Energy Laboratory in Golden Colorado. Measurements were taken using an ASD Inc. Field Spec Pro 2 that was mounted horizontally. A measurement of the sky was

taken, and then immediately afterwards a measurement was taken with the glass deposition plate covering the sensor. Transmission is calculated by:

$$\tau = \frac{I_p}{I_s} \tag{3.5}$$

where τ is the transmission, I_p is the irradiance measured through the plate and I_s is the irradiance of the sky. For clean plates the transmission is the percentage of incoming irradiance that is reflected or absorbed by the plate. The reflection and absorption by the glass plate is dependent on incidence angle. Using basic optical theory we can correct for this reflection and absorption changes resulting from angle of incidence changes by the method presented by Duffie and Beckman [17] and summarized here. The angle of refraction in the glass was determined using Snell's law:

$$n_1 \sin(\Theta_1) = n_2 \sin(\Theta_2) \tag{3.6}$$

where n_1 and n_2 are the refractive indices of the air and glass respectively. A value of 1 was used for the refractive index of air, and a value of 1.5 was used for the refractive index of the glass [17]. These values are approximate and may vary with wavelength, but no need was seen in this analysis to account for this variance. Θ_1 is the angle of incidence, the zenith angle for this experiment, and Θ_2 is the angle of refraction through the glass. The absorption of light by the glass is calculated by:

$$\tau_a = exp\left(\frac{-KL}{\cos(\Theta_2)}\right) \tag{3.7}$$

where τ_a is the transmission reduction caused by the absorption, K is the extinction coefficient of the glass and L is the thickness of the plate. In this research the value of K is found by fitting the transmission reduction to zero for clean plates. Values of 15.7 and 11.7 were found for the two types of plates used. These values are within the range expected for glass. Finally the total transmission through the glass plate can be calculated by the following set of equations:

$$r_\perp = \frac{\sin^2(\Theta_2 - \Theta_1)}{\sin^2(\Theta_2 + \Theta_1)} \tag{3.8}$$

$$r_\parallel = \frac{\tan^2(\Theta_2 - \Theta_1)}{\tan^2(\Theta_2 + \Theta_1)} \tag{3.9}$$

$$\tau_{theoretical} = \frac{\tau_a}{2}\left(\frac{1-r_{\parallel}}{1+r_{\parallel}}\right)\left(\frac{1-r_{\parallel}^2}{1-(r_{\parallel}\tau_a)^2}\right) + \frac{\tau_a}{2}\left(\frac{1-r_{\perp}}{1+r_{\perp}}\right)\left(\frac{1-r_{\perp}^2}{1-(r_{\perp}\tau_a)^2}\right) \tag{3.10}$$

where $\tau_{theoretical}$ is the theoretical total transmission through a clean plate at a given incidence angle. Finally to eliminate the effect of angle of incidence from the transmission data the corrected transmission is calculated by:

$$\tau_{corrected} = \tau - (1 - \tau_{theoretical}) \tag{3.11}$$

where $\tau_{corrected}$ is the transmission where any optical losses in the plate caused by changes in angle of incidence have been corrected.

3.5 Results and Discussion

3.5.1 Mass Accumulation

Mass accumulation rates in this study were observed in the range of 1-50 mg/m^2/day. These rates are dependent on deployment location, angle of deployment, and time of year. Results for mass accumulation rate are summarized in Table 3.3. It is important to note that these are dry deposition numbers, which are not effected by precipitation. While there is little precipitation in the winter months in the Colorado Front Range, see Table 3.2, and deposited particulates are likely to accumulate, there would be significant cleaning in the spring and summer months with the higher precipitation that comes with afternoon rain and thunderstorms. Higher precipitation also increases soil moisture reducing airborne dust.

Table 3.3: Summary of mass accumulation data collected in this study

Location	Position	Number of Samples	Mass Accumulation Rate ($\pm$ STD) mg/m^2/day
Commerce City	0°	130	47.3 (18.1)
	40°	53	34.3(15.5)
	180°	15	3.1(1.6)
Erie	0°	18	19.3 (11.3)
	40°	5	12.3 (8.2)
	180°	1	1.6

Comparing these results, with the previously published results, we find wide variability in the mass accumulation rates. The results from our study are much lower than the 200-330 mg/m^2/day mass accu-

mulations on horizontal plates and 100-170 mg/m^2/day mass accumulations on plates tilted at 40° to the horizontal that were found in the middle of Egypt [30], and the 125-440 mg/m^2/day mass accumulation found on a plastic plate tilted at 15° in Bangkok, Thailand [43]. However, these results are in the same range as the 15-20 mg/m^2/day found in Athens, Greece [33]. Therefore, not surprisingly, particle deposition is dependent on location.

The mass accumulation at the Commerce City site was much higher than the mass accumulation at the Erie site. This was most likely a result of higher concentrations of airborne particulate matter at the Commerce City site than at the Erie site. Data published by Clements and collaborators shows that the concentrations of PM are higher at urban sites in Colorado (including the Commerce City site, labeled as Alsup in their research) than at more rural sites [13]. Table 3.1 shows that the Erie site is in a much more rural area than the Commerce City site. The concentrations seen by Clements and collaborators at the Commerce City site are also much higher than the concentrations seen by Duhl and collaborators at the Erie site [18]. Differences may also be caused by different chemistry at the two sites [12], different size distributions of airborne particulates, and different meteorological conditions.

Table 3.3 shows how the angle of collection impacts mass accumulation. The plates deployed at 0° collect the highest mass of particulates followed by the 40° plates, and the 180° plates collect the least mass. Comparing our results to basic deposition theory, there are two main methods of deposition: gravitational settling, where large heavy particles fall out of the air, and diffusion, where smaller particles pushed around by the air molecules hit and stick to a surface. We would expect that particles depositing via gravitational settling or diffusion would deposit on the 0° plates, where as only particles depositing via diffusion would accumulate on the 180° plates. Therefore we would expect the mass to be higher on the 0° plates, followed by the 40° plates (they have a lower footprint on which the settling particles can accumulate), and finally the 180° plates. The significantly lower accumulations on the 180° plates indicate that there is a very low mass of PM smaller than $\sim$1 µm in diameter accumulating on the plates.

Throughout this experiment there has been a trend with the highest mass accumulation rates occurring during the summer, and lower mass accumulation rates during the winter. During the second year of this campaign the measurements of mass accumulation showed higher variability, and there was signifi-

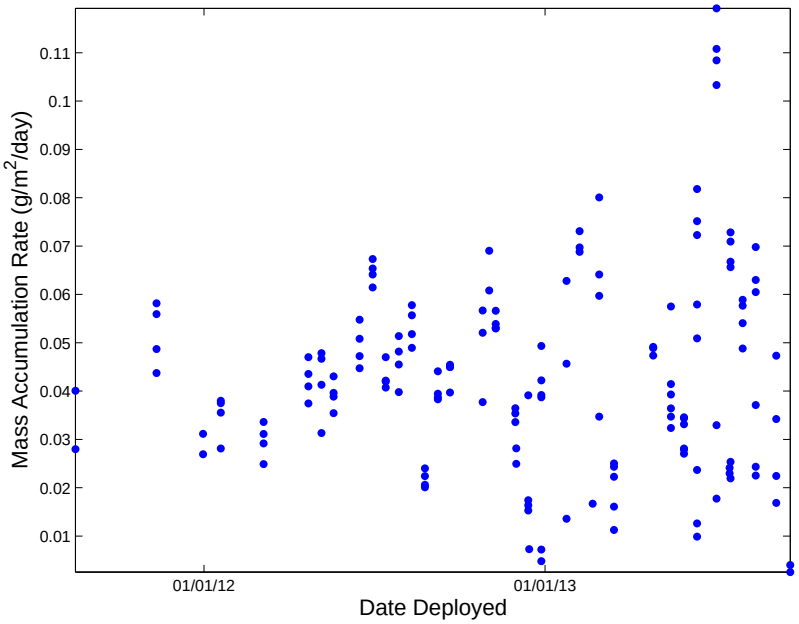

Figure 3.2: Rate of mass accumulation rate on horizontally deployed plates in mg/m^2/day plotted over the duration of the study. In the first year of deployment a clear seasonal trend is seen with a peak in the summer months. In the second year of the study this trend is less pronounced, and instead a wider range of mass accumulation rate values are seen.

cantly more spread in the mass accumulation rate particularly during the summer months.

3.5.2 Transmission

Transmission results were taken over the spectrum from 350 nm to 2500 nm wavelengths. However, the values above 1150 nm and below 375 nm were too variable and unrepeatable therefore only measurements from 375 nm to 1150 nm were considered here. A set of four transmission samples is shown in Figure 3.3. The samples shown were selected randomly, but are representative of what was seen for all plates.

Integrating over the set of wavelengths being considered, from 375 nm to 1150 nm, a single irradiance value is obtained. Then, using Equation 3.5 transmission was calculated. The transmission as a function of total mass accumulation on the plate is shown in Figure 3.4. Only data from the tempered glass plates, and not data from the conductive oxide glass samples is shown in Figure 3.4. There is significant spread in the data, largely caused by changes in the angle of incidence. Because samples are tested horizontally, we take the angle of incidence to be the zenith angle. There are several possible reasons for this angle dependence; one being increases in reflection and absorption by the glass plate as the angle of incidence angle increases as discussed in Section 3.4.3. The spread is reduced as seen in Figure 3.5, when this angle of incidence correction is applied by Equation 3.11.

Overall transmission measurements collected in this study do not show evidence of spectral dependence of naturally collected dust. However some of the samples do show spectral changes, particularly in the 600-800 nm wavelength range. An example is seen in Figure 3.3, where the 40° sample decreases much more quickly than any of the other lines in this region. These differences were not consistent across any of the samples, and do not correspond to the time they were deployed, angle of deployment, season, or any other factor examined here. These irregular differences may be an indication of difference in chemical composition of the deposited material, similar to that shown by Burton and King [8] or this could be an area where the sensor is not well calibrated, and changes seen in this range could be due to instrument uncertainty, similar to those seen by Qasem and collaborators [51]. Because this spectral irregularity is not reproducible and the change is small, we conclude that any spectral dependence on transmission is minor

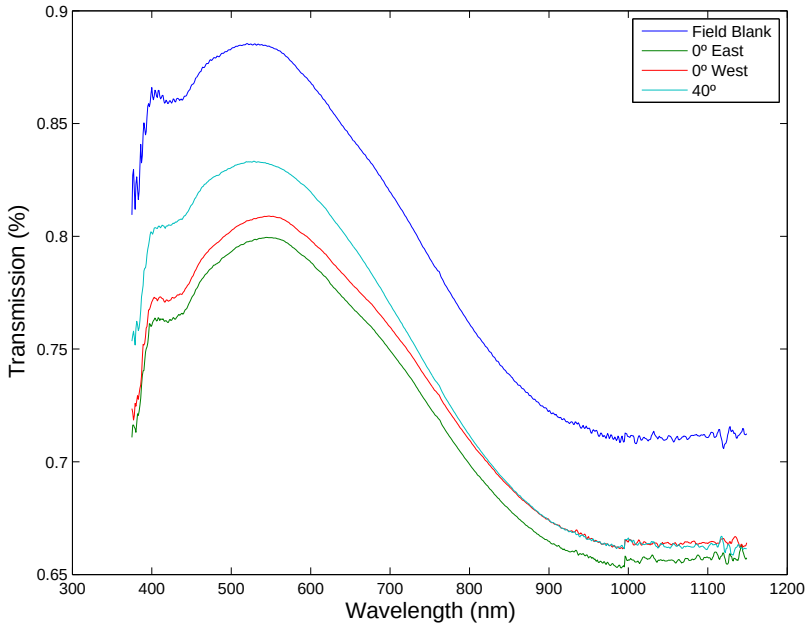

Figure 3.3: Average transmission through a random set of samples for each wavelength from 375nm to 1150nm. There are some differences in the transmission between samples, but these trends are not repeatable and do not seem to be influenced by any known variables.

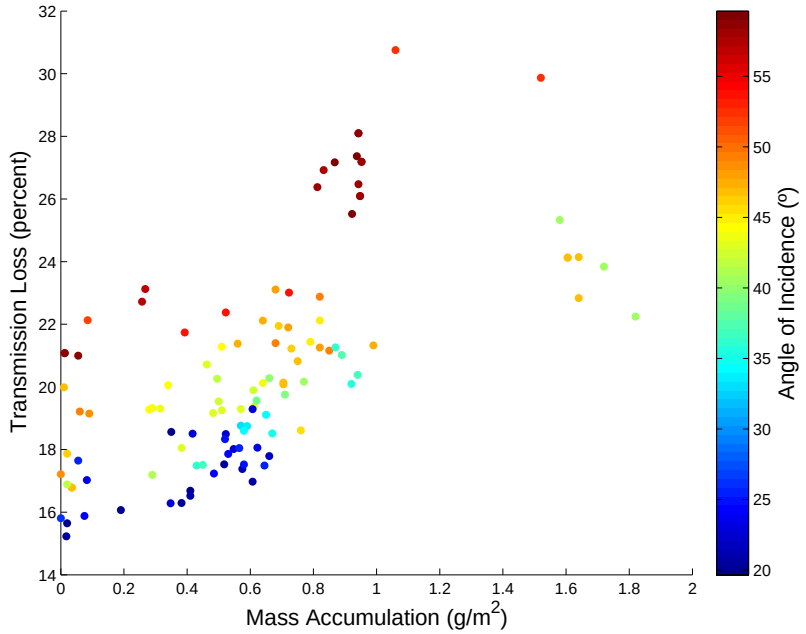

Figure 3.4: Transmission loss and mass accumulation for all tempered glass samples. The noticeable spread in the data is related to the angle of incidence of incoming light.

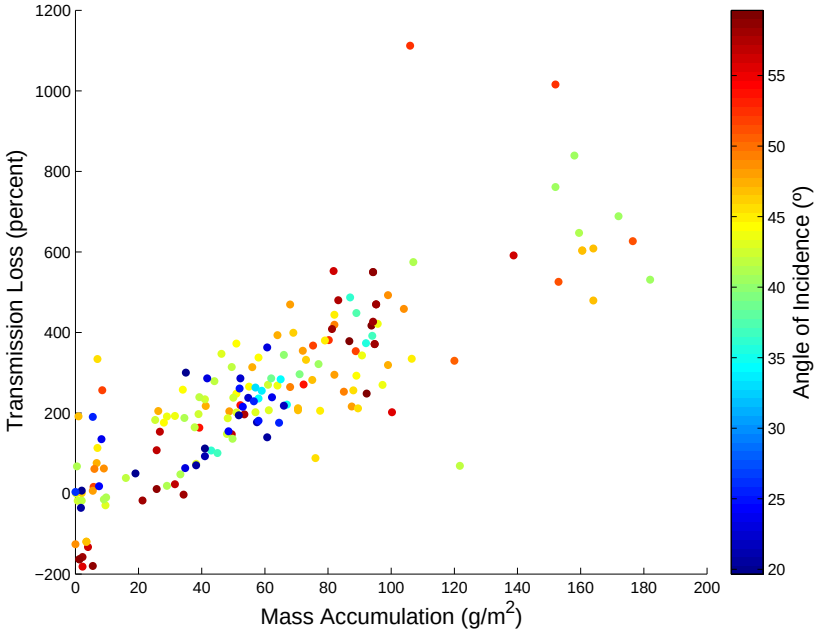

Figure 3.5: Corrected transmission loss and mass accumulation rate for all samples. There is significantly less spread in the data, and there is no longer a clear relationship with angle of incidence of incoming light.

and not a driving phenomenon. This indicates that we are in the geometric scattering regime, as apposed to Mie or Rayleigh scattering regime where there would be wavelength dependence. A lack of wavelength dependence will allow these results to be applied to a variety of solar energy applications in a straightforward manner regardless of the spectral dependence of the solar technology. This finding also supports the use of integrated transmission values as opposed to transmission values for individual wavelengths.

Previous researchers have found a dependence on incidence angle and the dust accumulated, beyond just the optical losses in the glass [2]. While this may initially seem true based on the data shown in Figure 3.4, correcting only for the reflection and absorption by the glass at different incidence angles by following the method outlined in Section 3.4.3 we were able to completely eliminate any incidence angle effect, as shown in Figure 3.5. While the samples collected so far in this study were not as highly soiled as those in other studies, they are realistic for natural soiling in this area of Colorado and other similar areas. The lack of incidence angle effect means that there is no time of day or day of year dependence on dust loss effects, and that tracking and stationary systems will see the same percentage loss for the same amount of accumulated dust.

Figure 3.5 shows a clear relationship between the amount of dust accumulated on the surface, and the transmission loss. At these soiling levels and transmission loss levels, a linear trend is sufficient to represent the data. The trend found in this work is:

$$\Delta\tau = 4.1\omega \tag{3.12}$$

For every g/m^2 of dust accumulated on the surface, 4.1% of the light transmission (and therefore energy production) is lost. This relationship is valid for angles of incidence between 20° and 60° and for dust accumulations in the range of 0 g/m^2 $\leq \omega \leq$ 2 g/m^2. This model was found to acceptably represent the data, with an R^2 of 0.69, and a residuals plot shown in Figure 3.6. The lack of trend in the residuals plot indicated that there was no additional trend in the data not captured in the simple linear model.

This linear relationship is similar to the two other relationships developed in previous research: by Hegazy , Equation 3.2, and by Elminir and collaborators, Equation 3.1 . Figure 3.7 compares these two previously published relationships to the one developed in this work. The trend line of Elminir and collaborators,

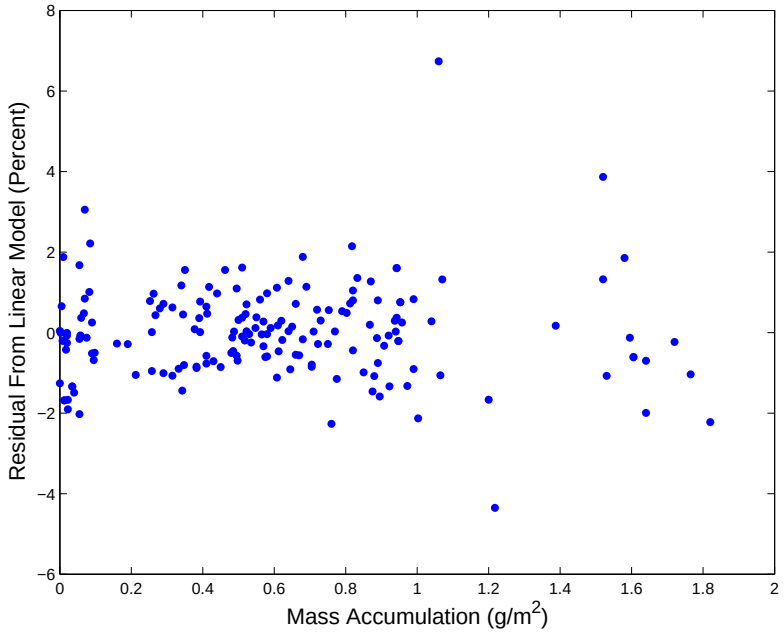

Figure 3.6: Residuals from linear model and mass accumulation. There are no obvious trends in the residuals indicating that the linear model developed in this work appropriately represents that collected data.

is only valid above 1.5 g/m^2, and agrees closely with the relationship found in this study. The relationship developed by Hegazy and collaborators is valid between mass accumulations of 0 and 10 g/m^2. While the Hegazy relationship appears to over estimate transmission loss as a function of mass accumulation, it is within a few percent, and follows the trend very well. While none of these relationships are exact matches, the similarity in values indicates that mass accumulation is the dominant factor in predicting transmission loss. Mass accumulation is more important than location, and likely more important than type of dust, although it is unknown how different the dust is between these locations.

3.5.3 Uncertainties and Errors

The error in mass measurements was found using the control samples. Since the control plates were weighed many times over a long period of time the uncertainty in these measurements can be used to find the error in mass measurements. The differences in mass of the control plates over many weighs are plotted in Figure 3.8 with the y-error. The average y-error over the range of observed mass differences was taken as the error in measurement of mass differences. This was used to calculate the error in measured mass accumulation following the procedure presented by Dutton and collaborators [19]. The error in mass was found to be 5.5x10^{-4} g. Figure 3.8 also shows that the masses of the plates were highly dependent on each other, justifying correction of the mass accumulation by Equation 3.3.

The error in the time deployed was estimated to be 15 minutes, based on the methods used for recording data and changing plates. Zenith angle uncertainty was determined to be 1°. Plate area was measured for a subset of 10 plates; the standard deviation of those measurements was used as an estimate of the error in the plate area and was found to be 0.2 cm^2. The error in the two types of plates was found to be nearly identical.

Using all of the uncertainties in our measurements and propagating the error for our mass accumulation rate calculations, we obtain a median error of 5.8 mg/m^2/day, compared with the y-error of co-deployed plates, which is 10.7 mg/m^2/day. This indicates that approximately half of the mass accumulation rate uncertainty is accounted for by uncertainties in mass measurements, deployment area, and time deployed, and the rest of the uncertainty was caused by environmental differences and deposition differences between

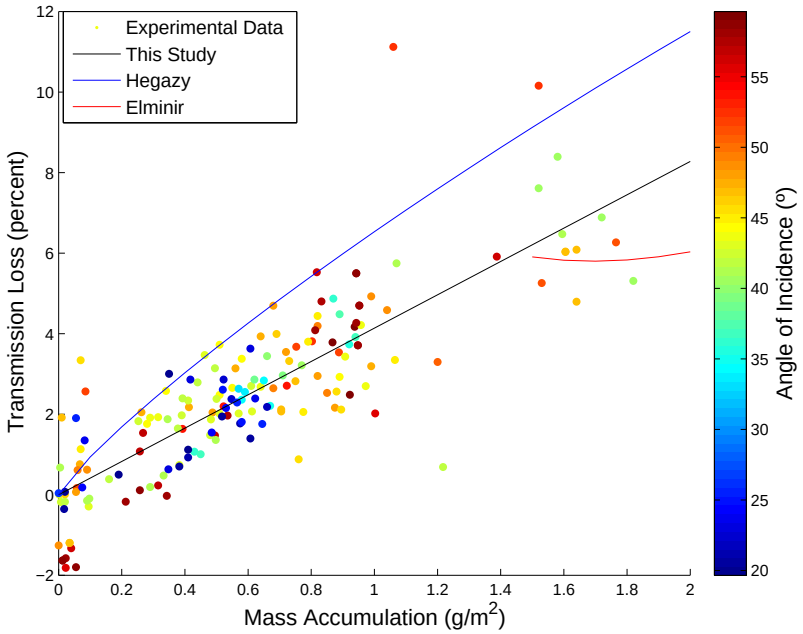

Figure 3.7: Comparison of relationships between mass accumulation and transmission loss. While there are differences between the three relationships presented here, they all seem to vary on the same scale and agree reasonably.

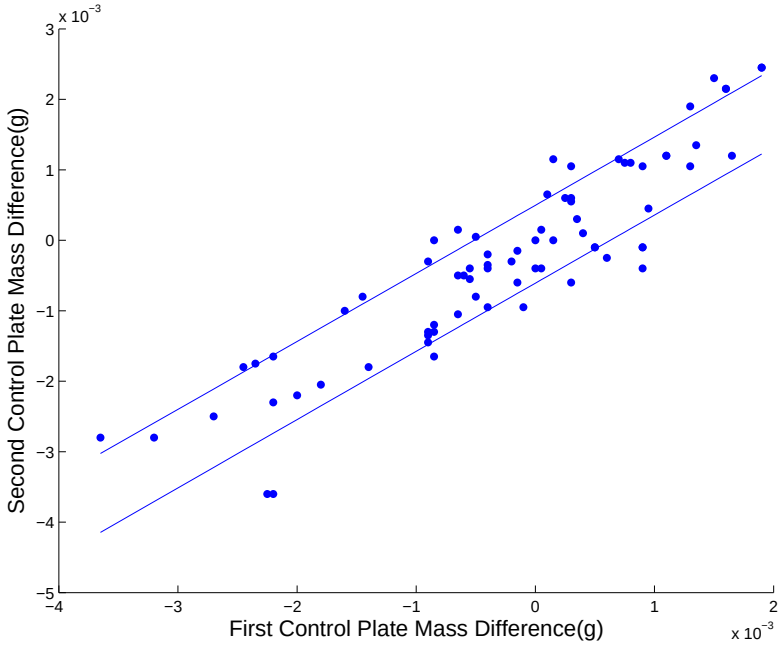

Figure 3.8: Mass uncertainty from control duplicates. Lines represent the y-error in the controls, taken as the error in the mass measurements.

the two plates. In the propagation of errors, the two dominant terms were the uncertainty in the area of the plate and the mass uncertainty.

The error in transmission measurements was calculated using three approaches. For the first approach we calculated the standard deviation of the measurements when at least three measurements were taken on a single plate; the uncertainty of the transmission measurements was 0.29%, based on 112 samples which is an indication solely of the error in the measurement. For the second approach the average transmission measurements from co-deployed plates were compared and an average uncertainty of 1.08% was found; this approach is shown in Figure 3.9. Finally propagation of errors through the transmission correction yielded an uncertainty of 1.36%, which is close to the y-error for the plates, indicating that we have accounted for all the sources of uncertainty in the transmission correction. Looking at all of the uncertainties in our calculations and re-creating Figure 3.5 with the uncertainties we obtain Figure 3.10.

3.6 Conclusion

As stated previously the residuals plot shows that there were no additional trends in the data not represented by the linear model, see Figure 3.6. Additionally a higher order model might be over-fitting data with higher uncertainty, as seen in Figure 3.10. Therefore a higher order fit is not appropriate and we recommend that future explorations of this relationship consider uncertainties of measurements in model creation. So far the model developed in this work, Equation 3.12, is consistent with other sites described in previous literature indicating that this relationship may be site independent, or applicable to a broad class of sites. As such we propose exploring more site types to investigate the application of this model more broadly. The sites examined in this work are in the same atmospheric environment and subjected to many of the same airborne particulates. Other studies were done in similar climactic regions (dry arid environments) and exploration of other climatic areas is needed. If this model is broadly applicable it will result in a relatively straightforward model for predicting solar energy yields across regions. While this research improves understanding of impacts that deposited particles have on light transmission and energy output, further understanding of the deposition process is needed. Additionally a better understanding of

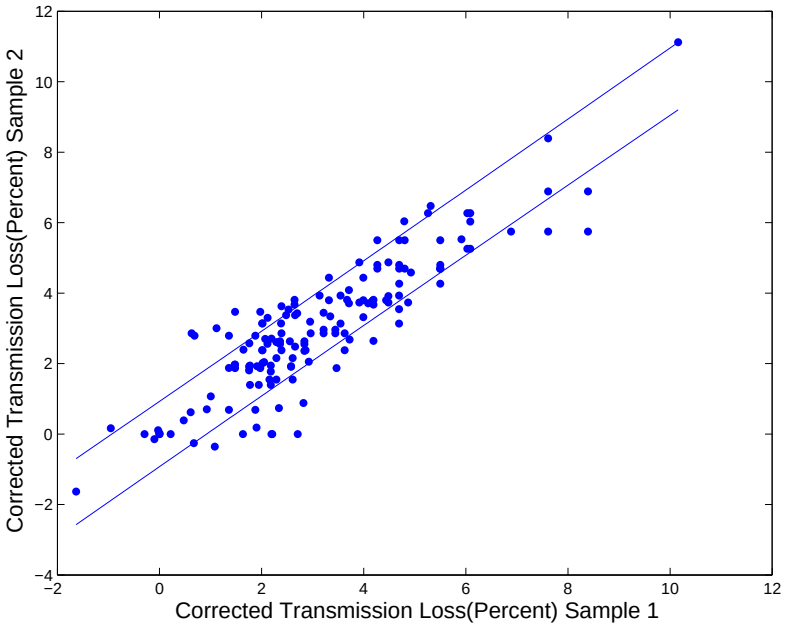

Figure 3.9: Transmission uncertainty duplicates. The middle line is the 1:1, and the secondary lines represent the y-error for co-deployed plates.

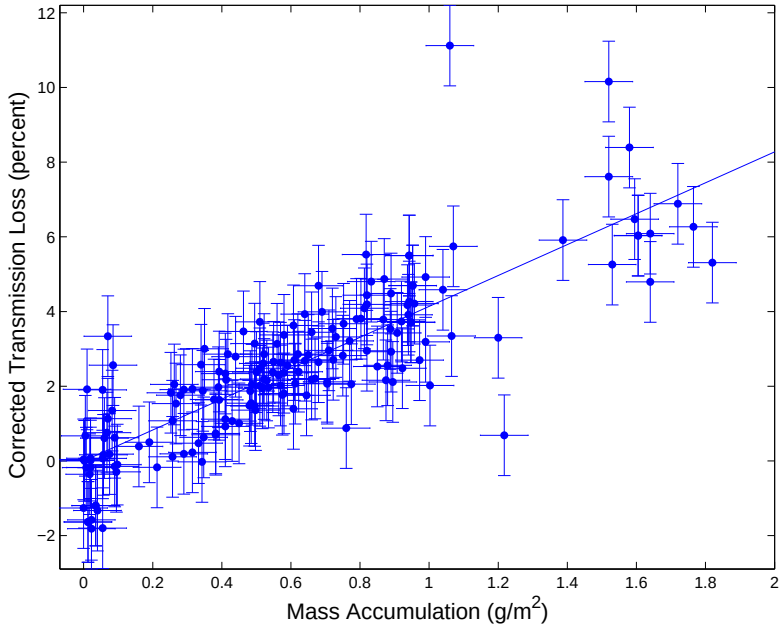

Figure 3.10: Transmission loss and mass accumulation for all samples with uncertainties. The linear relationship is included.

particle size, shape, and chemistry and their effect on deposition and transmission is needed. This is a major step that is necessary to improve predictions of energy loss due to dust accumulation.

3.7 Acknowledgements

This material is based upon work supported by the National Science Foundation Graduate Research Fellowship Program under Grant No. DGE 1144083. The authors would like to thank Daryl Myers, Afshin Andreas, and Aron Habte at the National Renewable Energy Laboratory for their help in collecting transmission measurements. The authors would also like to thank Zheng Zhang at the University of Colorado for help obtaining surface roughness measurements.

Chapter 4

ASSESSMENT OF PM DRY DEPOSITION ON SOLAR ENERGY HARVESTING SYSTEMS: MEASUREMENT - MODEL COMPARISON

Liza Boyle, Holly Flinchpaugh, Michael P. Hannigan

Department of Mechanical Engineering

University of Colorado, Boulder, Colorado, USA

4.1 Abstract

Soiling of solar energy systems, or the accumulation of particulate matter on their surface, can cause significant losses in energy conversion efficiency. However, predicting these losses is still not done, as no methods exist. Field measurements of mass accumulation and airborne PM_{10} were conducted for more than one year at two sites in the Front Range of Colorado with the objective of developing soiling prediction models. For this study, only dry deposition was examined. The two sites, despite having different PM_{10} concentrations have indistinguishable average effective deposition velocities of 2 cm/sec, although a large spread in the data was noted. These results are similar to results found in other deposition studies. The observed effective deposition velocities indicate that coarse particles are a dominant player in mass accumulation, and sampled airborne size distributions support this hypothesis. Using a model to calculate dry deposition yielded better agreement with deposition than a simple average deposition velocity data fit. This model combined with other research and models can be used for estimating average soiling rates and is most useful over long time scales especially months to years or longer.

4.2 Background and Motivation

The number of solar energy installations is growing rapidly [53]. This renewable energy has the potential to significantly reduce emissions from energy generation and provide electricity in remote and harsh environments. To improve feasibility assessment for solar energy harvesting, solar energy harvesting models need to more accurately predict energy output. These models are improving, however soiling is still a process that is not well understood and thus poorly implemented in these models. Soiling, or the loss of energy from dust or particulate matter (PM) deposition on the panels, can reduce energy production significantly. Previous studies have found soiling losses between less than 1% [32] and more than 88% [25], and soiling rates (loss of energy over time), between 0.1% per day [24], and 5% per day [58]. These large variations in losses can be attributed to location and meteorology, but generalization in the field has not been done.

Several previous studies have related the mass of deposited PM with the loss in solar energy. One study by Hegazy (2001) found a very clear relationship between the mass of deposited particles and the transmission reduction, regardless of angle of deployment [30], which led to the development of the equation:

$$\Delta\tau = 34.37\,\mathrm{erf}(0.17\omega^{0.8473}) \tag{4.1}$$

where $\Delta\tau$ is the transmission loss caused by deposited particles in percent, and ω is the dust deposition density (the mass of dust deposited per square meter) in g/m^2. This relationship is shown to be valid between 0 and 10 g/m^2 of accumulated dust, and may apply to more highly soiled samples. More research is needed to ensure that the transmission loss is generalizable to other locations, although a previous study has examined this [5]. Using this type of equation could result in much better predictions of energy loses due to soiling, but requires an estimate of the mass of deposited PM.

To understand the fate and transport of atmospheric PM, particularly those that can potentially impact human health, climate, or ecosystem health, researchers have been exploring the deposition process. Previous studies on deposition have found that for dry deposition the mass of PM deposited is related to

ambient concentration of PM by the dry deposition velocity:

$$m_{accumulated} = v_d * PM \tag{4.2}$$

where v_d is the deposition velocity, PM is the mass concentration of PM in the ambient air and $m_{accumulated}$ is the mass flux of deposited particles (mass per area per time). Deposition velocity is affected by wind speed, surface properties, particle size, and a number of other factors that make it difficult to calculate theoretically, however it is generally considered a useful tool for understanding deposition [61].

Previous ambient studies have shown that larger particles, often over 10 µm in aerodynamic diameter, are the dominant contributor to deposited mass [39]. Field and laboratory experiments have found a wide range of deposition velocities for particles, a snapshot of those studies that focused on larger size particles is shown in Table 4.1. Deposition velocities range from 0.17 cm/sec [16] to 21 cm/sec [22]. This large range of deposition velocities is a result of varying surface geometry, meteorological conditions, surrounding environment, size of depositing particles, and atmospheric stability.

Most deposition studies use greased or protected surfaces to prevent particle bounce. However for solar energy applications, where a particle can be resuspended, it is important to only collect particles that remain deposited over a long duration. A handful of studies have considered smooth surfaces, where particle bounce or resuspension is allowed. A study by Goossens considered dust accumulation on several surfaces and found good agreement between the mass accumulated on a glass and metal surface in a wind tunnel [27]. The results were also similar to a water surface, which indicates that geometry is more important than the surface composition.

Many models have been developed to predict deposition. Models are typically semi-empirical. The model developed by Zhang and collaborators [67] is used in this paper and employs a theoretical framework that separates the deposition process into several process steps. Each term that represents a process step is then calculated by a fit from deposition data. This model has seen good agreement with actual deposition in the past [67].

In this work we examine the deposition of particles on glass plates similar to those used as photovoltaic (PV) panel cover plates at two different sites in the Front Range of Colorado when samples were

Table 4.1: Summary of deposition velocities found in other studies examining coarse particulates.

Location	Deposition Surface	Orientation	Date	Deposition Velocity	Size Range	Notes	Source
New York	Greased micro-scope slides	Placed on ground	1962-1964	5 cm/sec	20 µm	Ragweed pollen	[52]
New York	Greased micro-scope slides	Placed on ground	1962-1964	12 cm/sec	32-35 µm	Timothy pollen	[52]
Champaign, Illinois	Teflon Plate	Horizontal and stationary	June, 1982	0.17 - 0.42 cm/sec	All	Only sulfate	[16]
Champaign, Illinois	Petri Dish	Horizontal and stationary	June, 1982	0.18 - 0.61 cm/sec	All	Only sulfate	[16]
South Chicago	Greased Mylar	Horizontal wind vane	July - Sep. 1986	11.7 cm/sec	>1 µm		[48]
South Chicago	Greased Mylar	Upside-down wind vane	July - Sep. 1986	4.2 cm/sec	>1 µm		[48]
Chicago area	Greased Mylar	Horizontal wind vane	July - Aug. 1991	5.3 cm/sec	PM_{10}		[31]
Chicago area	Greased Mylar	Horizontal wind vane	July - Aug. 1991	5.7 cm/sec	Coarse PM		[31]
Around Lake Michigan	Greased Mylar	Horizontal wind vane	Dec. 1993 - Oct.1995	0.2 - 12 cm/sec	Coarse PM	Metals only	[66]
Bursa Turkey	Greased Mylar	Horizontal wind vane	Oct. 2002 - June 2003	2.3 - 11 cm/sec	TSP	Metals only	[63]
Taiwan near an Airport	Greased Mylar	Horizontal wind vane	Sep. - Dec. 2005	2.3 - 11.7 cm/sec	TSP		[23]
Berlin	Beaker	Horizontal wind vane	Dec. 2007 - July 2009	0.4 - 1.3 cm/sec	PM_{10}	Used Sb as a tracer for PM_{10}	[38]
Taiwan near a Harbor	PVC	Horizontal wind vane	June - Nov. 2013	0.95 - 7.92 cm/sec	TSP		[22]
Taiwan near an Airport	PVC	Horizontal wind vane	June - Nov. 2013	1.8 - 21.4 cm/sec	TSP		[22]

collected for two to five weeks. Additionally we compare the observed deposition with ambient concentrations and modeled deposition results. The goal of this work is to collect a large data set for evaluating ambient PM concentrations and dry deposition to improve PV soiling models.

4.3 Methods

4.3.1 General Approach

Ambient PM and PM deposition samples were collected simultaneously at two different locations in the Front Range of Colorado. Ambient PM was collected using a dichotomous filter sampler such that particles with aerodynamic diameter between 2.5 and 10 µm ($PM_{10\text{-}2.5}$) are separated from particles with aerodynamic diameter less than 2.5 µm ($PM_{2.5}$). Deposition samples were collected on glass substrates similar to those used as covers for PV panels. Additional meteorological data were collected at both sites by other organizations: the Air Pollution Control Division of the Colorado Department of Public Health and the Environment (CDPHE) at the Commerce City site, and the National Oceanic and Atmospheric Administration (NOAA) at the Erie site.

The first sampling location was in Commerce City, Colorado, on the roof of a one story elementary school in a mixed industrial and residential area 10 km North of downtown Denver, Colorado. This site had several notable particulate matter sources nearby including an open gravel pit mine, and the intersection of Interstates 25, 76, and 270, and US Highway 36. This site was co-located with a CDPHE PM sampling location (AQS ID: 080010006). The second sampling location was in Erie ,Colorado, at the base of the Boulder Atmospheric Observatory tower in a rural and agricultural area 30 km North of downtown Denver. This site was surrounded by active farmland and native grasslands, with one freeway passing 2 km to the east. More information about these two sites was presented previously [5].

4.3.2 Airborne Particulate Matter

Ambient $PM_{10\text{-}2.5}$ and $PM_{2.5}$ were collected using dichotomous filter samplers located at both field sites, additionally the combined PM_{10} is examined in detail here. One of these samplers is shown in the

right side of Figure 4.1. These filter samplers pulled 50 L/min of air through a PM_{10} inlet. This flow is then passed through a virtual impactor that splits the flow into a 48 L/min $PM_{2.5}$ channel, and a 2 L/m $PM_{10\text{-}2.5}$ channel. Both flows are then split, with half going through a Teflon filter (47 mm, 2 µm pore size, Pall Gelman Teflo) and the other half going though a quartz fiber filter (47 mm, Pall Gelman Tissuequartz). Flow rates through each of the four filters were measured by flow totalizers as well as being controlled by critical orifices downstream. These filter samplers are described in more detail elsewhere [12]. The filters were changed every 3-10 days, typically 7 days, at the Commerce City site and 3-25 days, typically 14 days, at the Erie site to ensure that there were no flow restrictions caused by pressure drop due to heavily loaded filters. The filter samplers were run continuously between filter changings. Additionally filters were always changed at the same time as the deposition plates to ensure that the filters were collecting the same ambient PM that the plates were exposed to. The Teflon filters were weighed before and after deployment following the procedures described previously [19]. The Teflon filters were allowed to equilibrate in a temperature and relative humidity controlled chamber for 24 hour prior to being weighed at least twice on a LabServe model BP210D microbalance with an accuracy of 10 µg. If the difference in masses between the first two weights was more than 30 µg the filter was weighed a third time, and the mass was taken as the average of the closest two masses. Before and after deployment, the filters were stored in pre-cleaned petri dishes (Pall Life Sciences 50mm sterile petri dishes part number 25388-606) in a freezer -18° C $\pm$ 7° C. PM_{10} concentrations were found by:

$$PM_{10} = \frac{m_{10-2.5} + m_{2.5}}{V_{10-2.5} + V_{2.5}} \tag{4.3}$$

where $m_{10-2.5}$ and $m_{2.5}$ are the masses of the particles in the coarse and fine channels respectively and $V_{10-2.5}$ and $V_{2.5}$ are the volumes of air passed through the coarse and fine channels respectively. $PM_{2.5}$ concentrations are found by:

$$PM_{2.5} = \frac{m_{2.5}\left(1 + \frac{V_{10-2.5}}{V_{2.5}}\right)}{V_{10-2.5} + V_{2.5}}. \tag{4.4}$$

The correction factor in the numerator of the equation 4.4 is to account for the fine mass that is deposited on the coarse filter due to the nature of the virtual impactor. Analysis of blank samples and controls showed no systematic mass variation, and therefore these masses were not used for correcting the masses calculated

Figure 4.1: The experimental set-up at the Erie site. On the left is the deposition set-up, and on the right is the dichotomous filter sampler

by Equations 4.3 and 4.4. Although both Teflon and quartz filters were collected, only data from the Teflon filters are presented here. The quartz samples were collected for analysis of organic material, while Teflon filters were collected for gravimetric analysis and metals analysis. Chemical analysis, including organic analysis, has not yet been done and is not presented in this work, only gravimetric analysis of filters is presented here.

Airborne particulate samples began being collected in July of 2012 at the Commerce City site and December of 2012 for the Erie site. Sampling continued until May of 2014 at the Commerce City site, and until March of 2014 at the Erie site.

For examining effects of higher time resolution averaging, hourly PM_{10} measurements were used. These data were collected by the Colorado Department of Public Health and the Environment (CDPHE) at a monitoring site in Welby Colorado (AQS ID: 080013001), approximately 1.5 km northwest of the Commerce City site.

4.3.3 Deposited PM and Effective Deposition Velocity

PM deposition samples were collected in the same locations as ambient PM concentrations. Glass samples 10 cm x 10 cm were deployed at 0° and 40°, and a field blank was carried with each set of plates to observe contamination from handling, transportation, and storage. A few early samples were deployed at 180° at the Commerce City site, but stopped being deployed after it was found that no appreciable mass accumulation was occurring. The samples were covered by a roof to prevent effects of precipitation. The roof is to allow for only the consideration of dry deposition, and not wet deposition. The roofs were placed 45 cm above the samples to allow for as much natural air flow as possible without getting precipitation on the samples. Samples were deployed for between one and five weeks, with the typical deployment being two weeks at the Commerce City site and four weeks at the Erie site. The deployment is longer at the Erie site to ensure that enough mass has deposited on the plates to be significantly greater than the noise of the measurement. The deposition deployment structure is shown on the left side of Figure 4.1.

For more than a year of sampling at the Commerce City location deposited PM samples were collected without a roof covering the samples. While in this time period there was never an entire sampling period without rain, there were several with minimal, or rain that occurred very early in the sampling period. All of the samples without a roof collected close to or less than the same amount of mass accumulated on the covered samples (within measurement uncertainty when more mass was collected on the uncovered samples). From this analysis it was determined that the roof was causing a negligible effect on the dry deposition of particulates, and sampling continued with the roof.

Two types of glass plates were used, one a tempered glass and one a low iron glass coated with a transparent conductive oxide, no difference in deposited mass was observed between the two types of plates [5]. The tempered glass samples typically weighed around 117 g, and the low iron glass samples typically weighed around 79 g. The plates were thoroughly cleaned, and stored in cleaned glass petri dishes with aluminum foil covers. The same petri dish was used for pre and post deployment storage. Nitrile gloves were always worn when handling glass deposition samples to reduce contamination and care was taken not to disturb the exposed surfaces of the plates. After deployment samples were stored in the same freezer

as the filters, until they had been post-weighed.

Masses of samples were found by weighing the samples before and after deployment using the same method as the Teflon filters. Mass accumulation was found by subtracting the post masses from the pre masses, correcting for noise in the scale by subtracting the difference in the simultaneously weighed control samples as described in previous work [5]. The mass accumulation rate was calculated by:

$$\dot{m}_{accumulated} = \frac{m_{accumulated}}{A_{plate}\Delta t} \tag{4.5}$$

where $\dot{m}_{accumulated}$ is the rate of mass accumulated per unit surface area, $m_{accumulated}$ is the mass accumulated on the plate, A_{plate} is the area of the plate, and Δt is the length of time the plates were deployed. More information on weighing and deposition sample procedure are presented elsewhere [5].

In this work an effective deposition velocity is calculated. This is found by rearranging Equation 4.2, and using the PM_{10} as a surrogate for total airborne PM:

$$v_{effective} = \frac{\dot{m}_{accumulation}}{PM_{10}} \tag{4.6}$$

where $v_{effective}$ is the effective deposition velocity, and appropriate unit conversions are added, so that effective deposition velocity is presented in cm/sec in this work. Since we use PM_{10} to represent all the PM, $v_{effective}$ is biased high.

Sampling of deposited particulates at the Commerce City site began in August of 2011 and continued to June of 2014. It was nearly a year later that ambient PM samples began being collected at the Commerce City site, and effective deposition velocity calculations did not begin until then. At the Erie site deposited particulate sampling began in November of 2012 and continued until May of 2014. During the vast majority of sampling at the Erie site both airborne and deposited PM samples were being collected.

4.3.4 Deposition Model

To better understand the utility of deposition theory for estimating solar panel soiling, we used the PM deposition model described by Zhang and collaborators [67] to compare to the measured PM deposition rates. This model was chosen because it has been shown to be effective, its ease of application, and

because it allows for particle bounce. This model needs ambient PM concentrations including PM size distribution, surface characteristics, and meteorological parameters as inputs. This model uses the original structure developed by Slinn [62]:

$$v_d = v_g + \frac{1}{R_a + R_s} \tag{4.7}$$

where v_g is the gravitational settling velocity and R_a and R_s are the aerodynamic resistance and surface resistance respectively. This is a resistance model of deposition, which examines the processes necessary for deposition and attempts to quantify them individually. The aerodynamic resistance is calculated as:

$$R_a = \frac{\ln(z_R/z_0) - \Psi_H}{\kappa u_*} \tag{4.8}$$

where z_R is the height at which deposition is being calculated, taken at 5 meters here, z_0 is the roughness length, a value of 1 meter was used corresponding to an urban environment, Ψ_H is the stability function, κ is the Von Karman constant and u_* is the friction velocity. A simplified stability was used based only on windspeed, where windspeed above 5 m/s was considered unstable, between 3 m/s and 5 m/s was considered neutral, and below 3 m/s was considered stable. The corresponding stability functions from Bussinger and collaborators were used [9]. Friction velocity is calculated by:

$$u_* = \frac{\kappa \overline{u_x}(h_r)}{\ln(h_r/z_0)} \tag{4.9}$$

where $\bar{u_x}(h_r)$ is the windspeed at the reference height, h_r. The windspeed in this work was collected at 10 meters.

The surface resistance is calculated by:

$$R_s = \frac{1}{3u_*(E_B + E_{IM})R_1} \tag{4.10}$$

where E_B and E_{IM} are the collection efficiencies for Brownian diffusion, and impaction respectively, and R_1 is the percentage of particles that stay deposited on the surface. All of these factors have empirical fits from data collected in different experiments. Collection by interception is not included in the model used here due to the smooth surface of the solar collector. E_B is calculated by:

$$E_B = Sc^{-\gamma} \tag{4.11}$$

where Sc is the Schmidt Number, and γ is a parameter based on land use, a value of 0.56 is used here for the urban environment. E_{IM} is calculated by:

$$E_{IM} = 10^{-3/St} \tag{4.12}$$

where St is the Stokes number. This is based on a fit for a smooth collector [62]. Finally R_1 is calculated by:

$$R_1 = exp(-St^{-1/2}) \tag{4.13}$$

from Slinn [62].

Values for PM_{10} were obtained from the dichotomous filter samplers simultaneously deployed at the sites. Values for temperature, and wind speed were obtained from CDPHE at the Commerce City site and NOAA for the Erie site. The data from CDPHE are hourly averaged, and for use in modeling these values are averaged again to correspond to the time that glass coupons were deployed. Data from NOAA are one minute averaged, these data are again averaged to get one value for the time that corresponding glass coupons were deployed. At the Commerce City site, this data is publicly available at: `http://www.colorado.gov/airquality/report`. At the Erie site this data is publicly available at: `http://www.esrl.noaa.gov/psd/technology/bao/`. In this work we used the fit by Slinn [62] for the collection efficiency, since the glass coupons represent a smooth surface. For simplicity only deposition samples deployed at 0° were considered in comparisons of modeled and experimental mass accumulation.

4.3.5 Airborne PM Size Distributions

Airborne size distribution information was collected at the Commerce City site following the collection of deposition samples. A TSI Aerodynamic Particle Sizer (APS) Spectrometer (Model 3321) was deployed for a several week period in the Spring of 2015 beginning April 30th and continuing through May 21st. During this time the weather was especially rainy, with nearly daily rain showers. Because of the consistent rain the data are likely skewed slightly from typical size distributions in the area. Data were not collected for several days during this time period due to computer failure. Over this time a total of 902 size distribution measurements were taken. Each sample was a 20 second averaged size distribution. Size distributions

were collected and saved every 15 minutes while the system was operational. This instrument samples particle sizes from 0.5 µm to 20 µm in diameter by observing the time of flight of particles in an accelerating airflow. A lab calibration check of the instrument showed an uncertainty of 0.1 µm in particle diameter.

The median shape of these size distributions, as well as the size distributions individually, were used in modeling of particle deposition. When this was done the size distribution was scaled to match ambient concentrations based on the corresponding PM_{10} measurement.

4.4 Results and Discussion

4.4.1 Deposition

Mass accumulation rate (or deposition) values were collected over more than two years at the Commerce City site and more than one year at the the Erie site. The time series of these values is show in in Figure 4.2. Figure 4.2 differentiates the two sites as well as the 0°, 40°, 180°, and field blanks. From this figure we can see that the Commerce City site (abbreviated CC) in general has higher mass accumulation rates. Additionally the 0° plates show higher mass accumulation rates than the 40° plates. The 180° plates are nearly indistinguishable from the field blanks indicating that the main method of deposition is gravitational settling and not diffusion. This is reasonable as the majority of mass is in larger sizes of particles that deposit almost exclusively by gravitational settling. Small particles, which are preferentially removed via diffusion may be depositing on the 180° plates but do not have appreciable mass even with significantly longer deployment times (up to two months).

Summary statistics for mass accumulation rates are shown in Table 4.2. The highest values were seen in Commerce City where deposition values between 0.01 and 0.12 g/m^2/day were observed for horizontally deployed plates, and between 0.01 and 0.08 g/m^2/day for the 40° plates. Lower mass accumulation rates were seen at the Erie site where deposition values between 0.005 and 0.06 g/m^2/day for 0° plates and 0.005 and 0.02 g/m^2/day for 40° plates were observed. These are similar to results found by Holsen et al. outside Chicago [31], and lower than those seen by Fang and collaborators in Taiwan [23]. This is a likely indication of the respective concentrations of airborne particulates, since these two studies saw

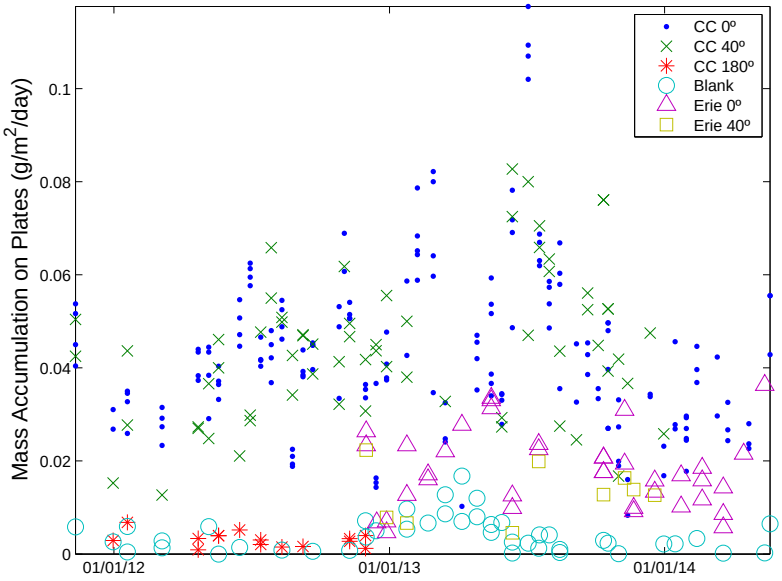

Figure 4.2: Plot of mass accumulation on the glass deposition plates. The samples are grouped by location and orientation to highlight the differences that location and angle of deployment have on mass accumulation. Note that only mass accumulations above zero are shown here, many blank and 180° samples have negative mass accumulation and are not presented in this figure

Table 4.2: Summary of mass accumulation data collected in this study

		Mass Accumulation Rate		Effective Deposition Velocity	
Location	Position	Number of Samples	Mean (± STD) $mg/m^2/day$	Number of Samples	Mean (± STD) cm/sec
Commerce City	0°	174	43.2 (17.8)	134	2.14 (1.03)
	40°	66	44.3(15.8)	48	2.42 (1.13)
Erie	0°	40	20.0 (11.6)	33	2.12 (1.05)
	40°	10	13.0 (5.6)	10	1.40 (0.58)

similar values for deposition velocity (see Table 4.1).

4.4.2 Effective Deposition Velocity

Deposition theory indicates that ambient PM concentrations and deposition are related by deposition velocity, Equation 4.2. Comparing PM_{10} concentrations with deposition rates yields Figure 4.3. Despite the wide spread in the data seen in Figure 4.3, the range of deposition velocities that were observed between the two sites were comparable. At the Commerce City site the range of effective deposition velocity values was 0.52 cm/sec to 5.7 cm/sec (174 samples) with a mean of 2.14 cm/sec, and at the Erie site the range of effective deposition velocity values is 0.61 cm/sec to 4.0 cm/sec (40 samples) with a mean of 2.12 cm/sec. The results for effective deposition velocity are summarized in Table 4.2. While the range of effective deposition velocities at the Commerce City site was slightly larger the mean effective deposition velocity at both sites were not statistically significantly different ($p = 0.92$). Additionally the variances of the two distributions are not statistically significantly different ($p = 0.86$). There were many more samples collected at the Commerce City site because sampling started earlier at that location and there were two deposition set-ups in Commerce City to assess measurement uncertainty [5] thus doubling the number of samples collected. Additionally the higher PM concentration allows samples to be collected more often.

The range in deposition velocities was also compared for the various deployment angles (0°, 40°, 180°, and field blanks). A box and whiskers plot of these data are shown in Figure 4.4. The median deposition velocity for both 180° samples and the field blanks is near zero, supporting the previous results that significant deposition is not being caused by diffusion of small particles. The large spread in the effective deposition velocity values particularly for the 180° plates may be caused by compounding of uncertainty in

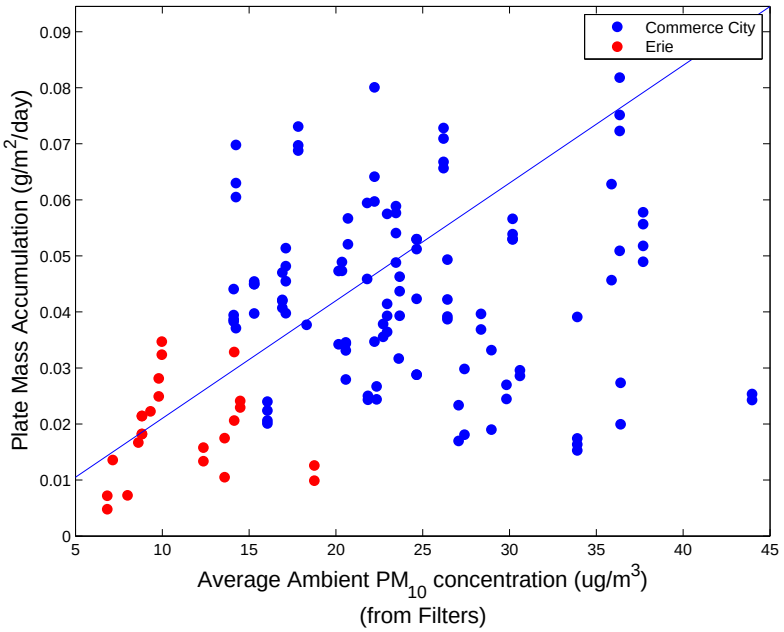

Figure 4.3: Comparison of Ambient PM10 and Mass Accumulation for the two sites in this study. A trend line shows a similar relationship between the two sites, which are statistically not differentiable.

PM concentrations as these samples were deployed longer, and the similar uncertainty in mass as the field blanks. The 0° and 40° samples have very similar deposition velocities, despite the 40° samples having been tilted. This may be due to particles depositing by impaction during wind events, or may be an result of the uncertainties in mass accumulation and PM_{10} concentrations.

These values for effective deposition velocity were similar to values previously observed, particularly for those studies that focus on larger particles (see Table 4.1). The range of effective deposition velocities seen in this work spans more than an order of magnitude, which makes generalization difficult, however the similarity between the two sites in this study, and other studies has some positive implications. If the similarity in deposition velocities, to smooth horizontal surfaces is minimally effected by airborne particle distributions, meteorology, and surrounding environment, than a first order estimate of mass accumulation on PV panels may be relatively easy, and accomplished with only knowledge of the relationship with PM_{10} concentrations.

When exploring the linear relationship between mass accumulation on the surface and airborne PM_{10} concentrations, PM_{10} concentrations accounted for 9% of the variability in mass accumulation. More of the variability can be accounted for by adding additional variables to this linear model, including temperature and windspeed. When using all three of these variables 26% of the variability can be accounted for. Neither $PM_{2.5}$ nor relative humidity were significant predictors of mass accumulation. Adding temperature and windspeed does improve the predictions of mass accumulation, however this model has been built and tuned to the data collected here. Section 4.4.4 provides a better estimate of mass accumulation with these same variables without tuning to this specific data set.

One reason that PM_{10} may be a poor predictor of mass accumulation is that particles larger than 10µm in aerodynamic diameter can deposit but are not counted in the PM_{10} measurement. PM_{10} can be a poor predictor of total airborne particulates. This is likely one of the driving factors in the variability of the effective deposition velocity and the spread in Figure 4.3.

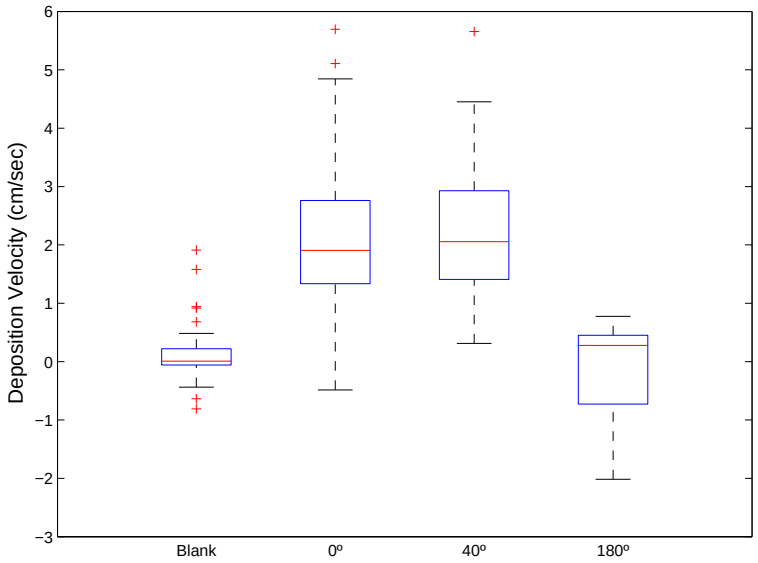

Figure 4.4: A comparison of the deposition velocities for plates deployed at different angles. The data from both sites are combined in this box and whiskers plot.

4.4.3 Airborne PM Size Distributions

Several days of size distribution data are shown in Figure 4.5. The frequent rainstorms are easily observable as the concentrations of coarse particles decrease drastically. There are also periods without rain, where we can see the quick rise in particle concentrations. The particle concentrations are not very stable, with the size distributions varying widely over even relatively short time scales (hour to hour for example) especially with the effects of precipitation. The median size distribution and interquartile range data show a clear single mode distribution in coarse particulates, see Figure 4.6.

Figure 4.5 shows that the size distribution can be highly variable with time and that using a single size distribution may not accurately represent the true conditions over long (in this case multi-week) time scales. Precipitation especially can affect the shape of the size distribution. The peak in coarse PM occurs around 14 μm, although the variability in this is quite high. Figure 4.6 shows the median normalized size distribution and the middle 25-75% quartiles. Size distributions were normalized so that the total mass in each size distribution was equal to one (the mass in each bin divided by the total mass in that sample). The median and quartiles are for each size bin individually across all of the samples and do not represent specific normalized size distributions, but represent how much of the airborne mass is typically in each of these bins. The lack of larger particles in the lower quartile is likely caused by the persistent precipitation that scavenged the larger particles, and may not be typical for the Front Range area. Figure 4.6 also indicates that there are likely larger particles that were not sampled by the APS, as seen by the shape of the distribution.

To use these size distribution data in modeling deposition, the median size distribution was used as time averaged size distribution of the particles, and the median size distribution was shown to match deposition results better than the mean size distribution. This was shown by running a comparison between deposition calculated every hour and every two weeks. Hourly averaged meteorological data was combined with bootstrapped size distributions to calculate a theoretical deposition for every hour over two weeks, and this was summed compared with the deposition calculated using two-week averaged meteorological data, combined with mean and median size distributions. Using this method with several years of meteorological

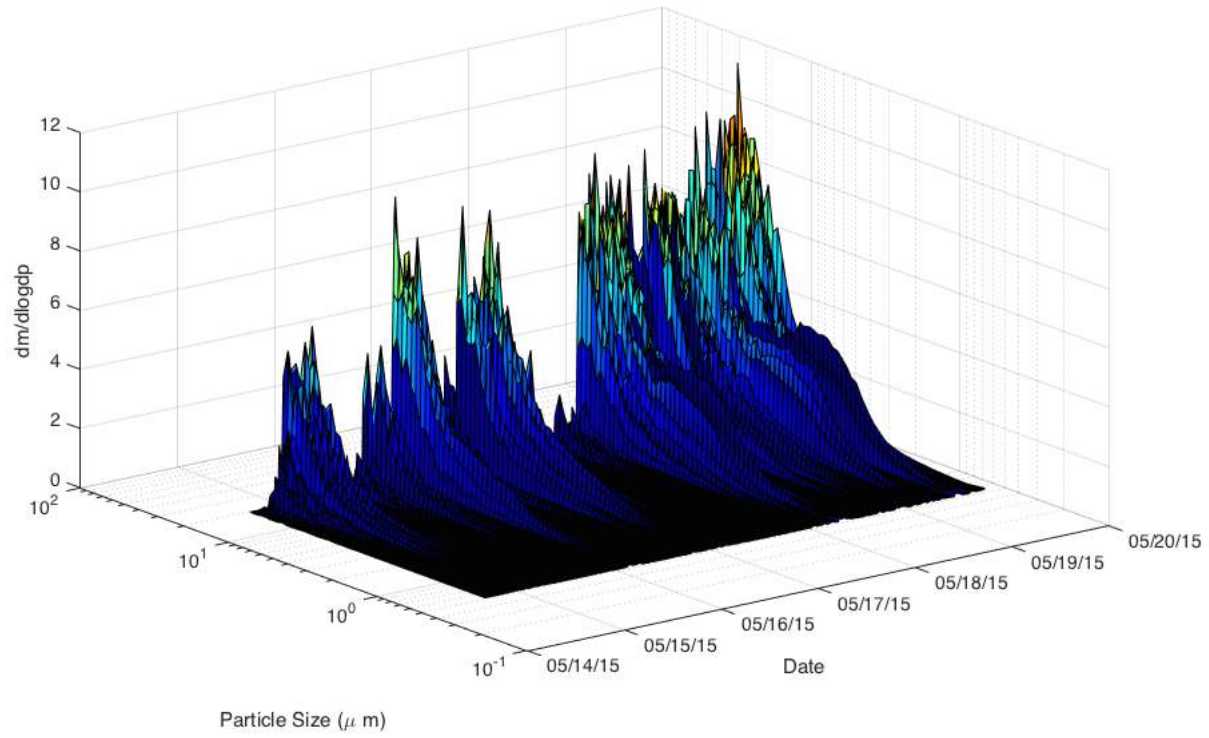

Figure 4.5: Size distributions collected for five days at the Commerce City site in May 2015. Frequent rainstorms are easily noted by the significantly lower PM concentrations. The APS used in this study samples particles up to 20 µm in aerodynamic diameter

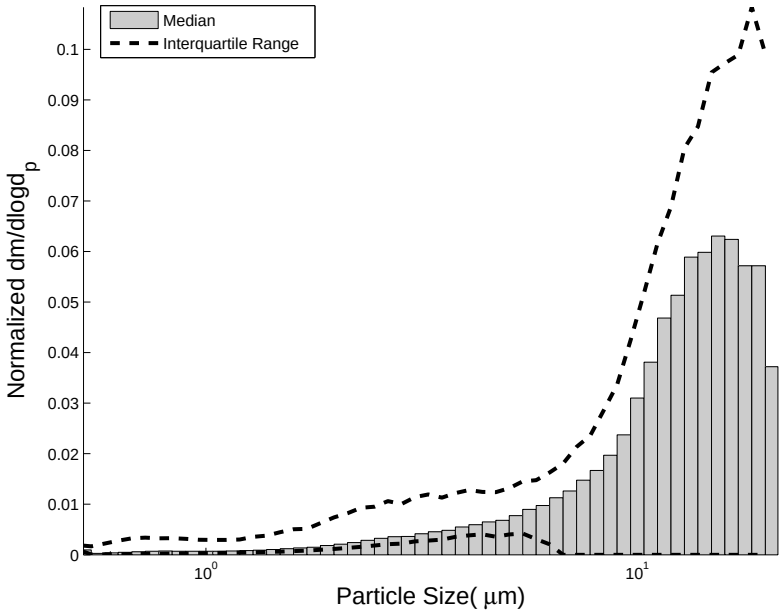

Figure 4.6: Variability in the size distributions collected in Spring of 2015 at the Commerce City site. The histogram is the median size distribution, and the two dotted lines represent where the 25th and 75th quartile distributions would be.

data the median size distribution was shown to better predict the hourly summed size deposition results than the mean size distribution. The PM_{10} concentration that was collected with the dichotomous filter sampler was used as a scalar to multiply the normalized size distribution by to get an average size distribution for the period of deployment of the plates.

4.4.4 Comparison Between Observations and Model

Figure 4.7 (b) shows the comparison between actual mass accumulation and modeled mass deposition, using the model developed by Zhang and collaborators (see Section 4.3.4) and using the median size distribution collected with the APS. These data have an R^2 value of 0.32, and smaller spread than the PM_{10} vs. mass accumulation plot (Figure 4.3) ($p = 0.46$). This indicates that this model does a better job of estimating mass accumulation than employing a single effective deposition velocity. The model does a good job of getting the right order of magnitude fit to the data and a regression of the data forced through the origin gives a slope of 1. Although the model makes a good first order approximation of deposition, there is still noticeable spread in the data of 0.018 $g/m^2/day$.

Figure 4.7 (a) shows the results of the same model as above but instead of using 52 size bins corresponding to the size bins of the APS, the model uses only two size bins one for $PM_{2.5}$ and one for $PM_{10\text{-}2.5}$. This model does almost as well as the model with 52 size bins ($R^2 = 0.31$), with less information. Not only is this likely the better model tested in this study, it shows that the same accuracy can be achieved with relatively rudimentary ambient size distribution information, as with a more specific size distribution. Both PM_{10} and $PM_{2.5}$ data are widely available in the US through the Environmental Protection Agency, and this model could easily be applied with this level of accuracy in many locations across the US.

Figure 4.7 shows similar magnitudes for results of both the 2-bin and 52-bin models, despite the 52-bin model including particles between 10 and 20 μm in diameter that are not included in the 2-bin model. This is most likely due to both models using the same mass of particles, just distributed between the bins differently. The 52-bin model has larger particles, but the total particle mass is still the same, so the model finds less deposition of the smaller particles. Additionally the 2-bin model uses simultaneously collected $PM_{2.5}$ and PM_{10}, so that more or fewer smaller particles may be represented in the model - compared with

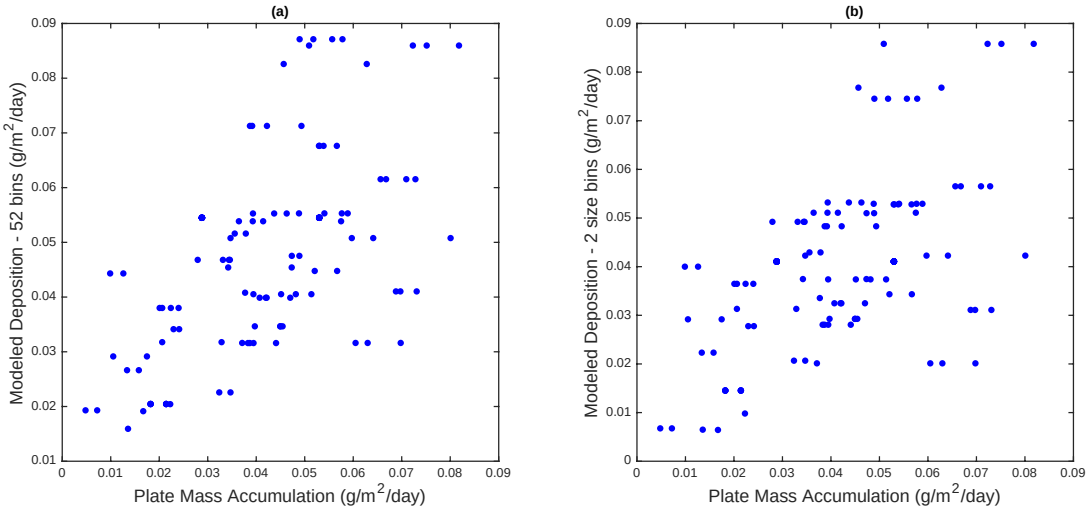

Figure 4.7: Comparison of mass accumulation and modeled mass deposition for the Commerce City site. Particulate concentrations were collected from the dichotomous filter sampler, and meteorological data averaged over the glass coupon deployment from data available from the CDPHE and NOAA. Plot (a) shows the model using size bins corresponding to the APS size bins, and plot (b) shows results using a simple 2 bin model with the $PM_{10-2.5}$ and $PM_{2.5}$ collected from the dichotomous filter sampler.

the 52-bin model which has one consistent size distribution.

Previous research has found that long time-averages for deposition significantly reduce the accuracy of model results and the relationship between ambient PM and deposition [47]. In an attempt to understand if this is a driver for the spread between modeled and predicted results a theoretical study was conducted. Real hourly PM_{10}, temperature, and wind speed data from the CDPHE were used to model deposition every hour over two week increments. Additionally the size distributions collected with the APS were bootstraped for these hourly calculations, choosing one size distribution at random for every hour. Then the median size distribution from the bootstrap population and the averaged PM_{10}, temperature, and wind speed data were used to calculate total deposition over the two week period and the deposition results were compared. The spread in the results was 0.005 $g/m^2/day$. As such, high time averaging was not able to fully explain the differences observed between modeled and observed deposition results in this experiment.

Another possible explanation for the spread is in the measurement uncertainty in calculating mass accumulation, caused by uncertainty in mass, time, and area measurements. This uncertainty has previously been shown to be on the order of 0.01 $g/m^2/day$ [5].

The uncertainty caused by lower time resolution and measurement uncertainty accounts for roughly two thirds of the difference between modeled and observed deposition. The remainder of the unexplained variance likely originates from model "inaccuracies" or inability of the model to fully capture real world deposition processes, meteorological variable uncertainties that are not examined here, and size distribution uncertainties. Another likely source of uncertainty in this approach is not accounting for particulates larger than 10 or 20 µm in aerodynamic diameter. These larger particles are in the atmosphere and depositing, but are not being included in the measurements of airborne particulates or the calculations of deposition. Previous experiments on solar energy systems have seen a peak in deposited size distributions around 20 µm [54] [4] [10], indicating that these larger particles are present and significant.

A sensitivity analysis of the model was conducted, examining the sensitivity to temperature, wind speed, PM_{10}, and particle size (increasing or decreasing the size of each particle by the given percentage). For each parameter the other parameters were kept constant while the parameter of interest was increased and decreased by five and ten percent for all the samples in the data set. The numerical output from this

Table 4.3: Summary of deposition model sensitivities given as the average percentage change in mass of particle dry deposition. Mean values for the range of input found in this experiment as well as the range of values observed are presented.

	Increase 10% Mean (Range)%	Increase 5% Mean (Range)%	Decrease 5% Mean (Range)%	Decrease 10% Mean (Range)%
Wind Speed	0.8 (-3.8 to -4.8)	0.2 (-2.6 to 2.7)	-1.3 (-3.3 to 2.0)	-3.0 (-7.2 to 4.7)
Temperature	1.7 (-3.0 to 5.7)	1.0 (-1.4 to 2.9)	-1.1 (-2.9 to 1.1)	-2.4 (-5.7 to 1.8)
Particle Size	1.60 (-1.9 to 6.0)	0.80 (-1.2 to 3.1)	-0.90 (-3.5 to 1.7)	-2.10 (-7.4 to 3.9)
PM_{10}	10 (10 to 10)	5 (5 to 5)	-5 (-5 to -5)	-10 (-10 to -10)

sensitivity analysis is shown in Table 4.3 The model was found to be most sensitive to PM_{10}, with any change in the input of PM concentration giving an equal percent change in the output. All the other parameters were less sensitive. Temperature and particle size, had similar sensitivities, with every percent change in the input in these parameters causing a 0.2 percent change in the modeled mass accumulation with wide variability across the input parameter space noted. Finally wind speed was the most variably sensitive parameter with every percent increase in wind speed causing a 0.06 percent increase in mass accumulation and every percent decrease in wind speed causing a 0.3 percent decrease in mass accumulation and wide spread in this relationship was again noted across the input parameter space.

4.5 Conclusions

An average effective deposition velocity of 2 cm/sec was observed at both sites in this study but an order of magnitude spread is observed in effective deposition velocity over the entire sampling campaign. A more complex model did a better job of predicting mass deposition but also required temperature, wind speed, and size distribution data. All methods showed significant spread in the deposition results when compared with experimental deposition, however these results represent a significant step forward in modeling soiling losses for solar energy. Because soiling happens over long time scales (months to years), an average effective deposition velocity is useful even if there is high variability on shorter time scales. For solar energy harvesting modeling, short term variability is driven by clouds and temperature, which dominate any effects that might be seen from soiling. However, monthly and yearly output of a system can be

greatly affected by soiling, and being able to predict these losses can significantly improve estimates of how much energy a PV system will produce over its lifetime, which dictates the payback period. The accuracy in predicting deposition achieved in this study is likely not useful for understanding short-term fate of airborne species, or high precision calculations of deposition.

Being able to predict mass accumulation on PV panels, or other solar energy harvesting devices, could improve prediction of energy loss due to soiling when paired with other study results and models. Here results are presented that indicate that mass deposition is related to ambient concentrations, even over periods of time greater than a week. This means that using readily available PM_{10} data, and easily implemented deposition models, even as simple as a constant effective deposition velocity, soiling losses could begin to be predicted at sites anywhere in the country or the world. Both the simple and more complex model are sensitive to PM_{10} concentration inputs, and high quality data for this parameter are necessary for accurately predicting mass accumulation. The more complex model was less sensitive to wind speed, temperature, and particle sizes indicating that lower quality data (from more distant stations, or with higher uncertainty) may be used in these parameters.

4.6 Acknowledgements

The authors would like to thank the Air Pollution Control Division, of the Colorado Department of Public Health and the Environment for generously sharing data. Especially to Bradley Rink for his continued help with data from CDPHE. Additionally the authors would like to thank the Physical Sciences Division, of the National Oceanic and Atmospheric Administration, for sharing data collected at the BAO Tower and Daniel Wolfe and Bruce Bartram for their support with sampling and instrument monitoring at the BAO Tower.

This material is based upon work supported by the National Science Foundation Graduate Research Fellowship Program under Grant No. DGE 1144083.

Chapter 5

SPATIAL VARIABILITY OF SOILING OF PHOTOVOLTAIC COVER PLATES: RESULTS FROM COLORADO, FLORIDA, AND NEW MEXICO

Liza Boyle[a], Patrick Burton[b], Holly Flinchpaugh[a], Victoria Danner[a], Charles Robinson[b], Ken Blackwell[c], Bruce King[b], Michael P. Hannigan[a]

[a]Department of Mechanical Engineering, University of Colorado, Boulder, Colorado, USA

[b]Sandia National Laboratory, Albuquerque, New Mexico, USA

[c]Florida Solar Energy Center, University of Central Florida, Cocoa, Florida, USA

5.1 Abstract

Soiling can cause large reductions in solar energy system production. To study the spatial variability of soiling, transmission loss and mass accumulation of particulates on PV cover plates were measured at five sites across the continental United States. Three sites were in the Front Range of Colorado in rural, suburban, and urban areas representing a semi-arid environment. One site was in Cocoa Florida in a hot and humid environment, and the final site was in Albuquerque New Mexico in a hot and arid environment. Simultaneously total suspended particulates (TSP) were measured at each site. Comparisons between transmission loss and mass accumulation measurements are made. Both mass accumulation and ambient TSP are shown to have some predicting power for transmission loss. Mean deposition velocities of 1 cm/sec were observed. For every g/m^2 of PM deposited on the PV cover plate a 5.5% reduction in transmission was observed independent of site. These results provide a method for estimating soiling rates at sites across

the United States.

5.2 Background and Motivation

Soiling, or the natural accumulation of dust and other particulates on the surface of photovoltaic (PV) panels, can lead to large losses in power output from PV systems. Many previous studies on soiling have looked at the losses caused by soiling in different locations. For example a study in Cambridge Massachusetts USA found an average loss of 1% from soiling, and a maximum loss of 4.2% after several months[32]. Another study in Saudi Arabia found losses of more than 60% after six months [55]. Researchers in India found losses between 52% and 7% for samples deployed at angles between 0° and 90° after six months [46].These and many other studies represent a body of research that has examined the scale of solar energy conversion loss that results from soiling in a variety of different locations. They also show that there is high variability in the magnitude of the losses that soiling can create.

Recently, a few previous studies have looked directly at the spatial variability of soiling. A study by Caron and Littmann installed solar panels and meterological stations at several locations in California that represented either rural agricultural areas or undisturbed desert. They found that location and season play a significant role in the losses incurred from soiling [11]. A study by Mejia and Kleissl looked at already installed PV systems in California, and estimated soiling losses at each site. This study found significant variability between sites, but these differences were not statistically significant by region [44]. Besides the tilt angle of the panels no predicting factors for variability in soiling were identified. A final study by Lombardo and collaborators looked at haziness of windows (very similar to PV panels), at 23 sites in Europe. They found wide variability in soiling, but found that it was not well correlated with the surrounding environment except in extreme situations [41]. Currently it is unclear how region and surrounding environment affect soiling of photovoltaic systems.

There are a couple of factors known to affect soiling levels. Tilt angle of panels has been shown in many studies to be related to the level of soiling [3] [54] [51] [30] [29]. Additional previous studies have found that the dust mass accumulated on the panel surface (the amount of soiling) is very clearly

related to the soiling losses [30] [21] [5]. A likely driving factor behind the amount of soiling is the quantity of airborne particulate matter (PM). This was examined in the study by Lombardo and collaborators, previously mentioned, but no significant conclusions were made with respect to PM concentrations [41]. Knowing that deposited mass is directly related to soiling losses, there are many studies that examine mass deposition with ambient particulates. Most previous work in this area has focused on understanding where and how PM leaves the atmosphere [61] and has not focused on soiling specifically. Previous research on deposition has indicated the airborne PM is related to the mass of deposited material by:

$$m_{accumulated} = v_d * PM \tag{5.1}$$

where $m_{accumulated}$ is the mass flux of deposited particles (mass per area per time), v_d is the deposition velocity, and PM is the mass concentration of PM in the ambient air [61]. Ambient studies have found deposition velocities ranging from less than 1 cm/sec [16] [22] [38], to 12 cm/sec [23] [52] depending on depositing particles' size, surface characteristics, and ambient meteorological conditions.

In this study we explore the links between airborne PM, PV cover plate soiling, and solar energy transmission reduction at five sites located around the continental United States. Using five sites allows for examination of the spatial variability of soiling processes, as well as a more comprehensive examination of the relationship between airborne PM and soiling. This expands previous results on the link between mass accumulation and transmission loss to additional sites, and expands the deposition process to focus on solar energy losses especially with larger particles.

5.3 Methods

5.3.1 General Approach

Locations with diverse landscapes and climates were used to collect soiling data in this study. At each site glass coupons similar to those used as cover plates for PV panels were deployed for two to four weeks. These glass coupon samples were collected continuously for six months, collecting a total of 89 samples. Mass accumulation and transmission of these glass coupons were measured. Additionally, the

mass concentration of airborne particulates was measured at each of the sites simultaneously with the deployment of the glass coupons.

5.3.2 Measurement Locations

Five sites were used to collect data in this study. Three were in the area surrounding Denver, Colorado, one in New Mexico and one in Florida. The first site in Colorado is located on the roof of a one-story elementary school in Commerce City, Colorado, 10 km north-northeast of downtown Denver. This site is surrounded by mixed residential and industrial areas with several freeways passing within 5 km of the site. The second site in Colorado is at the base of the Boulder Atmospheric Observatory (BAO) Tower in Erie, Colorado, a rural area 20 km north of downtown Denver. This site is surrounded by open native grasslands and agricultural land, and access to the site is on an unpaved road. The third Colorado site is on the main campus of the National Renewable Energy Laboratory, 15 km west of downtown Denver in a mixed suburban and rural area. The site is surrounded by several buildings, paved roads and native grasslands. These three sites are all in a semi-arid environment. The site in New Mexico is in Albuquerque, at Sandia National Laboratory, on a gravel lot in a light industrial area. This is located on the site of a Department of Energy Regional Test Center (RTC), and is surrounded by paved roads, research buildings, suburban areas to the north and barren land to the south. This site is in a hot and arid environment. The final site is at the University of Central Florida, in a grassy field in a rural and industrial area of Cocoa at a second RTC. The surroundings are a combination of dense forest and industrial buildings. This site is in a hot and humid climate. A map of the sites is seen in Figure 5.1, additionally average climactic data is presented in Table 5.1. In Table 5.1 the Denver, Colorado site is located between the Commerce City site and the Erie site in northern Denver. The Albuquerque site is located closer to downtown Albuquerque, north of where sampling for this campaign took place, and Titusville, Florida site is north of the Cocoa sampling location, but a similar distance from the coast. These five sites represent a diverse set of surrounding environments and weather patterns, and provide information about smaller scale differences in soiling in the Denver Metro area, and larger spatial variability of soiling across the United States.

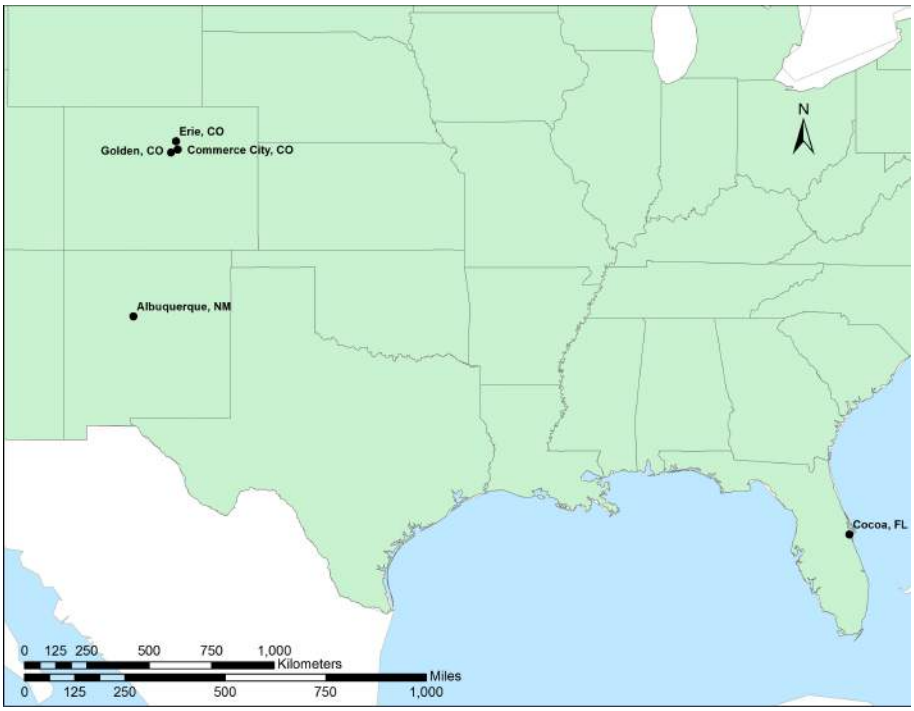

Figure 5.1: Map of the site locations used in this study. The sites in Albuquerque, NM and Cocoa, FL are at the sites of Regional Test Centers (RTC).

Table 5.1: Summary of temperature and precipitation at locations near the five sampling sites.

	Denver, Colorado		Albuquerque, New Mexico		Titusville, Florida	
	Average Precipitation (cm)	Average Daily Temp (°C)	Average Precipitation (cm)	Average Daily Temp (°C)	Average Precipitation (cm)	Average Daily Temp (°C)
Jan	0.94	0.9	0.97	2.4	6.99	15.5
Feb	0.94	1.9	1.22	5.2	7.19	17.10
Mar	3.05	6.0	1.45	8.9	9.96	19.40
Apr	4.67	9.70	1.55	13.3	7.04	21.8
May	5.61	15.1	1.27	18.7	7.75	25.1
Jun	4.24	20.5	1.68	23.8	16.76	27.4
Jul	4.75	23.8	3.81	25.7	17.53	28.3
Aug	3.89	22.9	4.01	24.6	20.02	28.3
Sep	2.57	18.10	2.74	20.7	17.96	27.3
Oct	2.46	11.4	2.59	14.2	11.99	24.6
Nov	1.88	5.10	1.45	7.2	7.47	20.7
Dec	1.42	0.3	1.27	2.4	6.5	17.2

5.3.3 PV Cover Plate Analysis

Mass accumulation and transmission measurements were taken using 5 cm by 6 cm by 0.32 cm float glass coupons available from Swift Glass (Elmira NY) deployed in acrylic frames. Two samples were deployed horizontally and one sample was deployed at angle of 40° to the horizontal facing south. Field blanks are transported and simultaneously analyzed with the deployed coupons for all sample sets. All the samples were covered with a simple roof to prevent cleaning and contamination by precipitation. A picture of the set-up in Cocoa, Florida is shown in Figure 5.2 on the right side of the image. Before being deployed the coupons were cleaned with soapy water, water, and isopropanol and visually inspected for any residual contaminants. Before deployment the samples were wrapped in clean aluminum foil. Nitril gloves were always worn when handling plates, and care was taken to only touch the edges of the plates and not the exposed surface. Samples were typically deployed for two week periods at the Albuquerque, Cocoa, and Commerce City sites, and four weeks at the Golden and Erie sites. After deployment the exposed surface was covered with a second identical coupon, cleaned in the same manner, the edges were wrapped in teflon tape, and the samples were re-wrapped in aluminum foil. This method was shown to not significantly affect the mass of particles collected, and samples were kept in this configuration except when being weighed and having transmission measurements taken. Samples were shipped once a month from the Cocoa and

Albuquerque field sites to the University of Colorado for weighing. Long term storage of samples was done in a freezer at -20 $\pm$ 5 °C.

5.3.3.1 Mass Accumulation

The mass of the glass coupons was measured before and after deployment to find the mass accumulated on the coupons. Mass measurements were taken using a LabServe model BP210D microbalance with an accuracy of 0.01 mg. The microbalance was in a temperature and relative humidity controlled chamber, where the coupons were equilibrated for 24 hours before weighing [19]. Each coupon was weighed twice and if those two masses differed by more than 0.03 mg a third mass was taken. The average of the masses was used, and when a third mass measurement was taken, the two closest mass measurements were averaged to obtain the mass of the plate. Plates were weighed in the same groups of four plates in which they were deployed, and for each group two control plates were weighed in the same manner. The control plates remain in the environmentally controlled chamber for the duration of the experiment. Mass accumulation was calculated by:

$$m_{accumulated} = [m_{post} - m_{pre}]_{plate} \tag{5.2}$$

where m_{pre} and m_{post} are the masses before and after deployment respectively. The mass accumulation rate on the plates is calculated by:

$$\dot{m}_{accumulated} = \frac{m_{accumulated}}{A_{plate}\Delta t} \tag{5.3}$$

where $\dot{m}_{accumulated}$ is the rate of mass accumulated on the plate, A_{plate} is the area of the plate, and Δt is the length of time the plates were deployed. And finally the mass accumulation density is calculated as:

$$\omega = \frac{m_{accumulated}}{A_{plate}} \tag{5.4}$$

where ω is the dust accumulation density or the g/m^2 of mass accumulated on the plates.

5.3.3.2 Transmission

After the post mass measurements were completed, coupons were repackaged using the same method mentioned previously and shipped from Boulder, Colorado to Sandia National Laboratory in Albu-

Figure 5.2: Set-up used for collection of samples at the Cocoa, Florida field site. On the left is the TSP filter sampler, and on the right is the deposition coupon deployment structure.

querque, New Mexico for transmission measurements. Transmission measurements were collected with a Varian Cary 5000 UV/vis/NIR spectrophotometer, which collects transmission every nm from 300 nm to 820 nm and every 4nm from 820 nm to 1800 nm. Transmission for individual wavelengths is examined as well as average transmission loss. Average transmission loss is calculated as:

$$\Delta\tau = 1 - \frac{\Sigma\tau_s}{\Sigma\tau_b} \tag{5.5}$$

where $\Delta\tau$ is the average transmission loss for the sample τ_s is the transmission values at each wavelength for the sample, and τ_b is the transmission value at each wavelength for the blank sample. These are summed over all the wavelengths to get $\Sigma\tau$.

5.3.4 Airborne Particulate Matter Concentrations

Total Suspended Particulates (TSP) were sampled at the same locations as the deposition coupons were deployed and for the same time period. TSP were used in this study as a single value to represent the particulates in the atmosphere that could deposit. This parameter is useful because it captures most the the particles in the atmosphere; however, it does not provide any information on the size distribution of these particles. The lack of size information can reduce the quality of the fit that we can expect from using this method. Previous studies have used PM_{10} [6], or a combination of PM_{10} and $PM_{2.5}$ [5], but these results do not capture the large amount of mass that can be present in particles larger than 10 µm in aerodynamic diameter.

TSP samples were collected using Hi-Vol TSP filter samplers such as the Tisch environmental TE-5000. An example is shown on the left side Figure 5.2. These samplers were set to pull 1000 L/min of air through a 8 inch by 10 inch quartz fiber filter (Whatman Pittsburg, PA). The flow rate was calibrated at the beginning of the sampling campaign using a critical orifice plate. The quartz fiber filters were cleaned by baking at 500° C for 12 hours in clean aluminum foil packets. After being baked the filters were weighed on the same balance and in the same manner as the glass coupons (see section 5.3.3.1). Two separate quartz filters were used as controls and kept in the weighing chamber at all times. Filters were always handled with cleaned metal tweezers when weighing and deploying the filters. After deployment the filters are weighed

in the same manner and the mass of the filter is calculated in the same way as the mass of the plate using Equation 5.2. TSP concentration was calculated by:

$$TSP = m_{filter}/[(1000L/min)(t_{deploy})] \tag{5.6}$$

where TSP is the mass concentration (typically μg/m^3) of particulate matter in the ambient air, m_{filter} is the mass accumulated on the filter, t_{deploy} is the time the filter is deployed in the running TSP sampler, and 1000L/min is the volumetric flow rate the calibrated TSP samplers pull through the filter. Field blanks were collected bi-monthly to establish the background level of contamination caused by sample preparation, transportation, and handling.

Deposition velocity was calculated by rearranging Equation 5.1, using the data collected in this study:

$$v_{TSP} = \frac{m_{accumulated}}{TSP} \tag{5.7}$$

where TSP is the TSP concentration in μg/m^3, v_{TSP} is the deposition velocity using total mass accumulated and the TSP concentration. Previous studies have used PM_{10} instead of TSP concentrations to calculate deposition velocity [6]. TSP concentration is used here because it provides a better metric of the particulates that are likely to deposit on the solar surface.

5.4 Results and Discussion

5.4.1 Mass Accumulation

Mass accumulation results are summarized in Table 5.2. Mass accumulation rates observed in this study covered a wide range, and were site dependent (p=0.005 for horizontal samples, 0.001 for 40° samples). The statistical significance in the difference of mass accumulation rate at the sites, indicates that soiling is site dependent. Additionally the difference in soiling rate at the three sites in the Front Range of Colorado (Commerce City, Erie and Golden) shows that soiling can not be predicted regionally, and must be examined on a smaller scale. Here despite the similar climactic influences in these three regional sites, differences in soiling indicate that local sources are a dominant contributor to PV soiling.

Mass accumulation rates were highest at the Commerce City and Coca sites, and lowest at the Erie and Albuquerque sites. It would be expected that the highest mass accumulation would be at the arid sites (Albuquerque, Commerce City, Erie and Golden), due to the prevalence of wind blown dust at these sites. The large deposition at the Cocoa site may be due to depositing sea salt, the site is 17 km from the ocean, however high deposition at the Cocoa site was more likely due to high relative humidity, increasing particle adhesion to the glass surface. Low deposition at the Erie and Albuquerque sites is likely due to low concentrations of ambient particulates (see Section 5.4.2, and Figure 5.3).

At all but the Cocoa site (p = 0.004), the mass accumulation on the horizontal and 40° sites are not significantly different (p values between 0.8 and 0.1). Many previous studies have found that higher tilt angles decrease the mass of accumulated PM, which makes sense from theory because tilted plates have less horizontal area for gravitational settling of particles. This was not observed in these results due to low sample numbers, and uncertainty in mass accumulation. There was also non-negligible mass accumulation on the blank plates, especially at the Cocoa site, although at all sites except the Cocoa site the value of the blanks is below the uncertainty in mass accumulation rate (see Section 5.4.4). This indicates that there may have been some mass accumulation being caused by sample handling, transport, and/or storage. The mass accumulation on the blank plates was significantly smaller than the mass accumulation on any of the deployed plates for all the sites and both angles of deployment. Blank masses could have been subtracted from the total mass accumulation, but due to the small values this was not done.

5.4.2 Deposition Velocity

Figure 5.3 shows how ambient particle concentrations were related to mass accumulation for each site. These were expected to be correlated by deposition theory (Equation 5.1) with some spread for variable locations, wind speeds, temperatures and humidities. Here, TSP concentrations were able to explain 25% of the variance in mass accumulation, while the other 75% was caused by other factors.

Deposition velocity was calculated by Equation 5.1, with the TSP concentration for PM. Results for deposition velocity are summarized in the right most columns of Table 5.2, and box and whiskers plots of the deposition velocity values is shown in Figure 5.4. Deposition velocity is generally around 1 cm/sec, with

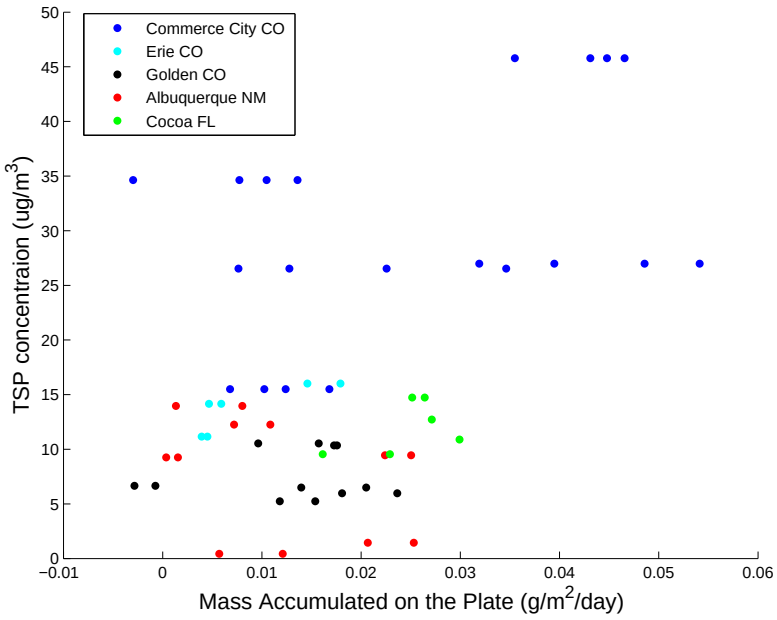

Figure 5.3: Comparison of mass accumulation rate with TSP concentrations at the five field sites used in this study.

higher values observed at the Golden site and for horizontal samples at the Cocoa site. The deposition velocity calculate for horizontal plates was found to be significantly different at the different sites (p=0.000), however for the 40° samples this same significant difference was not observed (p=0.06). This indicates that local variables, such as particle size distribution and meteorology are playing important roles in the deposition of particulates. The three sites in the Front Range of Colorado experience the greatest range of average deposition velocities, providing more evidence that regional variability can be very important, and understanding of local factors is important. Higher deposition velocity may be caused by a shift towards larger particles in the airborne particle size distribution as larger particles depositing by gravitational settling deposit faster than smaller particles. Higher deposition velocity could also be caused by higher wind speeds, or by fewer particles being removed from the surface, such as by high humidity helping particles stick at the Cocoa site. The Albuquerque site had standard deviations larger than the deposition velocity magnitude. This was caused by one deployment that may have an inaccurately low TSP value, or just had conditions appropriate for higher deposition velocity, most likely caused by high wind speeds.

The deposition velocity for field blanks is above zero as seen in Figure 5.4. This is most likely caused by the positive mass accumulation values that are seen for blank plates. While these values are important to note, they are lower than the deposition velocity values observed for 0° and 40° deployed plates.

These deposition velocity values are about half the deposition velocity seen in a similar previous study [6]. This difference is most likely caused by using TSP, instead of PM_{10} (only particles smaller than 10 μm in aerodynamic diameter) in calculating average deposition velocity. Here TSP was used which includes all PM mass while in that previous study only PM_{10} was used. TSP is a better metric in calculating total mass accumulation, because it is a measure of the total ambient particulates, instead of just those in a particular size range.

5.4.3 Transmission

Figure 5.5 shows the wavelength dependence of transmission. There was a distinct pattern noted in the transmission data with undulations having peaks around 500 and 1700 nm, and a low around 900 nm. This pattern was seen in all of the transmission samples, including the blanks. The pattern in transmission

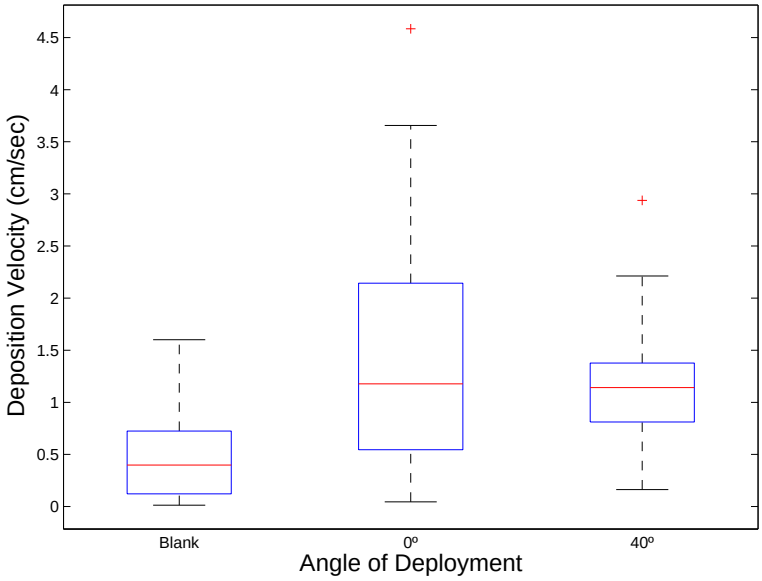

Figure 5.4: Box and whisker plot of deposition velocities observed in this study. Separated for angle of deployment, but not for location, this provided enough samples for these results to be meaningful.

with wavelength was most likely caused by the glass, which has a natural absorption spectrum. The relative transmission loss is shown for a subset of samples in Figure 5.6. In this plot we see that most samples have the largest relative transmission loss for the shortest wavelengths (375 nm to 400mn) with losses around one percent higher than the more typical relative transmission loss for the sample. Between 400 and 800 nm the relative transmission loss decreases to a more stable and typical relative transmission loss, which remains relatively constant above 800 nm with some small (tenths of a percent) changes. There are a couple of samples (including ones shown in Figure 5.6) that show noticeable jumps in transmission at 800 nm and agin at 1200 nm. These are most likely due to instrument errors, as there are three separate transmission sensors that these wavelengths are where the transmission measurements are made with different sensors. These samples are still used for analysis, but this is an added uncertainty in the overall transmission value that is used.

While some difference in transmission over the wavelength range tested here is noted, these changes are generally very consistent. For this reason, and for ease of analysis, a single transmission loss value is used in the remainder of this analysis. This single transmission value is taken as the average relative transmission loss from 375 nm to 1800 nm.

Transmission measurements were compared with the mass accumulated on the glass coupon, and are shown in Figure 5.7. This figure shows a clear relationship between mass accumulation and transmission loss. A linear fit through the data yields:

$$\Delta\tau = 5.7 \times \omega \tag{5.8}$$

or, for every g/m^2 of dust accumulated on the surface of a solar panel there is a 5.7% ($\pm$ 0.77%) reduction in the light transmitted through the surface. An ANOVA of the slopes for each site showed no significant difference for any of the sites used in this study ($p > 0.2$). which can be seen visually in Figure 5.7. While other studies have found very similar results to this for individual locations [30] [21] [5], this is the first to show a lack of location dependence. The Cocoa site provides an interesting point of comparison in this analysis. This site being near (17 km) the ocean is likely influenced by sea salt, which is a more transparent particle than other coarse particulates (dust, or pollen for example). The lack of difference in Equation 5.8

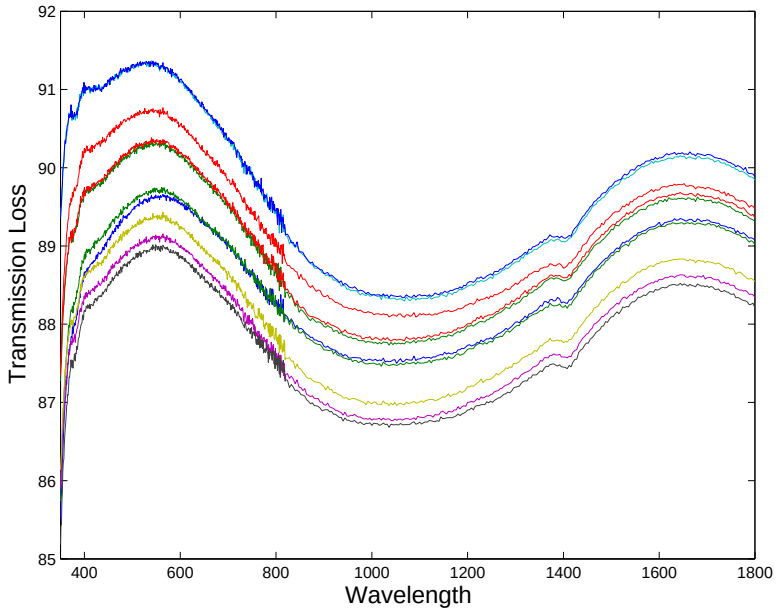

Figure 5.5: A sample of transmission measurements collected in this study.

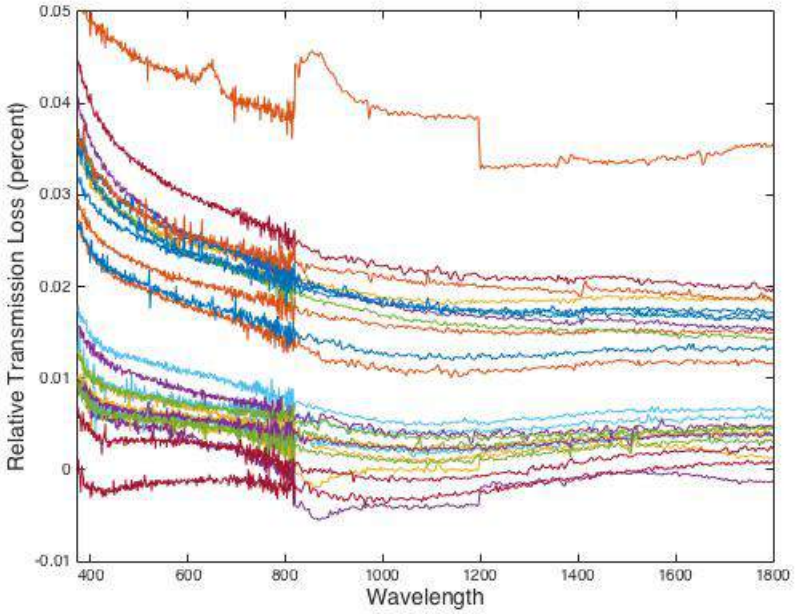

Figure 5.6: A sample of relative transmission loss measurements collected in this study. These are the relative difference in transmission loss between a deployed sample and the simultaneously collected field blank. Some wavelength differences are observed, generally less than one percent and typically in the lower region (up to 800 nm) where the instrument has the largest noise.

between this site and the other sites indicates that either the sea salt is not a significant fraction of the deposited particulates, or that the differences in transmission of varying chemistries, even ones that seem they should be quite different, is not a first order effect.

It is important to note that Equation 5.8 is based only on data between 0 and 0.8 g/m^2. While the same relationship may extend beyond this range, it is not validated for use beyond 0.8 g/m^2, and should be used with caution when estimating soiling of heavily loaded samples.

The logical next step in analysis is identifying if we can predict transmission loss from ambient PM concentrations without the intermediary step of mass accumulation. Figure 5.8 shows the comparison between transmission loss and the TSP exposure. The TSP exposure is just the TSP concentration multiplied by the time that the glass coupon was deployed, so that the two axes represent equivalent time scale (total deployment time of the glass coupons). This plot shows large spread in the data, but a clear trend towards increasing transmission loss with increasing airborne particulates. A simple linear regression yields:

$$\Delta\tau = 0.005 \times PM_{exposure} + 0.22 \tag{5.9}$$

where $PM_{exposure}$ is the Total Particulate Exposure in µg day/m^3, or the average TSP concentration multiplied by the time exposed in days. Using Equation 5.9 the TSP exposure was able to explain 45% of the variability in transmission loss. One reason that TSP exposure seems to do better than TSP concentration in predicting mass accumulation, is that time is a dominant factor here. This has significant implications for soiling. Mainly that, with time, soiling estimates using airborne PM concentrations improve. Soiling happens over longer time scales that examined here, often months to years. This improvement with time indicates we can likely do an even better job estimating average soiling losses when done for seasons, years, or a solar energy system life.

5.4.4 Uncertainty Analysis

Total uncertainty in mass accumulation rate and transmission were found by examining the y-error when plotting co-deployed samples. These samples included the two simultaneously deployed horizontal samples at all of the sites, and the co-deployed 40° samples at the Commerce City site. A total of 107

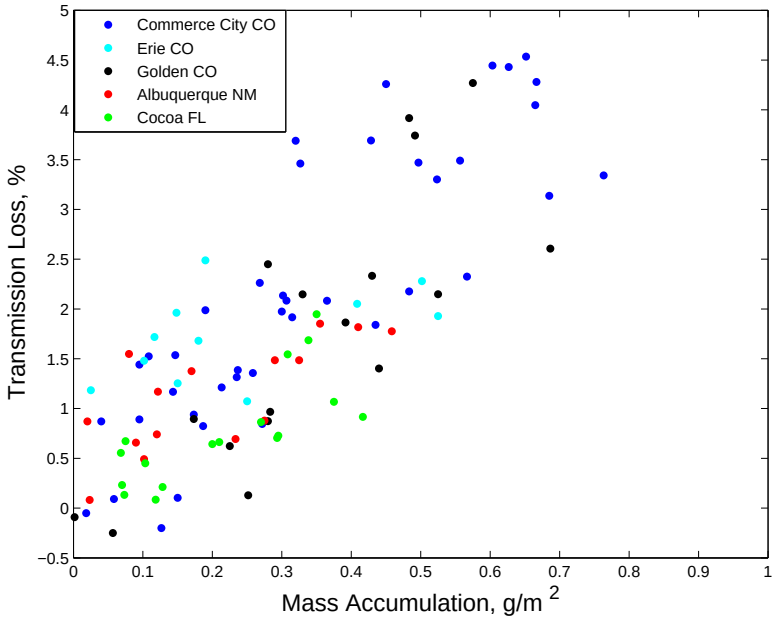

Figure 5.7: Comparison of mass accumulation on PV cover plate and transmission loss at the five sites used in this study. There is a clear relationship between mass accumulation and transmission loss that is not location dependent.

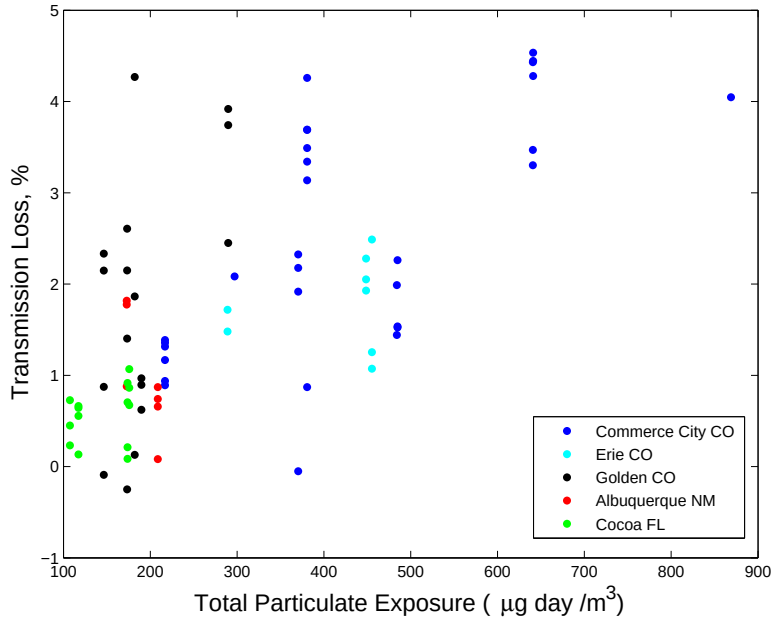

Figure 5.8: Comparison of ambient TSP exposure with transmission loss

comparisons were used for the error in mass accumulation rate, and 90 comparisons were used for the error in transmission. A y-error of 0.003 g/m^2/day was found for the mass accumulation rate and a y-error of 0.40% was found for transmission. For mass accumulation rate this is between 10 and 38 percent of the average mass accumulation rate at the sites and between 43 and more than 100 percent for the average blank samples at the five sites. The uncertainty in mass accumulation rate accounts for almost all, or all, depending on the site, of the variability in the blank samples, but can represent a large percentage of the mass accumulation rate.

Finding the uncertainty in TSP concentration was less straight forward because no simultaneously samples were collected at the same location. Instead uncertainties in the mass of the filters, flow rate, and time deployed were found or estimated, and combined to find a total uncertainty in TSP concentration. To find the uncertainty in the mass of the TSP filters, the two control filters were analyzed. Both TSP control filters that were weighed with each sample used in this analysis had a standard error of 0.012 g, and this is taken as the uncertainty in the mass of the TSP filters. The uncertainty in volume was taken as the uncertainty in calibration, 2% of the measurement based on instrument accuracy, or 20 L/min here, and the estimated drift. Limited data on drift and meteorological variability were collected. Based on that limited data we conservatively estimated 120 L/min of drift and meteorological variability over the sample period. Combined these give a 122 L/min uncertainty in the flow rate of air through the TSP filter. Finally the time is recorded to the minute when the collection is started and stopped, giving a maximum uncertainty of 2 minutes, which was used in further analysis. Using error propogation techniques, and the expected flow rate of 1000 L/min and mean values for sample deployment time a total uncertainty in the TSP concentration of 2.1 µg/m^3 was found. A couple of TSP values at the Albuquerque site were below this uncertainty however, most TSP samples were above 5 µg/m^3, with the highest values being near 50 µg/m^3. The uncertainty represents between 4 and 40 percent of the measurement for the majority of the TSP concentrations.

Combining uncertainties in mass accumulation rate, and TSP we can use error propagation to calculate the uncertainty in deposition velocity. Again using average values for TSP concentration and mass accumulation rate, an uncertainty of 0.20 cm/sec in deposition velocity was found. This is around 20% of the average deposition velocity that was found in this study - again indicating the variability in this value.

5.5 Conclusion

Using airborne PM concentrations to predict soiling losses is a novel method, and shows promise in accounting for spatial and temporal variability. Here we find the TSP concentration was related both to mass accumulated and to transmission loss, and that mass accumulation and transmission loss were strongly correlated. Better agreement was seen between TSP exposure and transmission loss than TSP concentration and mass accumulation rate, and because we integrated over the time the sample was deployed this indicates that longer time averaging will increase accuracy of soiling losses. Estimating soiling losses is important on a month to year time scale when small losses over time add up to significant energy loss. On shorter time scales solar energy output is dominated by the solar resource, which can be very variable especially with clouds. Soiling estimates improve with time, giving more confidence in the relationships presented here of soiling losses, since these relationships would primarily be implemented over longer time scales.

Unlike previous studies that have examined soiling rates at individual locations, the results presented here have been shown to be more broadly applicable. Samples were collected at three very different locations across the United States and collected for 6 months. Regional variability was shown to be important as was large geographic scale variability. These methods can help provide more accurate estimates of soiling both geographically and temporally, but require knowledge of local airborne particulate matter concentrations.

Table 5.2: Summary of mass accumulation and deposition velocity data collected in this study. Blank spaces in this table result from not enough reliable data.

			Mass Accumulation Rate		Deposition Velocity	
Location	Deploy Angle	Number of samples	Average ($g/m^2/day$)	STD	Average (cm/sec)	STD
Commerce City	0°	19	0.026	0.017	1.035	0.583
Commerce City	40°	13	0.028	0.013	1.093	0.400
Commerce City	Blank	2	0.002		0.090	
Erie	0°	6	0.009	0.006	0.681	0.391
Erie	40°	3	0.013	0.006	1.044	0.369
Erie	Blank	0				
Golden	0°	10	0.016	0.004	2.692	1.076
Golden	40°	4	0.012	0.003	1.910	0.829
Golden	Blank	4	0.004	0.004		
Albuquerque	0°	8	0.010	0.010	1.067	1.187
Albuquerque	40°	3	0.008	0.007	0.835	0.888
Albuquerque	Blank	3	0.002	0.001		
Cocoa	0°	6	0.025	0.005	2.404	0.498
Cocoa	40°	4	0.011	0.006	1.089	0.495
Cocoa	Blank	4	0.007	0.002		

Chapter 6

UNDERSTANDING PV SOILING: BEYOND DRY DEPOSITION OF AIRBORNE PM

6.1 Abstract

The results from several experiments conducted in Commerce City, Colorado are presented with the intent of providing results on how factors other than airborne particulate matter (PM) influence soiling. First precipitation and wet deposition are examined. These processes can both increase mass loading and the strength of particle attachment to the glass surface, as well as clean panels and reduce soiling. The experimental design used here is not well suited to understanding precipitation, but in general lower mass loadings and transmission losses were found when precipitation is allowed to interact with the surface. This effect is especially noticeable when rain has recently occurred. These results indicate that the dry deposition situation represents a 'worst-case' soiling scenario for the Commerce City location and that precipitation generally helps clean, and not dirty, the surface. Second micrometeorology was examined by comparing the results of deposition for samples placed adjacent to one another. This experiment was done first in an identical configuration, and then again in a slightly modified configuration. The results from both configurations indicate that there are not noticeable differences in soiling on distance scales less than 1 meter. For comparison the results of soiling at Commerce City and Erie sites are compared for simultaneously deployed samples. No correlation in this data is observed indicating that factors on the 10 km scale are significant for soiling. Finally, comparing samples deployed for four to twelve weeks saw no systematic or significant difference with the combined soiling samples deployed for two-week increments. These results provide no evidence for resuspension or soiling saturation at this location over time scales up

to three months.

6.2 Background

The previous chapters of this dissertation have addressed fundamental process-level aspects of soiling, identifying a method for estimating soiling loss rates, and the development of methods to due so. There are many other aspects of soiling that have not been examined in those chapters, or only discussed briefly, but that can affect soiling. This chapter provides details on a few additional experiments that were conducted to understand other parameters that may affect soiling. Some of these results were presented earlier, in Chapter 2, but this chapter provides more details on the experimental method and analysis, as well as a more detailed discussion of the results and their impact. Specifically this chapter focuses on the effects of precipitation, small scale meteorology, particle resuspension or soiling saturation, and the effect of the roof on particulate deposition sampling.

6.2.1 Precipitation and Wet Deposition

Rain and other precipitation, has the ability to clean solar modules, and eliminate or reduce the losses caused by soiling. Previous studies have examined how well precipitation cleans modules and general consensus indicates that some amount of precipitation completely, or almost completely restores (over 95% recovery) the output of modules to clean levels. These experiments are done by examining the power output from a PV module or system compared with either a clean calibrated module [24] or the theoretical output using solar irradiance, temperature, and windspeed data [37]. These studies have found a range of precipitation necessary to clean solar panels. Kimber and collaborators found insufficient evidence that any amount of rain, up to 0.4 inches was able to clean panels, and suggest that the precipitation rate should be investigated [37]. Caron and Littmann found around 1 mm (0.04 inches) of rain could clean panels [11], where as Garcia and collaborators found 4-5 mm (0.16 - 0.20 inches) of rain was necessary [24]. Meji and Kleissl found that less than 0.1 inches of rain increased soiling, and above 0.1 inches the panels were cleaned [44].

An increase in soiling caused by small amounts of rain has been seen in several studies [44] [35] [36]. This could be caused by any combination of three processes. First when water is present on the surface of a panel it can increase the sticky-ness of the surface. This makes it less likely for particles to bounce off of the surface and can increase the overall deposition. Second is by the scavenging and deposition of particles in the atmosphere by the rain. When rain occurs particles that are suspended in the atmosphere can scavenged from the air by the water droplets and deposited on the surface by the rain, this is called wet deposition and can be an additional source of particles on the surface of solar panels. Finally it has also been seen that small amounts of precipitation can cause particles to 'cement' to the surface making them harder to remove later [15] [35]. This is caused by water soluble particles, such as salts, dissolving in the water, and as the water evaporates these particles solidify along the surface of the panel often around insoluble particulates. This increases the surface area in contact with the glass for both insoluble and soluble particles making them more difficult to remove and blocking more light as the area covered by the particles increases.

6.2.2 Micrometeorology

Meteorology has the ability to change deposition on small scales. Previous wind-tunnel studies have shown that varying wind-speeds can cause varying mass depositions, and also varying deposition patterns [28]. This indicates that there could be varying mass depositions across a PV system as wind speeds are effected by the panels and surrounding environment. Another study, found that the tops of their samples had higher transmission rates then the bottoms of their samples. If this is due to micormeteorology, or particles 'falling' down the samples was not identified, but changes over centimeter scales were noted [29]. The scale of this effect in the real world has not been investigated, but could pose problems by introducing mis-match into solar energy systems, and making soiling more difficult to predict due to small scale variations.

6.2.3 Soiling Saturation and Resuspension

Many previous studies have seen soiling rates decrease over time [46] [29] [26] [35], however this is not always seen [54] [55]. This decrease over time could be caused by a saturation, that is, once a certain

number of particles have been deposited it is harder for more particles to deposit. Alternatively this could be caused by resuspension, or particles being removed by wind which would become more likely as more particles are deposited. It is unknown what processes are at play when this is seen, and which systems are more or less likely to see this effect.

6.3 Methods

6.3.1 Co-Deployed Samples

At the Commerce City site used in this study and described in previous chapters, there are three deployment structures placed side-by-side. Two are the same as all the set-ups used in this study, and the third was different. It was identical to all the other set-ups, except without a roof, as seen on the left side of Figure 6.1. These three set-ups were used both with the larger 10 cm x 10 cm plates (results presented in Chapters 3 and 4), and with the smaller 5 cm x 6 cm plates (results presented in Chapter 5). The two identical co-deployed set-ups allow for examination of micrometeorology, and soiling saturation or resuspension. The third set-up allows for the examination of both the effects of precipitation and the effect of the roof. This approach presented some problems, because there was often water in the acrylic set-up of the uncovered site - clearly allowing contamination on the unexposed side of the glass plate. Because of this, these results should be taken with caution. Moving forward the unexposed side of the plate should be cleaned before post-weighing, however that was not done for any of the samples presented here.

6.3.2 Precipitation

Rainfall data was obtained from two sources. First, rainfall data was obtained from the KDEN weather station at Denver International Airport maintained by the National Weather Service. This site is 23 km to east of the Commerce City site and provides hourly meteorological data including rainfall. The data from this site are publicly available (www.weather.gov/obhistory/KDEN.html). This data is utilized for identifying when significant rain events happen due to the higher time resolution that this data set provides.

Second, rainfall data was obtained from the Community Collaborative Rain, Hail and Snow Network

Figure 6.1: The three sample deployment structures used at the Commerce City site. The two on the right have roofs to prevent wet deposition of particles and cleaning by precipitation and represent the duplicate set-ups, while the one on the left does not have a roof, and is used for assessment of the impact of precipitation

(CoCoRaHS), which is a wide spread community initiative for collecting precipitation data. Volunteer citizens, with rain gauges record the previous 24 hour rain total every morning, and that data is made publicly available on the CoCoRaHS website (`http://www.cocorahs.org/`). The closest one to three rain stations were averaged, depending on data availability, to estimate the rainfall total at the Commerce City site and trace amounts of rain were taken as zero. These locations are generally around a 1 km away. The data is considered high quality, but there are not always consistent entries from the same sites, as such, the sites used varied widely across the time series. Data presented here was collected between March 2013 and August 2014, with the larger 10 cm x 10 cm plates. The CoCoRaHS data was used for total rainfall during sample deployment, due to the data collection being closer to the actual site.

6.3.3 Micrometeorology

To examine the effects of small scale meteorology and topology (10s of centimeters up to 1 meter), the results from the co-deployed samples at Alsup (middle vs. right most set-ups in Figure 6.1) were examined. Additionally, a second experiment was conducted where the 40° tilted sample was moved from between the two horizontally deployed samples, as seen in 6.1 and Figure 6.2(a), to even with the eastern most deployed sample in the middle set-up at the Commerce City site, Figure 6.2(b). This was intended to affected how winds coming from the south interact with the deployed horizontal plates. From the wind rose for the site, shown in Figure 6.3, we can see that winds from the south are common. Again all the co-deployed samples at the Commerce City site were examined. The first part of this experiment was conducted with the larger 10 cm x 10 cm plates, and the second part was conducted with the smaller 5 cm x 6 cm plates. This does not appear to affect the results, as shown later. This modification was an attempt to change the micrometeorological conditions, to see at what scale these changes are noticeable. For larger scale meteorology we can compare the results from co-deployed samples at the Commerce City site and the Erie site, which were 25 km apart.

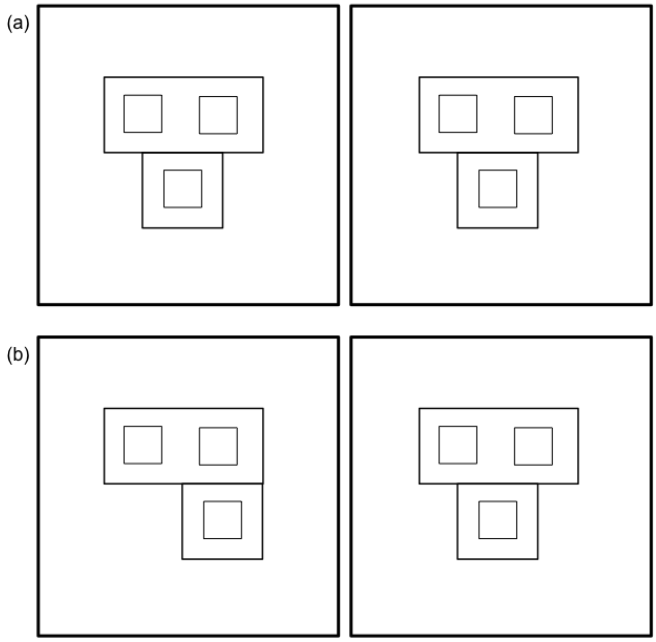

Figure 6.2: Birds-eye illustration of the modification to the experimental sampling station that was made to examine micrometeorology effects. (a) the original configuration, and (b) the modified configuration.

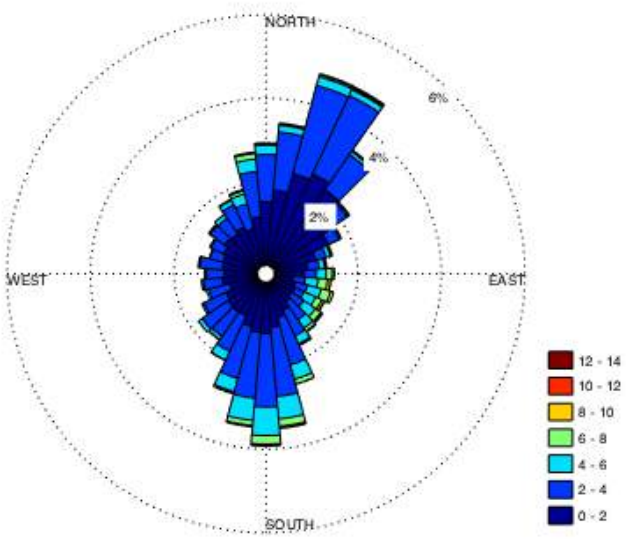

Figure 6.3: Windrose for the Commerce City site using hourly data from 2011 to 2014. Wind speeds are in m/s.

6.3.4 Soiling Saturation and Resuspension

To study soiling saturation the duplicate set-ups were used (middle and right-most set-ups in Figure 6.1). In this experiment the plates were changed in the typical manner on the right most set-up, and allowed to accumulate PM for varying amounts of time on the identical middle set-up. Then the mass of the shorter time deployments were added and compared with the mass accumulation for the longer time deployment. If saturation occurs then the summed mass of the shorter time deployments would be higher than the mass accumulated for the single longer time deployment. This experiment was conducted entirely with the 10 cm x 10 cm plates.

6.4 Results and Discussion

6.4.1 Precipitation and Roof Effects

A comparison between the mass accumulated on the covered and uncovered set-ups at the Commerce City site is shown in Figure 6.4. The plot is color-coded for the amount of precipitation received during the two week deployment. This plot shows that the covered set-up regularly accumulates more mass than the uncovered set-up. These results indicate that precipitation generally causes cleaning of the exposed samples, and not additional accumulation of PM, however there is no noticeable trend with the amount of precipitation and the difference in mass accumulation on the covered and uncovered set-ups. A visual analysis of the rainfall data showed that for each deployment time rainfall typically came in several events. Often one or two small rain falls, less than 0.1 inches, and one or two larger events with total rain falls of more than 0.2 inches.

The amount of time since the most recent significant rain was also examined. Here significant rain is taken as more than 0.05 inches in the hour, as recorded at the KDEN meteorological sample. This value was chosen based on the research performed by Garcia et al. [24] and Caron and Littmann [11]. A plot of the comparison between mass accumulation on the covered and uncovered set-ups, color coded for the time since the most recent significant rain, is shown in Figure 6.5. While there are no clearly significant trends, the samples with the largest differences between the covered and uncovered mass accumulation

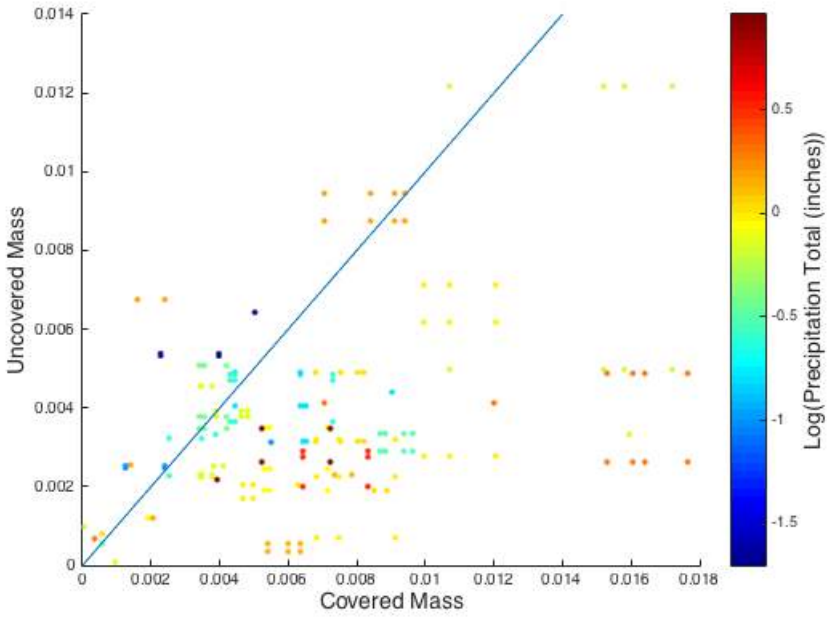

Figure 6.4: Comparison of mass accumulation on the samples with and without a roof color coded for the total amount of rain received during sample deployment. The solid line is the 1:1 line.

were exposed to the most recent significant rain events, occurring within the last few days (of a typical two week deployment).

The fact that the largest difference in mass accumulations between the covered and uncovered set-ups was shortly after significant rain indicate that significant rain can clean the surface of solar panels. This also provides anecdotal evidence that the level of 'significant' rain is close to an appropriate value, as lower amounts of recent rain did not cause as large a difference between deposited masses. Finally these results indicate that dry deposition only represents a worst-case scenario for soiling at the Commerce City site because rain was only seen to have a cleaning effect.

Figure 6.6 shows the relationship between mass accumulation and transmission loss for uncovered samples deployed at the Commerce City site. The data show the same trend as is seen for covered samples in Chapter 3 and Chapter 5. This data is from samples collected from the experiment described in Chapter 5 (5 cm by 6 cm plates), and are not the same samples shown in Figure 6.5, although the same relationship was seen in the data from the previous experiment as well. The relationship found with only this data is:

$$\Delta\tau = 5.0\omega \tag{6.1}$$

where $\Delta\tau$ is the transmission loss and ω is the dust deposition density in g/m^2. That is that for every g/m^2 of mass accumulated on the surface of a solar panel there is a 5% loss in light transmission. This is not significantly different than the relationship developed in Chapter 5 (p = 0.6)., indicating that results for comparison between mass accumulation and light transmission, presented earlier in this dissertation, are applicable even in conditions with precipitation. Additionally these results demonstrate that patterning or texturing that can be caused by precipitation does not change the light transmission per mass deposited (or at least not on the first order). Other researchers have found that texturing can change the light transmission per unit mass of deposited particulates [28], although this was found to be a small effect.

6.4.2 Micrometeorology

Comparing the mass accumulation on plates deployed in the two duplicate set-ups at the Commerce City site we see that there is only a minor difference, Figure 6.7. The blue data points, are the data collected

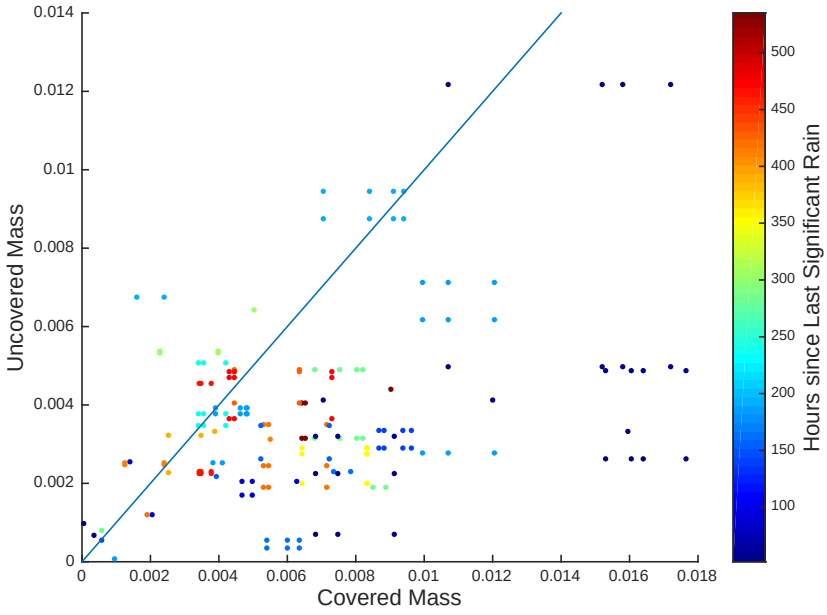

Figure 6.5: Comparison of mass accumulation on the samples with and without a roof color coded for the time since the most recent rain event.

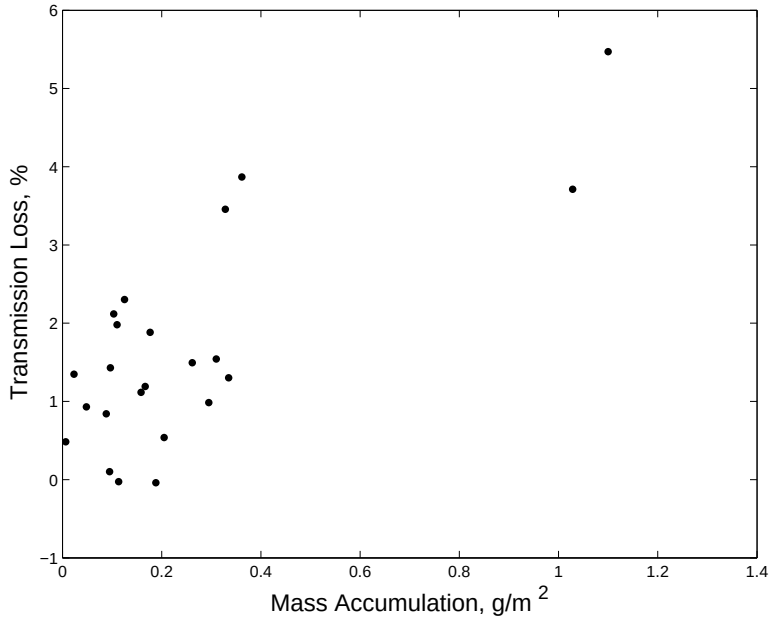

Figure 6.6: Transmission loss versus mass accumulation for plates that were deployed in the uncovered set-up at the Commerce City site.

in the original configuration shown in Figure 6.1 and in part (a) of Figure 6.2, and the red data points are collected with the 40° set-up on the middle set-up moved to the right most side of the sampling area as shown in part (b) of Figure 6.2. It is noted that the blue data points were collected with the 10 cm x 10 cm plates, and thus have higher mass loading than the red data which were collected on the 5 cm x 6 cm plates. This figure shows no significant difference between the samples ($p = 0.2$) in either configuration. These results indicate that meteorology on a scale up to 1 meter is not differentiable from the experimental uncertainty in this experiment.

The lack of significant differences in soiling on a meter scale has many positive implications. First it provides evidence that we can use models to generate a single soiling value for an entire PV system, and that value will likely be valid across the entire system. This makes modeling soiling losses easier and more reliable. Additionally uniform soiling means that there will not be mismatch in PV systems caused by soiling, which could cause compounding losses with soiling.

By comparison to the small scale meteorological differences, we can compare the mass accumulation at the Commerce City site with the mass accumulation at the Erie site. This is shown in Figure 6.8. This plot shows no noticeable relationship between the mass accumulation rate at the two sites, indicating that variations on a regional scale (10s of km) were very important whereas variations on a smaller scale (10s to 100s of centimeters) were less important.

We do not examine the effect of wind direction or speed over the sampling period. Wind direction likely plays a critical role in the micrometeorology, however due to the long time of deployment used here there are some averaging effects. The lack of significant differences between deployed plates seems to indicate that wind direction, wind speed, and other variables do not play an important role in small scale soiling effects, however this could be examined in more detail for specific configurations.

6.4.3 Soiling Saturation and Resuspension

Three sets of samples were deployed for a longer time. The first and second for four weeks, or the time for which two sets of the normally changed plates were deployed. The third for 12 weeks, or the time for which six normally changed sets of plates were deployed. During the second deployment, one of the

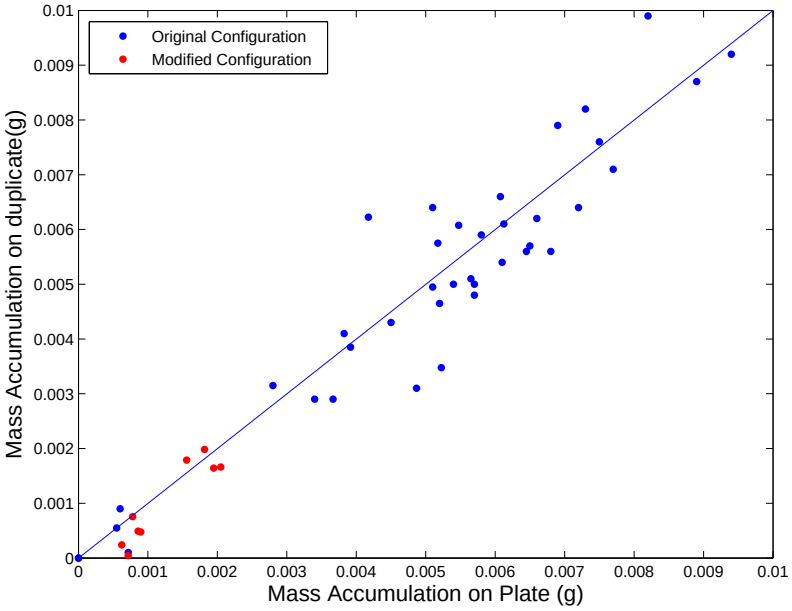

Figure 6.7: Comparison of mass accumulation of co-located samples at the Commerce City site. The blue data are from identically deployed samples, in Figure 6.2(a), and the red data are from one set-up being slightly modified in an attempt to more significantly change the micrometeorology seen by the two set-ups, in Figure 6.2(b).

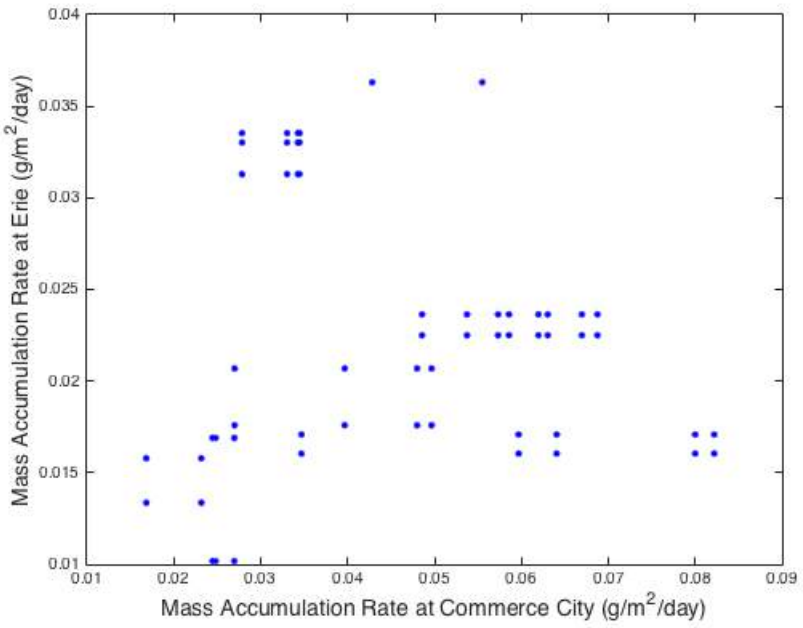

Figure 6.8: Comparison of mass accumulation rate at the Commerce City site and the Erie site for simultaneously deployed plates. Multiple data points at the Commerce City site represent shorter sampling times and two sampling set-ups at that site.

sets of regularly changed plates had both horizontally deployed plates blown from the acrylic set-up, and only the 40° sample from this sampling time is used. In total seven sets of mass comparisons are collected.

No systematic difference was observed in the mass accumulated on these samples, although large spread is noticed. The average percent difference between the long and short time deployed plates was 1.3%, with a standard deviation of 33%. These large errors are most likely caused by compounding mass errors leading to large percentage errors, especially when comparing the data for the third deployment. The differences are on the order of 0.004 g or 30 mg/m^2/day, which is about twice the uncertainty found in Chapter 3. The lack of consistent differences, even in the 12 week deployment, indicates that neither soiling saturation, nor resuspension are significant factors at the Commerce City site, and that the decrease in soiling rate over time, that is seen in other studies, was not observed here.

For modeling of soiling, these results indicate that at least some locations will predominately observe simple additive soiling. This would allow for a simpler model that does not require understanding of soiling saturation or resuspension.

6.5 Conclusion

There are many factors that affect soiling and there are still many factors that have not been examined here. In these experiments there were clearly effects caused by precipitation, with recent precipitation being responsible for cleaning. There was difficulty in identifying the amount of rain necessary for cleaning, and how timing, beyond very recent rains, affected soiling losses. Overall new methods are needed to explore precipitation.

Micrometeorology is a second or third order effect in distances less than 1 meter. However more work is needed to figure out at what scale variations in meteorology are important. This work indicates that that scale is somewhere between 10 and 10000 meters. This is still a large range, indicating the large solar systems could see different levels of soiling, but that co-deployed panels, in open environments, are unlikely to see significantly different soiling losses.

Identifying when saturation will occur is important in modeling soiling especially at dirty locations.

Identifying what factors affect this and when it will occur will be necessary for second order modeling of soiling losses. This effect is not seen here, and the factors contributing to it were not identified. Examining resuspension and soiling will most likely require much higher levels of soiling and time resolution to examine.

Chapter 7

CONCLUSION

7.1 Concluding Remarks

The results presented in this dissertation provide a framework for predicting soiling loss rates in any location using only ambient particulate matter (PM) and meteorological data. This was accomplished by examining two process steps individually. First, in Chapter 3 examining how deposited PM effects light transmission, and ultimately energy loss from a solar energy system. And second, in Chapter 4, by examining how ambient PM concentrations and meteorological conditions impact deposition of PM. These two process steps represent the theory behind how soiling happens, and examining them individually sheds light on where future work should most be addressed. Finally these two process steps are combined in Chapter 5 to look at estimating soiling exclusively from ambient PM data. Chapter 5 also examines spatial variability (both regionally and nationally).

The experiment conducted in Chapter 3 and Chapter 4 is nearly identical to the experiment conducted afterwards in Chapter 5. There are a few differences, including three additional field locations in Chapter 5, different glass samples used, and different instruments for measuring transmission and ambient particulate concentrations. It is important to note that these experiments did not yield identical results; the percentage transmission loss for every g/m^2 of mass accumulated is not the same in Chapter 3 (4.1%) and Chapter 5 (5.7%). These differences highlight the overall uncertainty in these experiments, primarily from measurement uncertainty. While these differences are important, the power that is gained in using them over the current soiling estimation method, which is pure speculation, is significant.

Similar differences exist between the deposition velocities observed in Chapter 4 (2 cm/sec) and Chapter 5 (1 cm/sec). These values are most likely different because of the different airborne PM concentrations that were used. In Chapter 4 PM_{10} was used and in Chapter 5 TSP (roughly PM_{100}) was used. Looking at the particle size distribution data presented in Chapter 4, more than half the particle mass is above 10 µm in diameter, so relatively the deposition velocity found in Chapter 5 may actually be higher than the one found in Chapter 4, however large uncertainty was found with both values.

This work aims at better predicting soiling losses, and the main application of this work is in models that predict power production from solar energy systems (such as the Solar Advisor Model). However there are many other applications of this work both in the field of soiling, and broader applications. Samples collected in this work were used at Sandia National Laboratory to investigate the minimum level of soiling that could be detected by various instruments [7], and also used to create a synthetic 'grime' that mimicked the PM deposited at the Commerce City site. This research could also be used in broader applications of deposition of particulates, such as soiling of windows and monuments. Finally concentrating solar systems represent an area where soiling losses are even less understood. The mass accumulation portion of this research combined with research on how mass effect losses in these systems could be used to predict soiling losses in concentrating solar systems such as parabolic trough collectors, or those that use Fresnel lenses.

Chapter 6 of this dissertation highlights a few of the many components of soiling that would be necessary to build a complete soiling model. Some of these have been examined in more detail in the literature. In addition to precipitation, micrometeorology, and soiling saturation, more work is needed to understand angle of deployment. Samples here are deployed only at 0° and 40° to the horizontal, but systems are deployed at nearly every angle between 0° and 90°. Other research has examined angle of deployment [54] [21] [29] [51] [56], and it is logical to assume a cosine dependence of soiling with angle of incidence, however caution should be used when using this research at varying angles of deployment of solar energy systems. More factors that have not been examined but that effect soiling are discussed below in Section 7.2.

Overall this research provides a complete method for estimating soiling rates at any location where

ambient PM concentrations are known, with better results possible with the inclusion of meteorological data. This is the first work of its kind to provide a method for predicting soiling rates. When combined with other research this work has the ability to provide a complete soiling model.

7.2 Future Work

A complete understanding of soiling is far from accomplished. Future work is needed in several areas to create a more robust and fully fledged model for estimating soiling losses. The first is an understanding of chemistry. Especially a focus on how the chemistry of airborne PM relates to the chemistry of deposited PM. Previous deposition work has found that not all species deposit at the same rate [15] [65] [49] or effect energy production equally [20] [34], but more work is needed to see how much this effects soiling.

Deposition studies have regularly looked at size distributions [14] [40] however no ambient soiling studies have looked at the effects of size distributions. This includes if size distributions are a necessary component of predicting total mass accumulation, and how ambient airborne and deposited size distributions vary, and if this is a contributing factor to light attenuation. Results presented in this dissertation indicated that deposited size distribution is not a contributing factor to light attenuation, however other studies have found that size is a contributing factor in artificially soiled samples [20].

The data in this research were almost entirely collected with a roof over the soiling samples (to prevent contamination and cleaning by precipitation). While this was a useful design component for understanding soiling, there are some particles that did not deposit on the samples because of the presence of the roof. Chapter 6 explored this issue, and found little if any effect, however further research examining the roof, and removing the effects of the roof would increase the applicability of research in this study. One method for doing this would be to model the roof as an extra deposition resistance, that could be removed when examining real PV systems.

Perhaps the most useful future research direction, is in validating the models and results presented here at more locations across the United States, with a focus on what data quality and proximity is necessary to accurately predict soiling losses. Many other studies have identified soiling rates [37] [24] [11] but studies

do not regularly report meteorological conditions, or ambient PM conditions. Gathering all this information together, and comparing modeled and measured soiling rates could validate the models presented here, and give confidence in using this method to estimate soiling losses.

Finally this research was conducted for wide implementation in solar models, and actually implementing this is large area of future work to be conducted. There are several key elements that need to happen before this is possible. First most solar models use typical meteorological year data sets (TMY or TMY3), which do not include ambient particulate concentrations. Either PM data needs to be added to the TMY data sets, or these results need to be extended to Aerosol Optical Depth (AOD) and/or horizontal visibility which are included in TMY3 data sets. Second most solar models include some sort of soiling option, but these should be modified to adapt to varying soiling rates and cleaning over time, ideally through the TMY data set.

Bibliography

[1] 1981-2010 Normals Data Access | National Climatic Data Center (NCDC).

[2] A Al-Hasan. A new correlation for direct beam solar radiation received by photovoltaic panel with sand dust accumulated on its surface. Solar Energy, 63(5):323–333, November 1998.

[3] Reinhart Appels, Buvaneshwari Lefevre, Bert Herteleer, Hans Goverde, Alexander Beerten, Robin Paesen, Klaas De Medts, Johan Driesen, and Jef Poortmans. Effect of soiling on photovoltaic modules. Solar Energy, 96:283–291, October 2013.

[4] S. A. Biryukov. Degradation of optical properties of solar collectors due to the ambient dust deposition as a function of particle size. Journal of Aerosol Science, 27, Supplement 1:S37–S38, September 1996.

[5] L. Boyle, H. Flinchpaugh, and M. P. Hannigan. Natural soiling of photovoltaic cover plates and the impact on transmission. Renewable Energy, 77:166–173, May 2015.

[6] Liza Boyle, Holly Flinchpaugh, and Michael Hannigan. Ambient airborne particle concentration and soiling of PV cover plates. pages 3171–3173. IEEE, June 2014.

[7] P.D. Burton, L. Boyle, J.J.M Griego, and B.H. King. Quantification of a Minimum Detectable Soiling Level to Affect Photovoltaic Devices by Natural and Simulated Soils. IEEE Journal of Photovoltaics, PP(99):1–7, 2015.

[8] P.D. Burton and B.H. King. Application and Characterization of an Artificial Grime for Photovoltaic Soiling Studies. IEEE Journal of Photovoltaics, 4(1):299–303, January 2014.

[9] J. A. Businger, J. C. Wyngaard, Y. Izumi, and E. F. Bradley. Flux-Profile Relationships in the Atmospheric Surface Layer. Journal of the Atmospheric Sciences, 28(2):181–189, March 1971.

[10] R. E. Cabanillas and H. Munguía. Dust accumulation effect on efficiency of Si photovoltaic modules. Journal of Renewable and Sustainable Energy, 3(4):043114, July 2011.

[11] J.R. Caron and B. Littmann. Direct Monitoring of Energy Lost Due to Soiling on First Solar Modules in California. IEEE Journal of Photovoltaics, 3(1):336–340, 2013.

[12] Nicholas Clements, Jenny Eav, Mingjie Xie, Michael P. Hannigan, Shelly L. Miller, William Navidi, Jennifer L. Peel, James J. Schauer, Martin M. Shafer, and Jana B. Milford. Concentrations and source insights for trace elements in fine and coarse particulate matter. Atmospheric Environment, 89:373–381, June 2014.

[13] Nicholas Clements, Ricardo Piedrahita, John Ortega, Jennifer L. Peel, Michael Hannigan, Shelly L. Miller, and Jana B. Milford. Characterization and Nonparametric Regression of Rural and Urban Coarse Particulate Matter Mass Concentrations in Northeastern Colorado. Aerosol Science and Technology, 46(1):108–123, 2012.

[14] Jan M. Coe and Steven E. Lindberg. The Morphology and Size Distribution of Atmospheric Particles Deposited on Foliage and Inert Surfaces. JAPCA, 37(3):237–243, 1987.

[15] Edward F. Cuddihy. Theoretical considerations of soil retention. Solar Energy Materials, 3(1–2):21–33, September 1980.

[16] Cliff I. Davidson, Steven E. Lindberg, Jill A. Schmidt, Lawrence G. Cartwright, and Laurence R. Landis. Dry deposition of sulfate onto surrogate surfaces. Journal of Geophysical Research: Atmospheres, 90(D1):2123–2130, February 1985.

[17] John A Duffie and William A Beckman. Solar engineering of thermal processes. Wiley, Hoboken, N.J., 2006.

[18] T Duhl, E Lee, M Hannigan, F Rosario-Oritz, N Clements, K Cawley, and L Blackwell. Vertical and temporal variability of carbonaceous aerosol and contributions from organic matter: Preliminary results from aerosol samples collected at the Boulder Atmospheric Observatory tower in Erie, CO. In Progress.

[19] Steven J. Dutton, James J. Schauer, Sverre Vedal, and Michael P. Hannigan. PM2.5 characterization for time series studies: Pointwise uncertainty estimation and bulk speciation methods applied in Denver. Atmospheric Environment, 43(5):1136–1146, February 2009.

[20] Mohammad S. El-Shobokshy and Fahmy M. Hussein. Effect of dust with different physical properties on the performance of photovoltaic cells. Solar Energy, 51(6):505–511, December 1993.

[21] Hamdy K. Elminir, Ahmed E. Ghitas, R.H. Hamid, F. El-Hussainy, M.M. Beheary, and Khaled M. Abdel-Moneim. Effect of dust on the transparent cover of solar collectors. Energy Conversion and Management, 47(18-19):3192–3203, November 2006.

[22] Guor-Cheng Fang, Hung-Che Chiang, Yu-Cheng Chen, You-Fu Xiao, and Yuan-Jie Zhuang. Particulates and Metallic Elements Monitoring at Two Sampling Sites (Harbor, Airport) in Taiwan. Environmental Forensics, 15(4):296–305, October 2014.

[23] Guor-Cheng Fang, Yuh-Shen Wu, Wen-Jhy Lee, Te-Yen Chou, and I-Chen Lin. Ambient air particulates, metallic elements, dry deposition and concentrations at Taichung Airport, Taiwan. Atmospheric Research, 84(3):280–289, May 2007.

[24] Miguel García, Luis Marroyo, Eduardo Lorenzo, and Miguel Pérez. Soiling and other optical losses in solar-tracking PV plants in navarra. Progress in Photovoltaics: Research and Applications, 19(2):211–217, 2011.

[25] H.P. Garg. Effect of dirt on transparent covers in flat-plate solar energy collectors. Solar Energy, 15(4):299–302, April 1974.

[26] Sanaz Ghazi and Kenneth Ip. The effect of weather conditions on the efficiency of PV panels in the southeast of UK. Renewable Energy, 69:50–59, September 2014.

[27] Dirk Goossens. Quantification of the dry aeolian deposition of dust on horizontal surfaces: an experimental comparison of theory and measurements. Sedimentology, 52(4):859–873, August 2005.

[28] Dirk Goossens and Emmanuel Van Kerschaever. Aeolian dust deposition on photovoltaic solar cells: the effects of wind velocity and airborne dust concentration on cell performance. Solar Energy, 66(4):277–289, July 1999.

[29] Jia Yun Hee, Lalit Verma Kumar, Aaron James Danner, Hyunsoo Yang, and Charanjit Singh Bhatia. The Effect of Dust on Transmission and Self-cleaning Property of Solar Panels. Energy Procedia, 15:421–427, 2012.

[30] Adel A. Hegazy. Effect of dust accumulation on solar transmittance through glass covers of plate-type collectors. Renewable Energy, 22(4):525–540, April 2001.

[31] Thomas M. Holsen, Kenneth E. Noll, Guor Cheng Fang, Wen Jhy Lee, Jui Min Lin, and Gerald J. Keeler. Dry deposition and particle size distributions measured during the Lake Michigan Urban Air Toxics Study. Environmental Science & Technology, 27(7):1327–1333, 1993.

[32] H. Hottel and B. Woertz. Performance of flat-plate solar-heat collectors. Trans. ASME, 64:91 – 104, 1942.

[33] J. K. Kaldellis and A. Kokala. Quantifying the decrease of the photovoltaic panels' energy yield due to phenomena of natural air pollution disposal. Energy, 35(12):4862–4869, December 2010.

[34] J.K. Kaldellis and M. Kapsali. Simulating the dust effect on the energy performance of photovoltaic generators based on experimental measurements. Energy, 36(8):5154–5161, August 2011.

[35] Soteris A. Kalogirou, Rafaela Agathokleous, and Gregoris Panayiotou. On-site PV characterization and the effect of soiling on their performance. Energy, 51:439–446, March 2013.

[36] Hussam Khonkar, Abdulaziz Alyahya, Mazzen Aljuwaied, Mohammad Halawani, Abdulrahman Al Saferan, Fawwaz Al-khaldi, Fawaz Alhadlaq, and Brent A. Wacaser. Importance of cleaning concentrated photovoltaic arrays in a desert environment. Solar Energy, 110:268–275, December 2014.

[37] A. Kimber, L. Mitchell, S. Nogradi, and H. Wenger. The Effect of Soiling on Large Grid-Connected Photovoltaic Systems in California and the Southwest Region of the United States. In Conference Record of the 2006 IEEE 4th World Conference on Photovoltaic Energy Conversion, volume 2, pages 2391–2395, May 2006.

[38] Marcel Langner, Martin Kull, and Wilfried R. Endlicher. Determination of PM10 deposition based on antimony flux to selected urban surfaces. Environmental Pollution, 159(8–9):2028–2034, August 2011.

[39] Jim J. Lin, Kenneth E. Noll, and Thomas M. Holsen. Dry Deposition Velocities as a Function of Particle Size in the Ambient Atmosphere. Aerosol Science and Technology, 20(3):239–252, 1994.

[40] Jui-Min Lin, Guor-Cheng Fang, Thomas M. Holsen, and Kenneth E. Noll. A comparison of dry deposition modeled from size distribution data and measured with a smooth surface for total particle mass, lead and calcium in Chicago. Atmospheric Environment. Part A. General Topics, 27(7):1131–1138, May 1993.

[41] T. Lombardo, A. Chabas, A. Verney-Carron, H. Cachier, S. Triquet, and S. Darchy. Physico-chemical characterisation of glass soiling in rural, urban and industrial environments. Environmental Science and Pollution Research, pages 1–8, April 2014.

[42] Monto Mani and Rohit Pillai. Impact of dust on solar photovoltaic (PV) performance: Research status, challenges and recommendations. Renewable and Sustainable Energy Reviews, 14(9):3124–3131, December 2010.

[43] G. A. Mastekbayeva and S. Kumar. Effect of dust on the transmittance of low density polyethylene glazing in a tropical climate. Solar Energy, 68(2):135–141, February 2000.

[44] Felipe A. Mejia and Jan Kleissl. Soiling losses for solar photovoltaic systems in California. Solar Energy, 95:357–363, September 2013.

[45] Krister Midtdal and Bjørn Petter Jelle. Self-cleaning glazing products: A state-of-the-art review and future research pathways. Solar Energy Materials and Solar Cells, 109:126–141, February 2013.

[46] N.M. Nahar and Jagdish P. Gupta. Effect of dust on transmittance of glazing materials for solar collectors under arid zone conditions of India. Solar & Wind Technology, 7(2-3):237–243, 1990.

[47] Kenneth E. Noll and Kenneth Y. P. Fang. Development of a dry deposition model for atmospheric coarse particles. Atmospheric Environment (1967), 23(3):585–594, 1989.

[48] Kenneth E. Noll, Kenneth Y. P. Fang, and Laura A. Watkins. Characterization of the deposition of particles from the atmosphere to a flat plate. Atmospheric Environment (1967), 22(7):1461–1468, 1988.

[49] Gregory C. Pratt, Evelyn J. Orr, Donald C. Bock, Rick L. Strassman, Dean W. Fundine, Clifford J. Twaroski, J. David Thornton, and Tilden P. Meyers. Estimation of Dry Deposition of Inorganics Using Filter Pack Data and Inferred Deposition Velocity. Environmental Science & Technology, 30(7):2168–2177, 1996.

[50] H. Qasem, T.R. Betts, and R. Gottschalg. Soiling correction model for long term energy prediction in photovoltaic modules. In 2012 38th IEEE Photovoltaic Specialists Conference (PVSC), pages 003397–003401, June 2012.

[51] Hassan Qasem, Thomas R. Betts, Harald Müllejans, Hassan AlBusairi, and Ralph Gottschalg. Dust-induced shading on photovoltaic modules. Progress in Photovoltaics: Research and Applications, pages n/a–n/a, 2012.

[52] G. S. Raynor. Experimental studies of pollen deposition to vegetated surfaces. In Atmosphere-Surface Exchange of Particulate and Gaseous Pollutants, pages 264–279, Richland, Washington, 1974.

[53] REN21. Renewables 2012 Global Status Report, June 2012.

[54] E. P. Roth and A. J. Anaya. The Effect of Natural Soiling and Cleaning on the Size Distribution of Particles Deposited on Glass Mirrors. Journal of Solar Energy Engineering, 102(4):248, 1980.

[55] S.A.M. Said. Effects of dust accumulation on performances of thermal and photovoltaic flat-plate collectors. Applied Energy, 37(1):73–84, 1990.

[56] Syed A. M. Said and Husam M. Walwil. Fundamental studies on dust fouling effects on PV module performance. Solar Energy, 107:328–337, September 2014.

[57] Travis Sarver, Ali Al-Qaraghuli, and Lawrence L. Kazmerski. A comprehensive review of the impact of dust on the use of solar energy: History, investigations, results, literature, and mitigation approaches. Renewable and Sustainable Energy Reviews, 22:698–733, June 2013.

[58] Sayigh, A.A.M. Effect of Dust on Flat Plate Collectors. In Sun: Mankind's future source of energy; Proceedings of the International Solar Energy Congress, New Delhi, India, January 16-21, 1978, volume 2, pages 960–964. Pergamon Press, Inc., Elmsford, N.Y., 1978.

[59] A. Sayyah, M.N. Horenstein, and M.K. Mazumder. Mitigation of soiling losses in concentrating solar collectors. In Photovoltaic Specialists Conference (PVSC), 2013 IEEE 39th, pages 0480–0485, June 2013.

[60] Arash Sayyah, Mark N. Horenstein, and Malay K. Mazumder. Energy yield loss caused by dust deposition on photovoltaic panels. Solar Energy, 107:576–604, September 2014.

[61] John H. Seinfeld and Spyros N. Pandis. Atmospheric Chemistry and Physics: From Air Pollution to Climate Change. Wiley Interscience, 2nd edition, 2006.

[62] W. G. N Slinn. Predictions for particle deposition to vegetative canopies. Atmospheric Environment (1967), 16(7):1785–1794, 1982.

[63] Yücel Tasdemir and Can Kural. Atmospheric dry deposition fluxes of trace elements measured in Bursa, Turkey. Environmental Pollution, 138(3):462–472, December 2005.

[64] MB Ullah, Julius Tan Kurniawan, Lam Khee Poh, Tham Kwok Wai, and PR Tregenza. Attenuation of diffuse daylight due to dust deposition on glazing in a tropical urban environment. Lighting Research and Technology, 35(1):19 –29, March 2003.

[65] Yee-Lin Wu, Cliff I. Davidson, Donald A. Dolske, and Susan I. Sherwood. Dry Deposition of Atmospheric Contaminants: The Relative Importance of Aerodynamic, Boundary Layer, and Surface Resistances. Aerosol Science and Technology, 16(1):65–81, 1992.

[66] Seung-Muk Yi, Usama Shahin, Jakkris Sivadechathep, Sait C Sofuoglu, and Thomas M Holsen. Overall elemental dry deposition velocities measured around Lake Michigan. Atmospheric Environment, 35(6):1133–1140, 2001.

[67] Leiming Zhang, Sunling Gong, Jacob Padro, and Len Barrie. A size-segregated particle dry deposition scheme for an atmospheric aerosol module. Atmospheric Environment, 35(3):549–560, 2001.